The structure and properties of the dihalo(dimethyl)germanes and related compounds

by

Heidi Rohwer

Thesis

submitted in fulfilment of the requirements
for the degree

Magister Scientiae

in

Chemistry

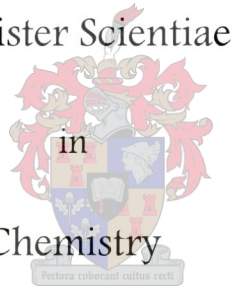

in the

Faculty of Science

at the

University of Stellenbosch

Supervisor : Prof Jan Dillen

March 2002

DECLARATION

I, the undersigned, hereby declare that the work contained in this thesis is my own original work and has not previously in its entirety or in part been submitted at any university for a degree.

Summary

There is limited experimental and computational information available on the structures of compounds of the form R_2GeX_2, where X is a halogen and R an alkyl group. Gas phase electron diffraction studies of the dihalo(dimethyl)germanes (R=Me) consistently give C-Ge-C angles in the range of 120-125°, about 10° larger than the corresponding C-C-C angles in the 2,2-dihalopropanes. However, in dimethylgermane, where the halogen atoms are substituted by hydrogen, the value of the C-Ge-C is very similar to the corresponding C-C-C angle in propane and deviates little from the tetrahedral value of 109.47°.

The unusually large influence of atomic substituents on the value of the valence angles in these compounds introduces a serious challenge to the development of empirical force fields, where the size of an angle is traditionally determined only by the atoms directly involved in the formation of the angle and not by the other substituents attached to the central atom. Unfortunately, the large experimental errors in the gas phase electron diffraction studies and the lack of representative crystalline compounds in the Cambridge Structural Database make it impossible to establish conclusively whether these large valence angles are significant or just statistical anomalies.

A systematic *ab initio* study of a number of compounds of the general form Me_2AX_2 with A=C, Si or Ge and X=H, F, Cl, Br or I has been initiated to verify the experimental results and to try to explain this observed deviation in valence angle in terms of electronic effects and existing theories of structure and bonding. The carbon and silicon analogs of the dimethylated germanes were included in the calculations to ascertain whether the observed effect is an anomaly or merely a periodic trend in the group IV elements. To obtain a clearer overall view, identical calculations were also performed on compounds of the form AH_nX_{4-n}, $MeAH_2X$, $MeAHX_2$ and Me_2AHX, where A and X have the same meaning as before.

The *ab initio* calculations confirmed that there is in fact a significant increase in the C-A-C angle from A=C to A=Ge in the compounds Me_2AX_2, although the calculated increase is smaller than the experimentally determined increase by a few degrees. Together with this observed increase in the C-A-C angle there is a corresponding decrease in the X-A-X angle. Calculation of the electron density of three representative compounds revealed a significant difference in electron distribution between the germanium compounds and their carbon analogs, suggesting that the ionicity of the bonds and the electronegativity of the substituents may play a role in the size of the C-A-C angle in compounds of this form. This is supported by a statistical analysis of compounds in the Cambridge Structural Database containing a C_2GeYZ fragment, where Y and Z may be any elements except carbon, which showed that the average C-Ge-C angle in compounds where Y and Z are electronegative is approximately 7° larger than in compounds where Y and Z are electropositive. The qualitative trends in the C-A-C and X-A-X angles have also been discussed in terms of three different bonding models.

To verify the results of the *ab initio* calculations experimentally, a representative compound, dichlorobis(phenethyl)germane, has been synthesized and its crystal structure determined by X-ray diffraction. The C-Ge-C angle was found to be 121.2°, which is in good agreement with both the *ab initio* and the gas phase electron diffraction results.

Furthermore, a force field for halogenated organic carbon, silicon and germanium compounds has also been developed based on the structural and vibrational data obtained from the *ab initio* calculations. Molecules of the form AH_nX_{4-n} and Me_2AX_2 with A=C, Si, Ge and X=H, F, Cl and Br were used in the training set and the bond lengths, bond angles and vibrational frequencies were used to optimize the force field. Calculations performed with the force field reproduce the C-A-C angles to within 1° of the observed values and the reproducibility for the rest of the experimental data is also good. Force fields have been developed for some of the simpler molecules in our training set and where this is the case, the force field parameters have been compared to the previously determined values.

Opsomming

Daar is 'n beperkte hoeveelheid eksperimentele en berekende inligting beskikbaar oor die struktuur van verbindings in die vorm R_2GeX_2, waar X 'n halogeen en R 'n alkiel groep is. Gasfase-elektrondiffraksie studies van die dihalo(dimetiel)-germane (R=Me) gee konsekwent C-Ge-C hoeke in die omgewing van 120-125°, ongeveer 10° groter as die vergelykbare C-C-C hoeke in die 2,2-dihalopropane. In dimetielgermaan egter, waar die halogene vervang word met waterstof, is die grootte van die C-Ge-C hoek soortgelyk aan die vergelykbare C-C-C hoek in propaan en wyk nie ver af van die tetrahedrale waarde van 109.47° nie.

Die buitengewone groot invloed van atoom substituente op die waarde van die valensiehoek in hierdie verbindings stel 'n ernstige uitdaging voor in die ontwikkeling van empiriese kragvelde, waar die grootte van 'n hoek tradisioneel bepaal word deur die atome direk betrokke in die vorming van die hoek en nié deur die ander substituente gebind aan die sentrale atoom nie. Die groot eksperimentele foute in die gasfase-elektrondiffraksie studies en die tekort aan verteenwoordigende verbindings in die Cambridge Strukturele Databasis maak dit ongelukkig onmoontlik om oortuigend vas te stel of hierdie groot valensiehoeke betekenisvol is of slegs statistiese afwykings is.

'n Sistematiese *ab initio* ondersoek van 'n aantal verbindings in die algemene vorm Me_2AX_2, met A=C, Si, Ge en X=H, F, Cl, Br of I, is ingelei om die eksperimentele resultate te bevestig en om hierdie waargenome toename in valensiehoek te probeer verduidelik in terme van elektroniese effekte en bestaande teorieë van struktuur en binding. Die koolstof en silikon analoë van die gedimetileerde germane is ingesluit in die berekeninge om vas te stel of die waargenome effek 'n afwyking is, of slegs 'n periodiese neiging in die groep IV elemente. Om 'n duideliker algemene prentjie te kry is identiese berekeninge ook uitgevoer op verbindings in die vorm AH_nX_{4-n}, $MeAH_2X$, $MeAHX_2$ en Me_2AHX, waar A en X dieselfde betekenis as voorheen het.

Die *ab initio* berekeninge het bevestig dat daar wel 'n betekenisvolle toename in die C-A-C hoek vanaf A=C tot by A=Ge in die verbindings Me_2AX_2 is, alhoewel die berekende toename 'n paar grade kleiner is as die eksperimenteel vasgestelde toename. Saam met hierdie toename in die C-A-C bindingshoek is daar 'n gepaardgaande afname in die X-A-X hoek. Berekening van die elektrondigtheid van drie verteenwoordiginde verbindings toon aan 'n betekenisvolle verskil in die verspreiding van elektrondigtheid is tussen die germanium verbindings en hulle koolstof analoë, wat suggereer dat die ionisiteit van die bindings en die elektronegatiwiteit van die substituente dalk 'n rol mag speel in die grootte van die C-A-C hoek van verbindings in hierdie vorm. Dit word ondersteun deur 'n statistiese analise van verbindings op die Cambridge Strukturele Databasis wat 'n C_2GeYZ fragment bevat, waar Y en Z enige elemente behalwe koolstof is, wat toon dat die gemiddelde C-Ge-C hoek in verbindings waar Y en Z elektronegatief is omtrent 7° groter is as in die verbindings waar Y en Z elektropositief is. Die kwalitatiewe tendense in die C-A-C en X-A-X hoeke is ook bespreek in terme van drie verskillende bindingsteorieë.

Om die resultate van die *ab initio* berekeninge eksperimenteel te verifieer, is 'n verteenwoordigende verbinding, dichlorobis(fenetiel)germaan, gesintetiseer en die kristalstruktuur bepaal deur middel van X-straaldiffraksie. Die C-Ge-C hoek in hierdie verbinding is 121.2°, wat goed ooreenstem met beide die *ab initio* en die gasfase-elektrondiffraksie resultate.

Verder is 'n kragveld ontwikkel vir gehalogeneerde, organiese koolstof, silikon en germanium verbindings, gegrond op die strukturele en vibrasionele data verkry vanaf die *ab initio* berekeninge. Molekules in die vorm AH_nX_{4-n} en Me_2AX_2 met A=C, Si, Ge en X=H, F, Cl en Br is gebruik in die oefenstel en die bindingslengtes, bindingshoeke en vibrasiefrekwensies is gebruik om die kragveld te optimiseer. Berekeninge met die kragveld reproduseer die C-A-C bindingshoeke tot binne die grense van 1° van die waargenome waardes en die herhaalbaarheid van die ander eksperimentele data is ook goed. Kragvelde is al ontwikkel vir 'n paar van die eenvoudiger molekules in ons oefenstel en waar dit die geval is, is die kragveld parameters vergelyk met die voorafberekende waardes.

Acknowledgements

- Professor J.L.M. Dillen, my supervisor, for always being available to help and guide, and for his endless patience during the writing up of this thesis.

- Dr. C. Esterhuysen for her help and encouragement.

- Dr. S. Cronje for her invaluable assistance with the synthesis.

- Dr. M. Bredenkamp for his help with solving the NMR spectrum.

- The University of Stellenbosch, the National Research Foundation and my supervisor, Professor Dillen, for their financial assistance.

- Gerhard Venter, my fellow theoretical chemistry student, for all his help with the practical aspects of computer use and for his company throughout the year.

- My mother and father for taking care of all the practical things I didn't always have the time or money for while writing up this thesis.

- My family and friends for their support, for keeping me sane and for putting up with the mood swings symptomatic of writing a thesis.

Publications and presentations

Portions of this work are being written up in the form of articles to be submitted for publication.

A poster was presented at Indaba III, Skukuza, Kruger National Park, South Africa, 6-11 August 2000: *"The molecular structure and properties of a range of halogenated germanium compounds as determined by ab initio molecular orbital calculations"*

Table of Contents

Glossary

A	Group IV element
CISD	Singly- and Doubly-excited Configuration Interaction
CSD	Cambridge Structural Database
DFT	Density Functional Theory
DZ	Double zeta
ECP	Effective Core Potential
ED	Electron Diffraction
ESMS	Electron-spray Mass Spectroscopy
HAO	Hybrid Atomic Orbital
HF	Hartree-Fock
IR	Infrared
LCP	Ligand Close Packing
Me	Methyl group
MM	Molecular Mechanics
MO	Molecular Orbital
MP2	Second order Moller-Plesset Perturbation
NBO	Natural Bond Orbital
NMR	Nuclear Magnetic Resonance
PEFF	Program for the Development of Empirical Force Fields
Ph	Phenyl group
QM	Quantum mechanics
R, R'	Alkyl group or alkyl derivative
RHF	Restricted Hartree-Fock
SCF	Self-Consistent Field
U	Isotropic Temperature Factor
UFF	Universal Force Field
VALBOND	Valence Bonding Force Field
VSEPR	Valence-Shell Electron-Pair Repulsion
X	Halogen (or hydrogen)
Y, Z	Any atom
χ	Electronegativity
ε	Van der Waals hardness
r_m	Van der Waals radius

CHAPTER 1: INTRODUCTION

1.1. Background

The dimethylgermanes are gases at room temperature and for this reason the only structural information available for these and related compounds is found by microwave spectroscopy [1-10] and gas phase electron diffraction [11-16]. The gas phase ED studies give C-Ge-C angles of 121(4)°, 121(4)° and 124(7)° for difluoro- [11], dichloro- [12] and dibromo(dimethyl)-germane [13] respectively. This is in strong contrast to the almost tetrahedral angles found in similar compounds containing carbon instead of germanium. Analogous silicon compounds also have C-Si-C angles close to the C-C-C angles found in the 2,2-dihalopropanes. Furthermore, the microwave spectrum of dimethylgermane [2], in which the halogens are replaced with hydrogen atoms, gives a C-Ge-C angle of only 110°. The C-Ge-C angles in the halo(trimethyl)germanes [3,4] also show deviations from the tetrahedral, but nowhere near as large as those seen for the dihalo(dimethyl)germanes.

If these experimental values are to be believed, the substitution of halogen atoms has a large effect on the C-Ge-C angle in compounds of the form Me_2GeX_2. Furthermore, it seems to be only the combination of germanium as a central atom and two halogen atoms as substituents that leads to these large angles. As soon as the halogens are replaced by hydrogen or the germanium replaced by carbon and or silicon, the angle reverts back to an approximately tetrahedral value.

Although these results seem to be quite remarkable, the gas phase ED studies from which the values were obtained contained large experimental errors for the C-Ge-C angles, making it impossible to state with any certainty that these angles are out of the ordinary and not just statistical deviations. Since these molecules are all gases at room temperature, X-ray diffraction data cannot be obtained and there are no known crystalline compounds that

have properties close enough to those of the dihalo(dimethyl)germanes that they can be considered representative of this group of compounds.

A search of the Cambridge Structural Database yields five crystal structures of the form R_2GeX_2, where R is an alkyl group or a derivative thereof. In all these compounds the R substituent is either bulky, has large electronic effects, or the C-Ge-C fragment forms part of a five- or six-membered ring, all of which could have a potentially large influence on the C-Ge-C angle. There is thus a shortage of sufficient, reliable and appropriate structural data on which to conduct an experimental study of the influence of halogen substitution on the C-Ge-C angle in R_2GeX_2 compounds.

Some computational studies have been conducted [17-19] and the results support the findings of the experimental data. These studies do not however, cover the whole range of compounds of the form Me_2AX_2, where A=C, Si and Ge and X=H, F, Cl, Br, but only selected cases. Furthermore, no satisfactory explanation has been offered for the large deviations from tetrahedral geometry in these germanium compounds. Calculations performed on analogous lead compounds indicate that the C-A-C angles in molecules of the form Me_2PbX_2 are also exceptionally large [20].

The large influence on bond angles of atomic substituents not directly involved in the formation of the bonds, presents a serious challenge to the development of empirical force fields. There are no force fields explicitly parameterized to calculated the geometries of halogenated organogermanium compounds and the generic force fields that are available for carbon, silicon and germanium are unable to correctly predict the trends in the C-Ge-C bond angles of the dihalo-(dimethyl)germanes. The Dreiding [21] and UFF [22] force fields both predict C-Ge-C angles close to the tetrahedral value of 109.47°. The values predicted by VALBOND [23] show a slight improvement but are still nowhere near those found by electron diffraction and *ab initio* studies.

The vibrational spectra of dimethylgermane, the dihalo(dimethyl)germanes and many other halogenated organogermanes have been extensively characterized [24-35] and modified valence force fields have been developed in a number of cases to test the assignments made. In the development of all of these force fields however, the assumption has been made that these substituted germanes have idealized tetrahedral, or close to tetrahedral, geometries. A few vibrational force fields have been developed for the simpler halogermanes [36-42], but these use experimentally determined geometries as input in the force field optimization and do not attempt to reproduce these geometries. Furthermore they are only parameterized for small groups of compounds.

1.2. Aims

In terms of the preceding discussion, the aims of this work are the following:

- To provide a set of consistent and reliable structural and vibrational data for compounds of the general form Me_2AX_2, where A=C, Si, Ge and X=H, F, Cl, Br, I, by means of *ab initio* calculation.
- To justify or explain the large C-Ge-C angle in the compounds Me_2GeX_2 in terms of existing theories of structure and bonding or propose an alternative to the existing theories.
- To synthesize a structure of the form R_2GeX_2, where R is an alkyl group and X a halogen, with properties similar enough to the dihalo(dimethyl)-germanes as to be representative of this class of compounds and from which reliable X-ray diffraction data can be obtained. A suitable R group will have to be chosen so that the compound is crystalline at normal temperatures.
- To develop a force field able to correctly predict the trend in the C-A-C angles of the compounds of the form R_2AX_2, where R is an alkyl group, A=C, Si, Ge and X=H, F, Cl, Br, and provide good estimates of the overall geometries and vibrational frequencies of these compounds and other halogenated organogermanes.

CHAPTER 2: LITERATURE REVIEW

2.1. Introduction

This chapter contains reviews of the group IV and group VII elements, an overview of computational chemistry and summaries of some general theories of structure and bonding. It also contains discussions of specific experimental and computational studies of the structure and vibrational behaviour of the halogenated organogermanes and related compounds and methods of synthesis for germanes. The results of searches of the Cambridge Structural Database for related molecules are also included.

Overviews of the physical and chemical properties of the group IV and group VII elements are given in **Sections 2.2.** and **2.3.** respectively. A large portion of this work concerns the effect of changes in A and X on molecules of the form Me_2AX_2, where A is a group IV and X a group VII element. Similarities, differences and general trends within these groups were therefore considered to be important. Although the information contained in these two sections can be found in any respectable inorganic textbook, they were nevertheless included here for this reason. Three different theories of structure and bonding in molecules are discussed in **Section 2.4.** with the view of using them later to explain the results of **Chapter 3**. An overview of computational chemistry is given in **Section 2.5.** for readers unfamiliar with the field, while the specific computational studies relating to this work are discussed in **Section 2.6. Sections 2.7.** and **2.8.** review respectively structural and vibrational studies of the halogenated organogermanes and some analogous silicon compounds. The structures and vibrations of the analogous carbon compounds were considered well known enough to be excluded. An overview of the development of synthetic methods for the organogermanes is given in **Section 2.9.** and **Section 2.10.** summarizes the results of searches of the Cambridge Structural Database for compounds related to the dihalo-(dimethyl)germanes. The conclusion is contained in **Section 2.11.**

2.2. The group IV elements

Germanium is a group IV element [43,44], along with carbon, silicon, tin and lead. Of all the elements on the periodic table, carbon has more known compounds than any other element except hydrogen. Silicon is also a diverse element with many and varied applications in Chemistry and a natural abundance second only to oxygen. Germanium, tin and lead on the other hand, are rare elements with low natural abundances.

Germanium was discovered in 1886 and although it is only found in small amounts, it occurs widely on the earth's crust. In comparison with the other group IV elements, relatively few germanium compounds exist. Its main use is in electronics, as a semiconductor or in the pure metal form. Tin and lead are also mainly used in their pure metal form, but they do have applications in organometallic chemistry and alkyltin and alkyllead compounds are synthesized on a large scale.

The group IV elements all have four electrons in their outer valence shells. Carbon in its ground state has the electronic structure $1s^2 2s^2 2p^2$ with the 2p electrons unpaired. In virtually all stable compounds however, carbon bonds with a four-covalence by promoting an electron to the empty p-orbital to form an electron state with configuration $2s2p_x2p_y2p_z$. On the whole carbon forms covalent bonds, although an approximation of a C^{4-} ion may exist in some carbides. In stable covalent compounds containing only single bonds, carbon will bond with four other atoms to form a structure with tetrahedral geometry.

All the Group IV elements can exist in either a divalent or a tetravalent state but carbon in its divalent state is only found in carbenes, which are inherently unstable compounds. The divalent state becomes increasingly stable down the group and is dominant for lead. Silicon and germanium can exist in the divalent state but both prefer the tetravalent state, forming

compounds analogous to carbon with similar geometries, such as the halides and hydrides.

Despite the similarities in the valence electronic structure, there is a striking discontinuity in general properties between carbon and silicon, unusual between first and second row elements in the same group. This is followed by a fairly smooth transition from non-metallic to metallic down the group, with germanium in the middle having metalloid character. Some general properties of the elements are given in table 2.1.

Table 2.1: Some general properties of the Group IV elements [30]

Element	Electronic structure	mp (°C)	bp (°C)	Ionisation enthalpies (kJ/mol)				χ	Covalent radius (Å)
				1st	2nd	3rd	4th		
C	[He] $2s^2 2p^2$	>3550	4827	1086	2353	4618	6512	2.50	0.77
Si	[Ne] $3s^2 3p^2$	1410	2355	786	1577	3228	4355	1.74	1.17
Ge	[Ar] $3d^{10} 4s^2 4p^2$	937	2830	760	1537	3301	4410	2.02	1.22
Sn	[Kr] $4d^{10} 5s^2 5p^2$	231.9	2260	708	1411	2942	3928	1.72	1.40
Pb	[Xe] $4f^{14} 5d^{10} 6s^2 6p^2$	327.5	1744	715	1450	3080	4082	1.55	1.44

The strength of single covalent bonds between the Group IV elements and other atoms tends to decrease gradually down the group. It is interesting to note however, that in the case of bonding to a halogen or to oxygen (the more electronegative elements), there is an initial increase in bond energy from C to Si, before a decrease begins from silicon onwards. For bonding to carbon or hydrogen, the decrease already begins at carbon. Also interesting is that the M-H bonds are stronger that the corresponding M-C bonds.

The group IV hydrides (MH_4) are all colourless gases and only monosilane (SiH_4) is of importance in the chemical industry. Chlorination of the group IV elements gives colourless liquids (MCl_4), with the exception of $PbCl_4$, which is a yellow solid. The principle uses of $SiCl_4$ and $GeCl_4$ are in the synthesis of pure silicon and germanium and both $SiCl_4$ and $SnCl_4$ are used in the synthesis of organometallic compounds. The fluorides are also liquids at room temperature, with the exception of SiF_4, which is gaseous.

2.3. The Halogens

Ionic and covalent halides are among the most important and common compounds known to man [43,44]. With the exception of the noble gases He, Ne and Ar all the elements in the periodic table form halides. On the whole they are easy to prepare and are often used as source materials for the synthesis of other compounds. The chemistry of organic halogen compounds is also extensive and varied and fluorine compounds especially have unique properties.

Molecular fluorine is a gas at room temperature and is the most chemically reactive of all the elements. It combines directly with all the elements other than nitrogen, oxygen and the lighter noble gases at normal temperatures, often spontaneously and with extreme vigour. Chlorine is a greenish gas at room temperature, bromine a dense, mobile, dark red liquid and iodine a black solid with a slight metallic luster, which sublimes without melting at normal atmospheric pressure. They all have interesting, unusual and unique properties, which give them great importance in chemistry.

The halogen atoms are only one electron short of the noble gas configuration and therefore readily form X^- anions or single covalent bonds. Halogen chemistry is essentially non-metallic and on the whole the properties of the elements and their compounds change progressively with increasing size. There are however, closer similarities within the group than in any other

group in the periodic table, with the exception of the Group I elements. In many instances fluorine behaves differently to the other halogens and this uniqueness can be attributed mainly to its small size, high electronegativity and consequent high electron density. However, rather than being different, its properties can be seen as being more pronounced than the others of its group, but essentially the same on a basic level.

Due to their reactivity, none of the halogens occur in their atomic state in nature, but exist as non-polar diatomic molecules with intermolecular forces similar to those between noble gas atoms. The trends in melting and boiling points are qualitatively the same for these two groups, the dominant factor being the increasing magnitude of the van der Waals forces as the size and polarisability of the atoms or molecules increases.

2.4. Theories of structure and bonding

2.4.1. The Valence-Shell Electron-Pair Repulsion (VSEPR) Theory

Early attempts to explain the shape of molecules used the directional nature of p and d orbitals to justify the directed valency of the central atom [45]. The direct application of this theory led to difficulties for a number of atoms, particularly carbon, and soon had to be modified to include the concept of hybridization. The concept of hybridization of atomic orbitals was able to fill in many gaps left by earlier theories, but it also had its limitations and fell short for more complex geometries and particularly those where d orbitals are involved in the bonding.

Development of a simple valence theory incorporated the idea that the shape of a molecule could be accounted for in terms of the arrangement of all the electron pairs (bonding and non-bonding) in the valence shell of the central atom, a given number of pairs always having the same arrangement [46]. As the theory developed, the role of lone pairs gained increasing importance, with contributions from Mellish and Linnett [47], Fowles [48] and Gillespie

and Nyholm [49]. Gillespie published a paper in 1963 [50], the purpose of which was to review the recent developments of the valence theory and to show that an understanding of a large number of the structural features of organic molecules can be gained by considering the repulsions between the electron pairs in valence shells, without making any use of the concept of hybrid orbitals. It attempts to give a consistent discussion of molecular shape from the point of view of this theory alone.

The theory proposes that the stereochemistry of an atom is determined primarily by the repulsive interactions between electron pairs in a valence shell. The electrons in the valence shell occupy essentially localized orbitals that are orientated in such a way around the nucleus and completed inner electron shells, as to maximize the average distance between them. In the common case of an atom or ion with space for eight electrons in its valence shell, bonding with other atoms or ions to form a neutral molecules leads to four essentially localized electron pairs in four tetrahedrally directed orbitals around the central atom. These orbitals are equivalent to the sp^3-orbitals of the valence bond theory.

A number of related postulates concerning the interactions between the valence-shell electron-pairs were presented to explain the finer details of molecular shape. Those that are relevant to the present work are listed below.

- The repulsions exerted by bonding electron-pairs decrease with increasing electronegativity of the ligand.

Any ligand attracts the bonding electron-pair to some extent, increasing the directional nature of the orbital and contracting it somewhat. The greater the electronegativity of the ligand, the more contracted the orbital and the nearer to the ligand the average distance of the bonding-pair. The overlap between the bonding orbital and neighboring orbitals, and therefore the repulsion between them, decreases as the electronegativity of the ligand increases.

This causes a decrease in the angle between electronegative substituents and a subsequent increase in the angle between electropositive substituents.

- Repulsions between electron-pairs in filled shells are larger than those between electron-pairs in incompletely filled shells.

Orbitals in a filled primary energy level effectively occupy all the available space surrounding the central atom. Any tendency towards reducing the angle between orbitals in this shell will cause considerable overlap and be strongly resisted. The orbitals in incompletely filled primary shells do not occupy all the available space and are more susceptible to factors that reduce the angle between orbitals, since more distortion of the angles can occur without causing appreciable overlap. Thus for first row elements the angles are always very close to tetrahedral, while for heavier elements that have unfilled d- and f-orbitals, more examples of deviations from idealized tetrahedral geometry are found.

- When an atom with a filled valence-shell and one or more unshared electron-pairs is bonded to an atom with an incomplete valence-shell there is a tendency for the unshared electron-pairs to be transferred from the filled shell to the incomplete shell.

This may be regarded as a means of compensating for the previous effect, namely that the repulsions between electron-pairs in filled shells are larger than those between electron-pairs in incompletely filled shells. Bond lengths in fluorides are often shorter than what one would expect for single bonds due to the delocalization of the unshared electron pairs of fluorine into the incomplete valence-shell of the central atom, giving the bond considerable double-bond character. Because of the consequent size increase in the bonding orbitals, there is more overlap between neighboring orbitals, stronger repulsion and an increase in bond angle. The other halogens have incompletely filled valence shells, there is little tendency for their electron pairs to delocalize and little or no double-bond character.

2.4.2. Bent's Rule

In 1960, Henry Bent [51] published an appraisal of valence-bond structures and hybridization in compounds of the first-row elements. The paper studies the effects of orbital hybridization and electronegative substituents on molecular properties from an empirical point of view. The conclusions drawn from the combination of these two concepts forms the basis of a general rule formulated to describe the effects of electronegative substituents on atom hybridization.

For first-row atoms that satisfy the octet rule, the four valence shell orbitals of the atom, namely the 2s and the three 2p orbitals, are considered to hybridize to form four equivalent orbitals that point to the corners of a regular tetrahedron, form angles of 109.47° with each other and are known as sp^3 hybrid atomic orbitals. It is also possible for the s orbital to hybridize with only two orbitals to form three sp^2 hybrid orbitals or only one to form two sp orbitals, which make angles of 120° and 180° respectively with each other. It is clear that as the s character in two equivalent hybrid atomic orbital increases, so too does the angle between them. The angle between two hybrid atomic orbitals can therefore be seen as an indication of the s content of those orbitals. If the two orbitals in question then bond with other atoms, and assuming as a first approximation that the orbitals point in the direction of the bonding atom, the molecular geometry can provide a good indication of the hybridization of and distribution of the s character in the atomic orbitals of the central atom.

As we have seen, the valence orbitals about an atom in a molecule can be pictured in localized orbitals, of which there are two distinct types. Orbitals occupied by unshared, nonbonding electrons are termed one-centered molecular orbitals and orbitals occupied by bonding or shared electrons, two-centered molecular orbitals. An interesting phenomenon that is observed is that molecules that differ in the number and/or distribution of their

extranuclear protons, but that contain the same total amount of protons, have remarkably similar electronic structures. Molecules related to each other in this manner are termed isoelectronic structures. The shape of a molecule is therefore largely determined by the hybridization of its heavy elements, which is in turn determined by the number of bonds between the heavy atoms, independent of the number of hydrogens in the molecule.

Bent goes on to discuss the effect of hybridization on molecular properties such as electronegativity. Since electronegativity is the measure of the ability of an atom to attract electrons, it follows that the electronegativity of an orbital increases as the energy of the orbital decreases. The electronegativity of an atomic orbital should therefore increase in the order $sp > sp^2 > sp^3$, as the lower energy s character of the valency increases. This view is supported by the fact that non-zero dipole moments are found along bonds between atoms that differ only in their hybridization.

One of the important results of Bent's paper, with regards to the present work, is the role of electronegative substitution on the hybridization of the central atom and therefore the geometry of the molecule. The hybridization of an atom containing only single bonds deviates from the ideal tetrahedral hybridization when there are one or more pairs of unshared electrons on the atom. Since these unshared electrons can be regarded as electrons bonded to atoms of extremely low or zero electronegativity, this leads to the idea that the electronegativity of a bonded atom or group can affect the hybridization and by inference, a number of molecular properties such as bond lengths and bond angles. A simple rule was formulated to describe and predict the effects of electronegative substituents on atom hybridization.

In compounds of the form AX_2 and AX_3 the valence angle X-A-X appears to correlate with the electronegativity of X, the valence angle decreasing as the electronegativity of X increases, in the absence of obvious steric effects. This suggests that, as the electronegativity of X increases, the central atom A diverts increasing amounts of s character to the orbitals occupied by lone-

pair electrons (substituents of zero electronegativity). The unshared electrons also capture an increasing amount of the s-character of the central atom as the electronegativity of the central atom A decreases and the difference in electronegativity between X and A therefore increases. Replacement of X in the structure X-A-Y with an atom more electronegative than X causes the adjacent A-Y bond to become shorter as more s character is directed towards it. It is interesting to note that these changes in geometry are often in the reverse direction from what one would expect on the basis of repulsions between non-bonded atoms.

The effects described here involve the influence of an atom on a bond one atom removed and in this respect the effect of electronegative substituents is similar to the inductive effect found in organic chemistry. The effect can be summarized in the form of this general rule:

"Atomic s character concentrates in orbitals directed towards more electropositive substituents."

For molecules of the type Y_2AX_2, where X and Y are substituents that may differ in electronegativity, and regarding unshared electrons once again as electrons in bonds to substituents of zero electronegativity, the effect on the Y-A-Y and X-A-X angles is summarized as follows:

- If X and Y are identical the four hybrid orbitals are equivalent and the angles will all be 109.47°.
- If X is more electronegative than Y, A will concentrate its s character in those orbitals directed towards Y, thereby diminishing the X-A-X angle below and increasing the Y-A-Y angle above the tetrahedral value of 109.47°.
- If Y is an unshared electron-pair and the electronegativity of X remains fixed, a decrease in the electronegativity of A has the same effect as an increase in the electronegativity of X

2.4.3. The Ligand Close-Packing (LCP) Model

The ionic and covalent models of bonding should be familiar to all chemists. Since their introduction, the covalent model has been the most widely used model for most molecular substances. Traditionally, the ionic model has been used to describe bonding only in substances that are able to conduct electricity in solution or in their molten states and therefore clearly consist of positive and negative ions. For most other molecules the bonding is seen as being predominantly covalent with possibly a degree of ionic character to it. However, there is evidence to support the theory that bonding in many molecules that are traditionally seen as having polar covalent bonds, is in fact better explained by considering them to be ionic and described by the ionic bonding model [52]. Just as the structures of many ionic crystals are determined by the close packing of anions around the central cations, so the bonding in these structures are determined by the packing of anion-like ligands around a cation-like central atom. The predominant interactions that determine the molecular geometry are therefore the interligand repulsions, or non-bonded interactions.

Experimentally determined homonuclear ligand-ligand distances in a large number of fluorides, chlorides, oxides, hydroxides and alkoxides of carbon, boron, beryllium, sulphur and phosphorus are almost constant for a given central atom [52], regardless of the coordination number or the presence of other ligands, and despite large variations in bond lengths and bond angles. A constant intramolecular contact radius that depends only on the central atom can be assigned for each of these ligands and these calculated contact radii are able to accurately predict interligand distances in species with mixed ligands.

Calculation of the atomic charges in these molecules support the view that they are predominantly ionic in nature and therefore better described by the ionic than the covalent model. Ligand charges, although large, are smaller than the full ionic charges and decrease with increasing electronegativity of

the central atom. It is proposed that the close packing of the ligands around the central atom determines the bond lengths and bond angles in these molecules and that the radius of the ligand is determined by its charge. This model is known as the Ligand Close-packing (LCP) model and it provides simpler explanations for the bond lengths and bond angles in many compounds traditionally seen as being covalent.

In a range of 3- and 4-coordinated fluorides of beryllium, boron and carbon for example, the F-F non-bonded distances remain almost constant for a given central atom, although there is great variation in the A-F bond lengths and F-A-F bond angles. The radii of the fluorine ligands are smaller than the radius of the fluorine ion and decrease as the electronegativity of the atom A increases, decreasing the charge on the fluorine. The LCP model provides a viable alternative to the frequently quoted π back-bonding explanation for the decrease in A-F bond lengths with increasing coordination number. The results for the chlorides and chlorofluorides of boron and carbon are in agreement with those for the fluorides.

The electronegativity difference between two atoms is often seen as a rough indication of the degree of ionic character in the bond between them. Yet the bonding in many compounds with large electronegativity differences between the atoms is still regarded as covalent on the basis of the type of atoms in the molecule. The polar nature of the bonds is indicated by the addition of $\delta+$ or $\delta-$ signs to the atoms, but these partial charges are regarded as small, implying that the bonds are covalent and have the directional properties of covalent bonds. However, despite the fact that a characteristic property of covalent bonding is its directional nature, a molecular geometry consistent with that predicted by the covalent bonding model does not necessarily imply covalent bonding. Close packing of anions around a central cation with an empty valence shell leads to the same molecular geometries predicted by the VSEPR model for covalent structures. No conclusions as to the nature of the bonding in these molecules should be made on the basis of the observed geometry alone.

Although electronegativity is a useful indication of the ionic nature of bonds, it is a qualitative one, as is the concept of electronegativity at this stage. To obtain meaningful quantitative information concerning bond polarity it is necessary to assign charges to atoms in molecules, which has only become possible on a large scale with the advent of *ab initio* calculations. The atomic charges in this review were calculated from the electron density distribution of the molecules using the Atoms in Molecules (AIM) Theory [53].

A comparison can be drawn between the VSEPR model of covalent bonding and the LCP model of ionic bonding. Where the VSEPR model is based on the assumption that the interaction between non-bonding and bonding electron pairs in the valence shell of the central atom is the major determining factor of molecular geometry, the LCP model assumes that it is the interaction between the ligands that determines the molecular geometry. For molecules of the form AX_n this difference is arbitrary and both models lead to the same geometries. In a few cases however, the LCP model succeeds in explaining geometries that the VSEPR model cannot. The VSEPR model, for instance, fails to explain the regular octahedral geometries of many AX_6E molecules. These molecules are usually said to have a stereochemically inactive lone pair and are often cited as exceptions to the theory. The LCP model on the other hand, is successfully able to account for this geometry. Also, 5- and 6-coordinated molecules of main group non-metals are often described as being hypervalent because they are exceptions to the octet rule of covalent bonding. However, these molecules invariably have very electronegative ligands for which the ionic model is particularly appropriate and successful.

2.5. An Overview of Computational Chemistry

2.5.1. Introduction

Computational chemistry has gained increasing importance as a means of gaining information on the structure and properties of both known and unknown compounds [54-60]. Used correctly and in combination with other experimental methods, it can be an extremely powerful tool. Since this work is largely computational in nature and since it is a field that is unfamiliar to many chemists in other fields, a general overview of the available and most commonly used computational methods is included here.

The basis of computational chemistry is the assumption that all molecular properties are related to the molecular structure [54]. It should therefore be possible to calculate the properties from the structure and vice versa, provided an algorithm can be developed which is able to calculate the structure from a given stoichiometry. In order to conduct a computational study of the properties of molecules, a molecular model must be established. This can be done experimentally or using a computational method such as quantum mechanics or molecular mechanics.

Since computational chemistry relies on the use of an acceptable model of the physical world [55], it is necessary that this physical model meet certain requirements in order to be a successful one. Firstly, it must be possible to calculate the energy of the system as a function of the atomic coordinates. Secondly, one must be able to calculate the change in energy of the system as a function of the change in position, or coordinates, of the atoms. It is assumed that the chemistry of the system is related to the energy of a specific geometry and the physical and chemical properties of the molecule to the change in energy [55, 56].

There are three main approaches in Computational Chemistry, namely electronic structure or *ab initio* methods, semi-empirical methods and empirical force field or molecular mechanical methods.

2.5.2. Quantum mechanical or *Ab initio* Methods

Ab initio molecular orbital theory uses the fundamental laws of quantum mechanics to predict the structure and properties of atomic and molecular systems [57]. The basis of all quantum mechanical calculations used in Computational Chemistry is the time-independent Schrödinger equation:

$$\left\{\frac{-h^2}{8\pi^2 m}\nabla^2 + V\right\}\Psi(\vec{r}) = E\Psi(\vec{r})$$

Ψ is the wavefunction of the particle, m its mass, h is Planck's constant, V is the potential field in which the particle is moving, E is the energy of the particle and the expression in parentheses is the Hamiltonian operator $\vec{H}$. This equation describes the wavefunction of a particle, but the Schrödinger equation for a collection of particles is similar, the only difference being that Ψ is a function of the coordinates of all the particles in the system.

The solutions to the Schrödinger equation correspond to different stationary states of the system of particles or molecule and the one with lowest energy is the ground state of the molecule. The starting point of any *ab initio* study is the calculation of the electronic wavefunction of this ground state and its associated energy. However, since it is impossible to find an exact solution to the Schrödinger equation for any system containing more than two particles, *ab initio* methods make use of a variety of mathematical transformations and approximation techniques to solve the fundamental equations [57].

The most basic of these approximations, and one that is frequently used, is the Born-Oppenheimer approximation, which separates the nuclear and

electronic motions. The full Hamiltonian for a molecular system consists of both kinetic and potential energy terms for the nuclei and all their electrons. In the Born-Oppenheimer approximation, an electronic Hamiltonian is constructed which neglects the kinetic energy term for the nucleus. This Hamiltonian is then used in the Schrödinger equation describing the motion of electrons in a field of stationary nuclei. Solving this equation yields an effective nuclear potential energy term, which is dependent on the nuclear coordinates and describes the potential energy surface for the system. This term is in turn used as the effective potential in the Schrödinger equation for the nuclear motion, which is able to predict the energy states of the nuclei. The Born-Oppenheimer approximation usually yields good results, since the neglect of nuclear-electron coupling is a minor problem in comparison to other errors [56].

Methods aimed at solving the electronic Schrödinger equation and finding the potential energy surface for a molecule are broadly referred to as electronic structure calculations. The simplest and least computationally intensive of these methods is known as Hartree-Fock (HF) theory. Since Ψ^2 is interpreted as the probability density of the particle described by Ψ, it is required that Ψ be normalized and antisymmetric. In molecular orbital theory the wavefunction Ψ is decomposed into a combination of normalized, orthogonal molecular orbitals (ϕ_1, ϕ_2, ..., ϕ_n) and the simplest way of doing this is by forming their Hartree product:

$$\Psi(\vec{r}) = \phi_1(\vec{r})\,\phi_2(\vec{r})\ldots\phi_n(\vec{r})$$

However, the Hartree product does not account for the antisymmetry of the wavefunction and is therefore inadequate. Furthermore, it does not allow for the two possible spin states of the electrons in these orbitals. To rectify this, two spin functions α and β are defined. The product of the molecular orbital function and either α or β is known as a spin orbital and is a function of both the location and spin of the electrons. In this way the electron spin is

included in the overall electronic wave function and the component spin orbitals are both orthonormal and antisymmetric.

A closed shell wavefunction is then built by defining n/2 molecular orbitals for a system with n electrons and assigning electrons to these orbitals in pairs of opposite spin. The mathematic form of the wavefunction is that of a determinant, in which each row represents all possible assignments of an electron *i* to all orbital-spin combinations. This determinant therefore mixes all of the possible orbitals of all the electrons in the molecular system to form the wavefunction.

A further approximation used by Hartree-Fock theory involves expressing the molecular orbitals as linear combinations of a pre-defined set of one-electron functions known as basis functions. These basis functions are usually centered on the atomic nuclei and bear some resemblance to atomic orbitals, but this need not be the case and any set of appropriately defined functions may be used. An individual molecular orbital is defined as:

$$\phi_i = \sum_{\mu=1}^{N} c_{\mu i} \chi_\mu$$

The coefficients $c_{\mu i}$ are known as molecular orbital expansion coefficients and the basis functions χ_μ are chosen so that they are normalized.

Gaussian and other *ab initio* electronic structure programs make use of gaussian-type atomic functions, which have the general form:

$$g(\alpha, x, y, z) = c x^n y^m z^l \exp\left(-\alpha r^2\right)$$

The constant α determines the radial extent of the function and c is a normalization constant, which is dependent on α, l, m and n and chosen so that the integral of g^2 over all space is one.

The actual basis functions, known as contracted gaussians, are linear combinations of these primitive gaussians and have the general form:

$$\chi_\mu = \sum_p d_{\mu p} g_p$$

The constants $d_{\mu p}$ are fixed within a given basis set and it is also common practice to normalize the contracted functions. A large number of basis sets are available and they differ from each other in the number and type of basis functions they contain. The choice of basis set can have a large influence on the results and care must be taken in choosing an appropriate basis set.

The problem then becomes one of solving for the set of molecular orbital expansion coefficients $c_{\mu i}$, and HF theory does this using the variational principle [57,58]. The variational principle states that for the ground state of any antisymmetric normalized function of the electronic coordinates, the expectation value for the energy corresponding to this state will always be greater than the energy for the exact wavefunction. The energy of the exact wavefunction is therefore the lower limit of the energies of all the other normalized antisymmetric functions.

The equations describing the molecular orbital expansion coefficients that arise through use of the variational principle are known as the Roothaan-Hall equations. They are non-linear matrix equations and must therefore be solved iteratively. At convergence the energy is a minimum and further iterations will produce the same average electron field and set of orbital coefficients. The method is therefore known as the Self-Consistent Field (SCF) method. A set of both occupied and virtual orbitals is produced, the total number of which is equal to the number of basis functions used.

In Hartree-Fock theory, each electron sees all of the other electrons as an average distribution and no instantaneous electron-electron interaction is

included. Although major correlation effects arising from pairs of electrons with the same spin, known as exchange correlation, are implicitly included in the requirement that the wavefunction be antisymmetric, the motion of electrons of opposite spin remains uncorrelated. Higher levels of theory attempt to remedy this neglect of electron correlation in various ways. Any method that goes beyond SCF in treating this phenomenon is known as an electron-correlation, or post-SCF method [57].

Møller-Plesset perturbation theory for example, adds higher excitations to Hartree-Fock theory as a non-iterative correction. Perturbation theory is based upon dividing the Hamiltonian into two parts:

$$H = H_0 + \lambda V$$

H_0 is soluble exactly and in Møller-Plesset perturbation theory is defined as the sum of one-electron Fock operators of Hartree-Fock theory. λV is a perturbation applied to H_0, which is assumed to be small in comparison to it. The assumption that V is a small perturbation to H_0 allows the perturbed wavefunction and energy to be expressed as a power series in V, which is usually done in terms of the parameter λ. The perturbed wavefunction and energy are then substituted back into the Schrödinger equation. Expansion of the products and the equation of the coefficients on each side of the equation for each power of λ, yields a series of relationships representing successively higher orders of perturbation.

Substitutions close to the ground state make larger contributions to the perturbation and the stronger the mixing between a state and the ground state, the larger too its contribution to the perturbation. It can also be shown that the value of the first perturbation to the Hartree-Fock energy is always negative, although higher order corrections may be positive. A reasonably accurate result can therefore be obtained without having to consider many perturbations. MP2 theory, for example, calculates only the second order perturbation, MP3 the second and third order perturbations and so forth.

Density Functional Theory, although also an *ab initio* method, uses electron density rather than the electronic wavefunction to calculate the energy of a system. It is based on the Hohenberg-Kohn theorem, which demonstrates the existence of a unique functional able to calculate both the ground-state electronic energy and the electron density exactly [56,57]. The fact that there exists a one-to-one correspondence between these two properties means that the energy can be determined solely by the electron density. The exact form of this functional is not known and the goal of DFT methods is therefore to design functionals that relate the energy to the electron density. In practice, DFT calculations are performed in an iterative manner, analogous to an SCF computation.

2.5.3. Molecular Mechanics or Force Field Methods

Molecular mechanics can be considered to arise from the Born-Oppenheimer approximation [54], namely that the motions of the nuclei of a molecule are independent of the motions of the electrons. In molecular mechanics (MM) the arrangement of the electrons are assumed to be fixed relative to the nuclei and the positions of the nuclei are calculated.

The basis of all molecular mechanics calculations is that a good estimate of the geometry of a molecule can be obtained by taking into account all the forces between the atoms, calculated using a classical mechanics approach. To optimize the geometry of a molecule, the total energy that arises from these force, or stresses, is minimized by computational methods. The minimized energy is an indication of the strain in the molecule and is related to its potential energy and stability, since it is a measure of how much the individual parameters in the molecule deviate from their ideal value.

The parameters that define the forces present are derived, in first instance, from experimental observables such as infrared vibrational frequencies and then modified empirically to enhance the reproduction of experimentally

determined geometries and other properties. Because the parameters used to derive the strain energies from these functions are fitted quantities, which are based on experimental data, molecular mechanics is sometimes referred to as empirical force field calculations.

The quality of the calculations is strongly dependent on the reliability of the potential energy functions and the corresponding parameters that make up the force field. The selection of experimental data used to optimize the force field parameters, is therefore one of the most important steps in a MM study. An empirical force field calculation is essentially a method whereby the structure and strain energy of an unknown molecule are interpolated from a series of similar molecules with known structures and properties.

There are two types of force fields, those that are explicitly parameterized to study a specific group of compounds and generic force fields, which are more general and are parameterized for a larger range of atom types. Individual force fields differ from each other in the number and type of interactions, as well as the atom types for which they are parameterized. Atom types depend, not only on the atomic number, but also on the type of chemical bonding the atom is involved in.

In a conventional force field, each interaction is explicitly defined for each possible combination of atom types. The number of constant parameters required to define a function describing the interaction is proportional to the number of atom types directly involved in the interaction. The total number of constants required to define a particular type of interaction is thus proportional to N^m, where N is the total number of atom types and m is the number of atom types involved in the interaction. The grand total of all the parameters needed to describe the force field as a whole, is therefore equal to the sum of all the above N^m terms and this can be quite a large number, depending on the number of interactions defined for the force field.

Generic force fields offer an alternative to the large number of constants and experimental parameters required to describe a traditional force field. The parameters that enter into the equations describing the different interactions in generic force field are calculated from constant atomic properties rather than taken from experimental values [55]. This reduces the number of parameters required to define the force field to being linearly proportional to the number of atom types N.

For routine applications of molecular modeling, generic force fields are ideal, since they produce results for any combination of elements and can therefore be applied to a wide range of compounds. However, along with this general applicability comes the disadvantage that they do not give results as accurate as explicitly parameterized force fields. Where they work well for conventional textbook geometries, they often fail to accurately describe compounds with interesting and unusual properties. Specifically, since the parameters are calculated from the atom types, generic force fields are unable to account for geometries where the influence of substituents not directly involved in an interaction plays a significant role in determining the geometry.

The first generic force field was aptly named the Universal Force Field (UFF). This force field suffers from a number of inherent deficiencies, one of which is that the bond angles are based on an ideal hybridization of the central atom and are thus very approximate [55]. The Valence Bonding Force Field (VALBOND) improves on the description of bond angles by using the concept of hybridization. However, VALBOND uses bond parameters rather than atomic parameters and is therefore not strictly generic, since the number of parameters is proportional to N^2 rather than N. The force field Dreiding reduces the number of parameters required by not considering hydrogens explicitly, but incorporating them into other atom types by increasing the van der Waals radius of the other atom.

2.5.4. Semi-empirical Methods

A semi-empirical calculation is one that makes use of quantum mechanical methods for the calculation of the potential energy surface, but relies partly on experimental data for calibration [58]. It is basically a mixture of the previous two techniques and in it a compromise between the accuracy of the *ab initio* methods and the speed of the force field methods is reached. As it is a technique that is not used in the present work and a summary can be found in most textbooks on Computational Chemistry, no further details will be discussed here.

2.5.5. Quantum Mechanics vs. Molecular Mechanics

The differences between quantum mechanics and molecular mechanics arise largely due to the fact that Quantum Mechanics is based on first principles, whereas Molecular Mechanics incorporates chemical ideas in an empirical way. In terms of usefulness neither method is better that the other, rather they are complementary methods and the choice of which one to use is based on the requirements of the problem at hand rather than the validity of the method.

In QM, atoms are considered to consist of nuclei and electrons, the latter being described by orbital wave functions that overlap and interact. The difference in properties of the same atom in different chemical environments is a result of the interactions of the wave functions of that atom with those of surrounding atoms or groups. In MM, atoms are differentiated based on chemical knowledge and the same atom in different chemical environments is treated as a separate atom type with its own unique properties.

Whereas in MM, the positions of the nuclei are calculated by assuming that the arrangement of the electrons is fixed, in QM, the electronic states are calculated by assuming the nuclei to be in fixed positions. MM also assumes

the concept of a chemical bond and connectivity between atoms has to be specified, whereas in QM the existence of a bond is the result of calculation.

In QM, the only interaction that is considered between the particles is the electrostatic interaction. In MM, the interactions are differentiated at a much higher level. Bonding interactions, angle interactions, torsion interactions and any number of others are defined based on what is previously known about the system or similar systems. The number and type of interactions is varied according to the size and properties of the molecule or system.

In MM, all of these interactions contribute to the total energy of the system and physical properties such as bond length are related to the energy by means of a mathematical formula. The total energy of the system is obtained by a summation of all the energy contributions due to all the different interactions. These formulas need not have any theoretical basis and are mostly fitted empirically to experimental data. Often the potential energy functions are similar to functions used to analyze vibrational spectra for example. This is in strong contrast to QM, where the energy of a system is calculated from the approximate solution of the Schrödinger equation and therefore has a theoretical basis.

2.6. Computational Studies

2.6.1. Ab initio Calculations

George Vacek, Vladimir Mastryukov and Henry Schaefer undertook an *ab initio* investigation of Me_2SiF_2, Me_2SiCl_2, Me_2GeF_2 and Me_2GeCl_2 to examine the deviations from idealized tetrahedral geometry [17]. Basis sets of the double-ζ (DZ) quality and DZ with the addition of a set of d-type functions on all the heavy atoms (DZd) were used in conjunction with the Hartree-Fock (HF) self-consistent field method and the single and double excitation configuration interaction method. The geometry optimizations were done

under C_{2v} symmetry constraints and the individual methyl groups have C_s symmetry. The predictions of molecular geometry corroborated the electron diffraction results to the extent that all four molecules have C-A-C bond angles significantly larger than 109.47°, but the calculated values were smaller than those concluded by ED and this calls into question some of the experimental values. At the DZd/CISD level of theory, C-A-C bond angles of 115.9°, 114.3°, 120.9° and 117.6° were found for the molecules Me_2SiF_2, Me_2SiCl_2, Me_2GeF_2 and Me_2GeCl_2 respectively. In addition to the optimized geometries, the calculated rotational constants, dipole moments, harmonic vibrational frequencies and IR intensities were also given.

V. Jonas, C. Boehme and G. Frenking investigated the structure of a number of transition metal compounds in terms of Bent's rule [18]. The equilibrium geometries of Me_2ACl_2 for A=C, Si, Ge, Sn, Pb, Ti, Zr and Hf were calculated at HF and MP2 levels of theory using a 6-31G(d) basis set for H, C, Si and Cl, an effective core potential (ECP) with a (31/31/1) valence basis set for Ge, Sn and Pb, and an ECP with a (441/2111/N1) valence basis set for Ti, Zr and Hf (N=4 for T, 3 for Zr and 2 for Hf). Results of the calculations show that the Cl-A-Cl angle for A=C, Si, Ge, Sn, Pb is always smaller than the C-A-C angle, which is in agreement with experimental data, previous calculations and Bent's rule. The calculations also show that the Cl-A-Cl angle decreases and the C-A-C angle increases continuously from A=C to A=Pb and that the angles calculated at HF and MP2 levels of theory do not differ significantly from each other.

For the transition metal compounds the trend is exactly the opposite, with the calculated Cl-A-Cl angle being significantly larger than the C-A-C angle for A=Ti, Zr and Hf. The difference in the Cl-A-Cl and C-A-C angles between the main group and transition metal compounds was explained in terms of the energy levels of the orbitals involved in the hybridization of the central atom. The transition metals have mainly sd^n-hybridized bonds while the main group elements have sp^n-hybridized bonds and while the valence s orbital of a main group elements is energetically always below the valence p

orbitals, the valence s orbital of a transition metal is above the valence d orbital. On the basis of the trends in the Cl-A-Cl and C-A-C angles, the relative energies of the atomic orbitals and the hybridization of the central atoms, Bent's rule [51], which states that *"Atomic s character concentrates in the orbitals directed toward electropositive substituents"* was reformulated more generally to *"The energetically lower lying valence orbital concentrates in bonds directed towards electropositive substituents"*. Later computational studies on other transition metal compounds however, have given results which are in contradiction with this general form of Bent's rule and Frenking himself has said that the theory is incorrect [61].

In an earlier ab initio study by Jonas, Frenking and Reetz [19] a total of 25 species with general formula Me_nACl_{4-n}, where A is a group IV element, were investigated. However, the focus of the study was different and they did not address the issue of the C-A-C bond angles. Only the C-A-Cl angles, which are almost always close to the tetrahedral value, were reported and the C-A-C angles cannot be determined from the given information.

Quasirelativistic *ab initio* model potential calculations on group IV hydrides (XH_2, XH_4; X=Si, Ge, Sn, Pb) and oxides (XO; X=Ge, Sn, Pb) were performed by Zoila Barandiaran and Luis Seijo [62] and a systematic comparison was made between the values of the bond lengths, bond angles and vibrational frequencies for these three groups.

An *ab initio* study has been conducted to try to explain the destabilization of inorganic and organolead compounds by electronegative substituents [20]. Inorganic Pb(IV) compounds are mostly either unknown, unstable transient species or highly reactive. In contrast, organic lead compounds such as R_4Pb, where R is an alkyl or aryl group, are relatively stable in comparison with the corresponding divalent species. The stability of mixed species of the form R_nPbX_{4-n}, where X is an electronegative substituent, decreases with decreasing n, so that monohalogenated and dihalogenated compounds are known, but the trihalogenated species are uncommon.

The study showed that all the unsymmetrically substituted tetravalent species (n=1-3) deviate substantially from the idealized tetrahedral geometries. This is particularly notable in the methyl fluoride series, the results of which are summarized in table 2.2. The C-Pb-C angles are considerably larger than 109.47°, whereas the C-Pb-X and particularly the X-Pb-X with X=F angles are smaller. In the dihalogenated species Me_2PbF_2, the C-Pb-C angle is 134.8°, while the F-Pb-F angle is only 101.4°.

Table 2.2: HF structural parameters of for Me_nPbF_{4-n} (n=0-4) [26]

Molecule	Pb-C	Pb-X	C-Pb-C	C-Pb-X	X-Pb-X
Me_4Pb	2.248	-	109.5	-	-
Me_3PbF	2.227	2.045	116.4	101.1	-
Me_2PbF_2	2.202	2.010	134.8	104.1	101.4
$MePbF_3$	2.198	1.964	-	115.5	102.8
PbF_4	-	1.924	-	-	109.5

The study also develops a general bonding model for lead compounds to explain this destabilization with increasing electronegative substitution. The concept of sp^n hybridization is modified to accommodate heavier main group elements by removing the restriction of orthogonal hybrids. Valence p-orbitals are in general significantly larger than the corresponding s-orbitals, except in first-row compounds and particularly carbon. The relative p-orbital contribution to covalent bonding in compounds of heavier main group elements is therefore smaller than expected from symmetry considerations and orthogonal hybrids, resulting in smaller sp^n ratios. The direction of the deviations of the bond angles in the unsymmetrically substituted species R_nPb_{4-n} (n=1-3) from the tetrahedral is attributed to Bent's isovalent rehybridization rule.

2.6.2. Semi-empirical Calculations

A series of semi-empirical molecular orbital calculations of the infrared band intensities of some simple polyatomic molecules have been performed. A number of the halogenated methanes, silanes and germanes were included in these studies [63-65].

In one study by J. Bunnell, B. C. Crafford and T. A. Ford [63], theoretically computed dipole moment derivatives were used to calculate the infrared band intensities of CH_3F, CH_3Cl, CH_2F_2, CH_2Cl_2, CHF_3 and $SiHCl_3$, for comparison with experimental values, and of SiH_3F, SiH_3Cl and $SiHF_3$, for which no experimental data existed at the time. The complete neglect of differential overlap (mark II) (CNDO/2) parameterization was used for these dipole moment derivative calculations. For CH_3F, CH_2F_2 and CHF_3 the calculations were performed at INDO level and for the remaining molecules at the CNDO level. The L matrices of SiH_2F_2 and SiH_2Cl_2 were not available at the time and the calculated dipole moments could not be transformed into band intensities.

J. Bunnel and T. A. Ford [64] augmented these calculations to include the brominated methanes and silanes at the CNDO level. The infrared band intensities, equilibrium dipole moments and molecular geometries of the molecules CH_3Br, CH_2Br_2, $CHBr_3$, SiH_3Br and $SiHBr_3$ were calculated. The molecular geometry of SiH_2Br_2 was not accurately known at the time and was therefore omitted from the study. The band intensities of SiH_2F_2 and SiH_2Cl_2 were also calculated from the previously determined dipole moment derivatives [63] and force fields that had not previously been available.

The calculation of the infrared band intensities of fluoro-, chloro- and bromogermane, dichloro-, dibromo- and trichlorogermane, by J. Bunnell and T. A. Ford [65], completed the series of semi-empirical calculations on the halogenated methanes, silanes and germanes of C_{3v} and C_{2v} symmetry. No reliable molecular structures were available for difluoro-, trifluoro- or

tribromogermane or any of the iodated compounds and they were therefore excluded. The calculations were compared to those previously performed on the halogenated methanes and silanes, in an attempt to establish any periodic trends in the band intensities. The conclusion that was reached was that trends exist only for some normal modes, or only for limited groups of molecules.

In each of the studies the band intensities, dipole moments, bond lengths and bond angles were compared with such experimental results as were available at the time. In the case of the band intensities, the authors acknowledged that the CNDO/2 methods used were capable of reproducing experimental values to within an order of magnitude at best. Their justification for the calculations lay in the fact that they were examining trends rather than absolute values and they felt these to be correctly reproduced. The use of *ab initio* rather than semi-empirical methods was considered, but at the time of publication of these studies the basis sets for heavier elements such as Br and Ge were not yet well established and the computational labour involved would have been extensive.

The dipole moments were mostly found to be considerably overestimated or underestimated, depending on the central atom, the type of halogen and the number of halogen atoms attached to the central atom. On the whole, the agreement between calculation and experiment is therefore not very good. The calculated molecular geometries are in better agreement with the experimental values than the dipole moments. Certain parameters are also systematically under- or overestimated but for others the agreement is very good. However, the Cl-A-Cl and Br-A-Br angles in many of the molecules were grossly underestimated and this is attributed to the basis set used in the CNDO/2 parameterization.

Thus, although the studies may have been of value at the time, they cannot be compared in quality to the results that can be achieved with *ab initio* methods today. Furthermore, the focus was on the vibrational behavior of

the molecules rather than their geometries and only the simple halogenated methanes, silanes and germanes were considered. None of the methylated compounds, which are the focus of the present study, were considered or included in the calculations.

2.6.3. Force Field Calculations

Within the Cerius2 software package [66], there are three generic force fields that are parameterized for all the atoms in the range of molecules being studied in the present work, namely the Dreiding [21], Universal [22] and Valence Bonding [23] Force Fields. The optimized heavy atom geometric parameters for the molecules Me_2AX_2, with A=C, Si, Ge and X=H, F, Cl, Br and I, calculated with these three force fields using Cerius2, are shown in tables 2.3. to 2.5. Both UFF and Dreiding clearly use an idealized tetrahedral bonding model to calculate the valence angles and even VALBOND, although improving on the previous two, fails to reproduce the large C-A-C angles seen experimentally in the dihalo(dimethyl)germanes.

Vibrational force fields have been determined for some molecules of the form AH_nX_{4-n}, where n=1-3, A=C, Si, Ge and X=F, Cl, Br. These force fields are mostly parameterized for small groups of molecules only and attempt to reproduce experimentally determined vibrational data rather than structures.

R. Aroca, E. A. Robinson and T. A. Ford [36] obtained force constants and compliance constants for the trihalomethanes and trihalosilanes, using the vibrational frequencies of CHX_3, CDX_3, $SiHX_3$ and $SiDX_3$. Force fields were obtained separately for the two groups of molecules. The force constants and compliance constants were closely related and showed self-consistency of the final results. Moreover, the force fields reproduced the frequencies with an error of less than 0.6% gave reasonable values for the Coriolis coupling constants, centrifugal distortion constants and mean amplitudes of vibration.

Table 2.3. Selected Dreiding 2.21 geometric parameters for Me_2AX_2

A	C				Si				Ge			
X	CAC	XAX	AC	AX	CAC	XAX	AC	AX	CAC	XAX	AC	AX
H	112.9	108.1	1.545	1.930	110.9	109.0	1.701	1.258	109.5	109.5	1.970	1.530
F	112.4	107.5	1.548	1.377	110.7	108.8	1.702	1.539	109.5	109.5	1.970	1.811
Cl	111.8	106.8	1.550	1.765	110.5	108.6	1.703	1.926	109.6	109.5	1.970	2.197
Br	112.3	107.4	1.546	1.933	110.7	108.8	1.702	2.095	109.6	109.5	1.970	2.367
I	112.4	107.5	1.545	2.125	110.8	108.9	1.701	2.288	109.6	109.5	1.970	2.560

Table 2.4. Selected UFF 1.02 geometric parameters for Me_2AX_2

A	C				Si				Ge			
X	CAC	XAX	AC	AX	CAC	XAX	AC	AX	CAC	XAX	AC	AX
H	111.3	108.4	1.526	1.111	109.5	109.6	1.866	1.470	109.3	109.7	1.944	1.550
F	111.0	108.8	1.527	1.384	109.5	109.5	1.867	1.686	109.3	109.5	1.944	1.756
Cl	110.8	108.5	1.529	1.785	109.5	109.5	1.867	2.094	109.4	109.6	1.944	2.165
Br	110.8	108.4	1.529	1.942	109.5	109.5	1.867	2.255	109.4	109.6	1.944	2.327
I	110.9	108.2	1.528	2.142	109.5	109.5	1.866	2.463	109.4	109.6	1.944	2.536

Table 2.5. Selected VALBOND 1.01 geometric parameters for Me_2AX_2

A	C				Si				Ge			
X	CAC	XAX	AC	AX	CAC	XAX	AC	AX	CAC	XAX	AC	AX
H	112.9	107.6	1.524	1.111	110.8	108.2	1.866	1.470	110.5	108.4	1.944	1.550
F	111.8	108.7	1.526	1.384	114.3	105.2	1.866	1.686	111.4	107.6	1.944	1.756
Cl	111.0	108.5	1.529	1.785	111.8	107.3	1.866	2.093	110.1	108.9	1.944	2.165
Br	110.2	109.6	1.529	1.941	110.5	108.5	1.866	2.255	110.0	109.0	1.944	2.327
I	109.9	110.0	1.529	2.142	110.4	108.7	1.866	2.462	110.0	109.0	1.944	2.536

In a continuation of the series by the same authors [37], the vibrational constants of the dihalomethanes were determined by means of normal coordinate calculations.

In another study, J. Bunnell and T. A. Ford [38] determined the molecular vibrational constants of difluoro- and dichlorosilane, dichloro- and dibromo-germane and trichlorogermane. These were the only members of the series AH_2X_2 and AHX_3 for which molecular geometries had been published and which accurate force field determinations could therefore be made. The force constants were used to calculate centrifugal distortion constants, Coriolis coupling constants and mean amplitudes of vibration and these were then discussed in relation to previously published data on other molecules of the form AH_nX_{4-n}.

The reliability of the force fields computed for the dihalomethanes, -silanes and -germanes was tested by calculating the fundamental vibrational wavenumbers of seven molecules of the type $MHDX_2$ from those of the series AH_2X_2 and AD_2X_2 [39]. The potential energy distributions calculated for the $AHDX_2$ series were used to clarify the assignments of the vibrational spectra of the AH_2X_2 and AD_2X_2 molecules.

Mercau et. al. [40] extended the above force field calculations to include the AH_3X molecules, where A=C, Si, Ge and X=F, Cl, Br and I. Once again the force constants and compliance constants obtained were used to calculate the centrifugal distortion constants, Coriolis coupling constants and mean amplitudes of vibration. These were compared to available experimental data and were furthermore shown to be self-consistent with the AHX_3 and AH_2X_2 force fields.

Previous vibrational force fields developed for the molecules AH_nX_{4-n} only calculated the symmetry force constants. Aron et. al. reported the valence force constants and compliance constants of 26 halogenated methanes, silanes and germanes of C_{3v} and C_{2v} symmetry [41], calculated using the

previously reported symmetry force constants [36-40]. The study was carried out mainly to ascertain the effect of changing the atoms A and X on the vibrational properties of these molecules and it was for this reason that the valence rather than the symmetry constants were determined. Symmetry constants are subject to initial choices of symmetry coordinates, while the valence coordinates are intrinsic molecular properties and not constrained to arbitrary choices in their computation. Correlations were noted between the primary force constants and the nature of the atoms A and X, as well as with the number of attached halogen atoms. Relationships were also found between the bond lengths and bond strengths and the force and compliance constants.

J. S. Weaving and T. A. Ford [42] examined the intramolecular coupling of vibrational modes and assignments of the partially deuterated methyl, silyl and germyl halides. The fundamental vibrational wavenumbers of AH_2DX and AHD_2X were determined by transferring the force fields developed with the experimental wavenumbers of AH_3X and AD_3X (A=C, Si, Ge and X=F, Cl, Br and I). The normalized potential energy distributions determined as part of the force field transfer process were interpreted as an indication of the extent of intramolecular coupling between vibrational modes and served also to clarify some of the assignments made previously for AH_3X and AD_3X.

2.7. Structural Studies

2.7.1. Electron Diffraction Studies

As part of an investigation into the molecular structures of halo(methyl)-germanes of the type Me_nGeX_{4-n} with X=F, Cl, Br or I, the structures of difluoro(dimethyl)germane and trifluoro(methyl)germane [11] , as well as their chlorine [12] and bromine [13] analogs were determined by vapour phase electron diffraction. Specifically the variations and trends in bond lengths and valence angles were investigated. The general findings where that both the Ge-C and the Ge-X bond lengths decrease with increasing

halogen substitution and that the angles decrease in the order C-Ge-C (Me_2GeX_2) > C-Ge-F ($MeGeX_3$) > C-Ge-F (Me_2GeX_2) > F-Ge-F ($MeGeX_3$) > F-Ge-F (Me_2GeX_2). In all the dihalo(dimethyl)germanes the C-Ge-C angle is considerable larger than the other valence angles and deviates significantly from the normal tetrahedral angle. Some of the more important structural parameters are reported in table 2.6.

Table 2.6: Structural parameters of some organogermanes

Molecule	Parameters								
	C-Ge	Ge-H	Ge-X	H-C-Ge	C-Ge-C	C-Ge-X	H-Ge-H	H-Ge-X	X-Ge-X
H_2GeCl_2 [21]	-	1.56	2.130	-	-	-	-	106.4	107.2
H_2GeBr_2 [21]	-	1.52	2.277	-	-	-	-	109.0	108.4
Me_4Ge [22]	1.945	-	-	108.2	109.5	-	-	-	-
Me_2GeF_2 [18]	1.928	-	1.739	111.5	121.0	107.3	-	-	105.4
$MeGeF_3$ [18]	1.904	-	1.714	116.0	-	113.2	-	-	105.5
Me_2GeCl_2 [19]	1.928	-	2.143	110.5	121	108	-	-	105
$MeGeCl_3$ [19]	1.893	-	2.132	110.5	-	112.3	-	-	106.4
Me_2GeBr_2 [20]	1.911	-	2.303	109.5	124	107	-	-	104
$MeGeBr_3$ [20]	1.889	-	2.276	109.5	-	111.6	-	-	104
$MeGeH_3$ [13]	1.9453	1.529	-	-	-	-	109.3	-	-
Me_2GeH_2 [14]	1.950	-	-	-	110.0	-	-	-	-
$MeGeCl_3$ [17]	-	-	2.135	-	-	106.0	-	-	-
Me_3GeCl [16]	1.939	-	2.169	-	112.8	105.89	-	-	-
Me_3GeBr [15]	1.94	-	2.323	-	112.4	106.3	-	-	-

The structural trends are basically the same for F, Cl and Br and seem to depend only on the number of halogen atoms attached to the central atom and not on the species of halogen atom involved. The major changes in geometry correlate strongly to changes in the charge distribution of the molecules and also the polarity of the bonds. For the fluoro(methyl)germanes

a linear increase in both the Ge-C and Ge-F bond lengths is observed as the bond polarity increases. Similar trends are found for Si-F and C-F bonds in analogous carbon and silicon compounds.

Both the Valence Shell Electron Repulsion (VSEPR) Model and the Hybrid Atomic Orbital (HAO) Model can explain the trends in bond length and are able to correctly predict the dependence of the bond length on polarity of the bond. The valence angles are in turn influenced by the changes in bond length and the relative numbers of Ge-C and Ge-X bonds and these trends can also be qualitatively explained by the theories. However, no explanation is given for the abnormally large deviations of the C-Ge-C angle in all three dihalo(dimethyl)germanes.

In a related study, the gas phase structures of the halogermanes GeH_2Cl_2 and GeH_2Br_2 where determined [14]. A similar trend was observed when the geometric parameters were compared with other molecules of the form GeH_nX_{4-n}, with the Ge-X bond lengths decreasing with increasing halogen substitution. The structure of tetramethylgermane [15] was also re-determined as a prelude to studies of the Me_nGeX_{4-n} (X=F, Cl, Br, I) series.

The gas-phase electron diffraction structures of some analogous silicon compounds, the fluoro(methyl)silanes, have been determined [16]. The study was performed mainly to investigate the validity of the theory of (p-d) π back bonding in these compounds. Some interesting trends in bond lengths and bond angles were seen and it was noted particularly that the C-A-C angle increases with increasing fluorination.

Unfortunately, gas phase electron diffraction can sometimes contain large experimental errors, due to the fact that only radial distributions are directly determined and the bond lengths and bond angles are calculated from these distances. The height of the peaks in the spectrum is dependent on the atomic number of the atoms involved in the interaction, as well as the interatomic distance. Added to the broadening of peaks due to the molecular

vibrations and the fact that peaks can often overlap or completely cover one another, this can sometimes lead to large uncertainties in measurement. In the studies of the halo(methyl)germanes, many of these problems were encountered. Therefore, although the large C-Ge-C angles seem significant, the large experimental errors make it impossible to state this with any certainty.

2.7.2. Microwave Spectral Studies

Microwave studies of methylgermane [1], dimethylgermane [2] and some of the halo(methyl)germanes [3-5] have been conducted and the heavy atom structural parameters of these molecules calculated. These results are summarized in table 2.6.with the structural parameters obtained by gas phase electron diffraction studies of the organogermanes.

The spectrum of 28 isotopic species of methylgermane (CH_3GeH_3) was measured by Victor W. Laurie in 1958 [1] and some of the structural parameters calculated. There were 34 effective moments of inertia available for calculation of the structure and each of the atoms was isotopically substituted at least once. Structures were calculated using two different methods and the results were in fairly good agreement, although the one method was thought to give values closer to the equilibrium structure. The barrier to internal rotation around the C-Ge bond and the dipole moment of the molecule were also calculated and comparisons made to analogous carbon and silicon compounds.

The study of dimethylgermane, by Thomas and Laurie, followed in 1968 [2]. The spectrum of the five Ge isotopic species of Me_2GeH_2 was investigated and the rotational constants and barrier to internal rotation calculated. There was insufficient information available to completely determine the structure, but with the assumption of methyl-group parameters, the heavy-atom parameters were determined. The dipole moment of the molecule was also calculated.

Durig and Li investigated the rotational spectra of five Ge and two Br isotopic species of bromo(trimethyl)germane [3] in 1973. The ground state rotational constants for 9 isotopic species were calculated. The r_s value of the Ge-Br bond distance was found using Kraitchman's equations and by assuming the structural parameters for the methyl groups, some additional structural parameters could also be calculated. The calculated structural parameters were compared to those of similar molecules. Notably, it was found that the C-Ge-C angle opens up appreciably on substitution of a chlorine or bromine atom for the hydrogen in trimethylgermane.

In 1975, the rotational spectrum of chloro(trimethyl)germane [4] and that of trichloro(methyl)germane [5] was investigated by Durig and Hellams and Durig, Cooper and Li respectively. In both studies, ground state rotational constants were obtained for a number of isotopic species of the molecules and an r_s value for the Ge-Cl bond distance was calculated from the rotational constants. Additional heavy atom structural parameters were once again calculated by assuming the structures of the methyl groups and these were compared to those of similar structures. The structural parameters of chloro(trimethyl)germane were included in the discussion in the previously cited study of bromo(trimethyl)germane.

In microwave studies on analogous silicon compounds some structural parameters of methylsilane [6], dimethylsilane [7] and bromo(trimethyl)silane [8] were determined. The microwave spectra of the non-methylated germanes trichlorogermane [9], iodogermane and bromogermane [10], have also been determined.

2.8. Vibrational Studies

The organogermanes have been extensively and successfully characterized by means of numerous spectroscopic techniques. The vibrational spectra of this group of compounds especially, have been characterized through the analysis of the infrared and Raman spectra of the molecules.

In 1964, James E. Griffith [24] reported the vibrational spectrum of dichloro-(dimethyl)germane in both gaseous and liquid states in the infrared (250-400 cm^{-1}) and the liquid phase in the Raman (40-3200 cm^{-1}) region. Frequencies were assigned to normal modes of vibration and compared with those of analogous carbon, silicon and tin compounds. Up to this point, compounds of the type X_nAY_{4-n} where A is a group IV element and Y may be H, CH_3 or a halogen, had been examined in detail by various spectroscopic methods for A=C, Si and Sn, but not yet for A=Ge. This study completed the series of vibrational spectra for Me_2ACl_2 and allowed for comparison of results. The transition in vibrational frequencies down group IV in this series is smooth and germanium fits in with the general trend. The fundamental frequencies tend to shift down with increasing mass of the group IV elements, as is to be expected.

In the same year, James R. Aronson and James R. Durig [25] recorded the infrared and Raman spectra of trichloro(methyl)germane and assigned the 11 active fundamental vibrations of the molecule. The frequency of the inactive torsional vibration was also estimated and the height of the torsional barrier calculated. The Raman study was undertaken only when several of the fundamentals could not be located in the infrared study. The results where then compared to the previously obtained vibrational spectra of CH_3ACl_3 with A=C, Si and Sn.

R.J. Cross and F. Glocking [26] undertook a general study of the infrared spectra of 80 organogermanes in the region 2500-200 cm^{-1}, with the main objective of assigning group frequencies. The symmetric and asymmetric

Ge-C stretching bands were given for methyl-, ethyl-, isopropyl-, butyl- and benzylgermanes, while absorption bands due to C-H stretching vibrations were ignored. For methyl derivatives, useful methyl-germanium bands were listed, with the methyl rock being the most characteristic. It was found that the Ge-C stretch is stronger and at higher frequency than for most other alkylgermanes. A number of strikingly characteristic bands are also given for organogermanium hydrides, deuterides and halides.

In 1969, Durig et al [27] recorded the infrared and Raman spectra of chloro-(trimethyl)germane over the frequency range of 33-4000 cm^{-1}. Normal modes and force constants were calculated and assignments for the normal modes were made on the basis of band types, Raman depolarization values and characteristic frequencies. The valence force field was used to calculate the frequencies and potential energy distribution for the molecule and these corresponded well to the assignments given in this study. The infrared spectra above 400 cm^{-1} and the Raman spectra of the Me_nGeCl_{4-n} series had previously been reported by Van de Vondel and Van der Kelen [28] and the observed frequencies assigned to normal modes. Some changes where made to their assignments however, which permitted calculation of the spectrum to a far greater precision with fewer force constants than were previously necessary. The results, when compared to previously published results for Me_3ACl with A=C, Si, Ge and Sn, showed a need for the re-determination of the force fields of the heavier members of the series.

A study of the vibrational spectra of the bromo(methyl)germanes [29] was undertaken by Van de Vondel, Van der Kelen and Van Hooydonk in 1970. The infrared and Raman spectra were measured and vibrational assignments proposed on the basis of characteristic group frequencies, rotational splitting in the gas phase infrared and Raman polarization data. In the study of Me_nGeCl_{4-n} cited above the number of bands observed at low frequency was notably less than the number of fundamentals. The accidental degeneracy thought to have caused this, could be cancelled by a change in the relative mass of the halogen vs. the carbon atom. The use of the laser as a light

source in the Raman effect improved the resolution of the spectra with respect to previous studies and the intensity gain due to laser excitation allowed for observation of the rocking vibrations of the methyl group.

Two separate studies of the vibrational spectra of iodo(methyl)germanes were conducted in 1971. Durig et al. recorded the Raman spectra of liquid and solid triiodo(methyl)germane and triiodo(perdeuteromethyl)germane (CH_3GeI_3 and CD_3GeI_3) and the infrared spectra of the liquids from 33-4000 cm^{-1} [30]. The spectra were interpreted in detail and all 12 normal modes for the molecules assigned. The torsional mode was observed in CH_3GeI_3 and the threefold barrier restricting rotation calculated. The study was part of an overall program to determine the relative effects of various halogens on the torsional barrier of the methylgermanes. The valence force field was used to calculate the frequencies and potential energy difference for the molecules and the results support the assignments made. Furthermore, the force constants are consistent with those previously reported for halogermanium and organogermanium compounds and appear to be reasonably transferable to other germanium compounds.

The second study by Anderson et al. [31] recorded the infrared and Raman spectra of the series of iodo(methyl)germanes, $MeGeI_3$, Me_2GeI_2 and Me_3GeI_3. A normal coordinate analysis was done based on a modified valence force field and this confirmed the assignments for all fundamental frequencies except the torsional modes. The results were in good agreement with those published by Durig et al. for $MeGeI_3$. The study was part of a continuing program of vibrational analyses of methylated and halogenated derivatives of germane and was done to assist the interpretation of the spectra of the halo(methyl)germanes of lower symmetry and confirm the assignments of previous authors.

In 1973, Anderson et al. recorded the infrared and Raman spectra of the fluoro(methyl)germanes $MeGeF_3$, Me_2GeF_2 and Me_3GeF [32]. Once again the fundamental frequencies for each molecule were assigned and confirmed by

normal coordinate analyses based on a modified valence force field. The observed vibrational frequencies were reproduced with a precision better than 2%. The frequencies were mostly fitted to the liquid Raman data but in cases where fundamentals were weak, infrared data was used. The fluorides completed the series Me_nGeX_{4-n} (X=F, Cl, Br, I and n=1-3), providing the opportunity of comparing the trends due to changing halogen substitution for a series with a specific n value.

It is important to note that in the normal coordinate analyses, the molecules were assumed to have tetrahedral angles and the bond lengths were based on literature values for related species. The same assumption concerning bond angles was made in all of the previously discussed normal coordinate analyses for related molecules. Furthermore, the calculations do not account for intermolecular interactions that could play a role in the condensed phase and the force constants are not unique, since the final values are dependent on both the interaction terms and the order in which they are introduced.

The high yield syntheses and spectroscopic analyses of Me_2GeHX (X=F, Cl, Br, I) and Me_2GeHPs (Ps=CN, N_3, NCO, NCS, Oac), monohalogen and mono-pseudohalogen derivatives of dimethylgermane where reported by Barker, Drake and Hemmings in 1974 [33], in a continuation of the work done on the dihalo(dimethyl)germanes. The species were identified by NMR, infrared, Raman and mass spectroscopy, as well as other physical methods. A normal coordinate analysis based on a modified valence force field was done as a confirmation of the assignments of all the fundamental frequencies, except the torsional modes, in the vibrational spectra of the compounds.

The Raman spectrum of trichloro(methyl)germane in the gas phase was re-recorded with its microwave spectrum [5] in an attempt to eliminate the uncertainty in some of the assignments given in the previous study [25]. It was hoped that the addition of the structural data obtained from the microwave spectrum would improve the normal coordinate analysis, which was subsequently performed using (once again) a modified valence force

field. The barrier to internal rotation around the Ge-C bond was calculated using the assignments made for the torsional overtones.

In a further continuation of the work on organogermanes, the infrared and Raman spectra of the monohalo(methyl)germanes [34] and dihalo(methyl)-germanes [35] were studied in 1971. As with all previous vibrational studies assignments were made for the frequencies and a normal coordinate analysis was done using structural parameters from the literature.

2.9. Synthesis

Work was being performed on the synthesis of the phenyl derivatives of germane as far back as the 1920's. Morgan and Drew [67] prepared tetraphenylgermane and other phenyl derivatives and Tabern, Orndorff and Dennis [68] prepared tetraphenylgermane and other quaternary alkyl and aryl germanium compounds. Kraus and Foster investigated the triphenyl-germane group [69]. The isolation of diphenylgermane and the preparation and properties of some of its derivatives [70] was investigated by Kraus and Brown in 1930. The three diphenyl gemanium halides Ph_2GeX_2 (X=F, Cl, Br) and diphenyl germanium oxide were synthesized. Dibromo(diphenyl)germane was prepared by direct bromination of tetraphenylgermane in boiling carbon tetrachloride. The mixture of bromides formed was converted to oxides, which were in turn converted to the corresponding chlorides. Dichloro-(diphenyl)germane was obtained from this mixture by fractional distillation. Converting the dichloride to its oxide and treating it with hydrobromic or hydrofluoric acid gave the pure dibromide and difluoride compounds.

The reduction of GeO_2 with hydroborate [71] was reported in 1957 by Piper and Wilson to give germane in 75% yield. Up until this point germane had been difficult to prepare. Furthermore, although adequate methods were available [72] for the synthesis of substituted germanes of the type R_nGeH_{4-n} (n=1-3 and R=alkyl), these required the use of non-aqueous solvents or highly flammable hydrides, which made them rather inconvenient.

In 1963, James E. Griffith reported the synthesis and properties of methyl-, dimethyl- and trimethylgermane [73], based on the method for germane using hydroborate. The main motivation for the study was the fact that the methyl-substituted germanes serve as prototypes for the entire class of alkyl-substituted germanes, the chemistry of which was not well understood at the time. A brief discussion of the factors affecting the yield of germane is also included. The result of the study was that both germane and its methyl derivatives Me_nGeH_{4-n} (n=1-3) were prepared in virtually quantitative yield and it was thought that the reaction could be extended to include aryl and cycloalkyl derivatives.

A synthesis of methylgermanium halides [74] using germanium powder, copper and the respective methylhalide CH_3X (for X=Cl, Br, I) was reported by K. Moedritzer in 1966 and improved on the previous direct synthesis [75] reported by E.G. Rochow. A mixture containing all three of the germanium halides Me_nGeX_{4-n} (n=1-3) was obtained in each case, although the quantity of the trimethylgermanium halide was very small. Data indicated that the yields were considerable increased in comparison to previous methods.

Johnson [76] presented a general review of organogermanium compounds in 1978, which included recommendations on nomenclature, general methods of synthesis and a discussion of some of the properties of these compounds. Organogermanium compounds were defined, by analogy with organosilicon compounds, as substances having at least one carbon atom attached to a germanium atom. Most of these carbon-containing germanium compounds are then considered as derivatives of the simple germanes, namely germane, GeH_4; digermane, Ge_2H_6 and trigermane, Ge_3H_8.

Seven general methods of synthesis were mentioned in the review, namely substitutions by dialkylzinc and diarylmercury compounds, substitution by Grignard reagents, the use of alkyl- or aryllithium compounds, coupling reactions with sodium, reduction with lithium aluminium hydride and a

direct synthesis from elemental germanium. Although the number of known carbon-containing germanium compounds were too few and too little data was available on those that were known to allow for any generalizations, a number of facts became apparent. Considerable variation in the strength of the Ge-C bond was found to depend mainly on the nature of the carbon radical. Also, in the case of halogenated germanes, the halogens are readily replaced by hydrogen through reduction and by a hydroxyl-group through hydrolysis, particularly in alkaline media.

Following on this general study, specific methods of synthesis were reported for tetraphenylgermane [77], hexaphenyldigermane [78], diphenylgermane [79], bromo(triphenyl)germane and triphenylgermane [80]. Of these, only tetraphenylgermane is a crystalline solid at room temperature. The other four are all liquids. The diphenylgermane obtained, a colourless liquid with a boiling point of 95° at 1 mm, can be brominated directly to diphenyl-dibromogermane.

The synthesis of dichlorobis(pentachlorophenyl)germane and some of its derivatives [81] was reported by Fajari et al. in 1994. The preparation of dichlorobis(pentachlorophenyl)germane was performed by the treatment of tetrachlorogermane with either pentachlorophenyllithium or pentachloro-phenylmagnesium chloride in a molar ratio 1:2. The product was reduced to bis(pentachlorophenyl)germane by $LiAlH_4$ in THF and converted to the dibromo- and diiodo- analogs with a tetrachloroethylene solution containing bromine and iodine respectively. The dichlorogermane was also converted to dimethoxy(pentachlorophenyl)germane by prolonged boiling in methanol. The molecular structure of diiodobis(pentachlorophenyl)germane was then determined by X-ray crystallography.

2.10. The Cambridge Structural Database

2.10.1. Molecules of the form R'RGeYZ

A search of the Cambridge Structural Database (version 1.3.) [82] for structures containing a C_2GeYZ fragment, where Y and Z are any elements on the periodic table excluding carbon, yielded 169 compounds of this form. A statistical analysis of the group, gave an average C-Ge-C angle of 108.8°, very close to the tetrahedral angle. The results are shown in figure 2.1.

Figure 2.1: Histogram of the C-Ge-C angle for RR'GeYZ compounds

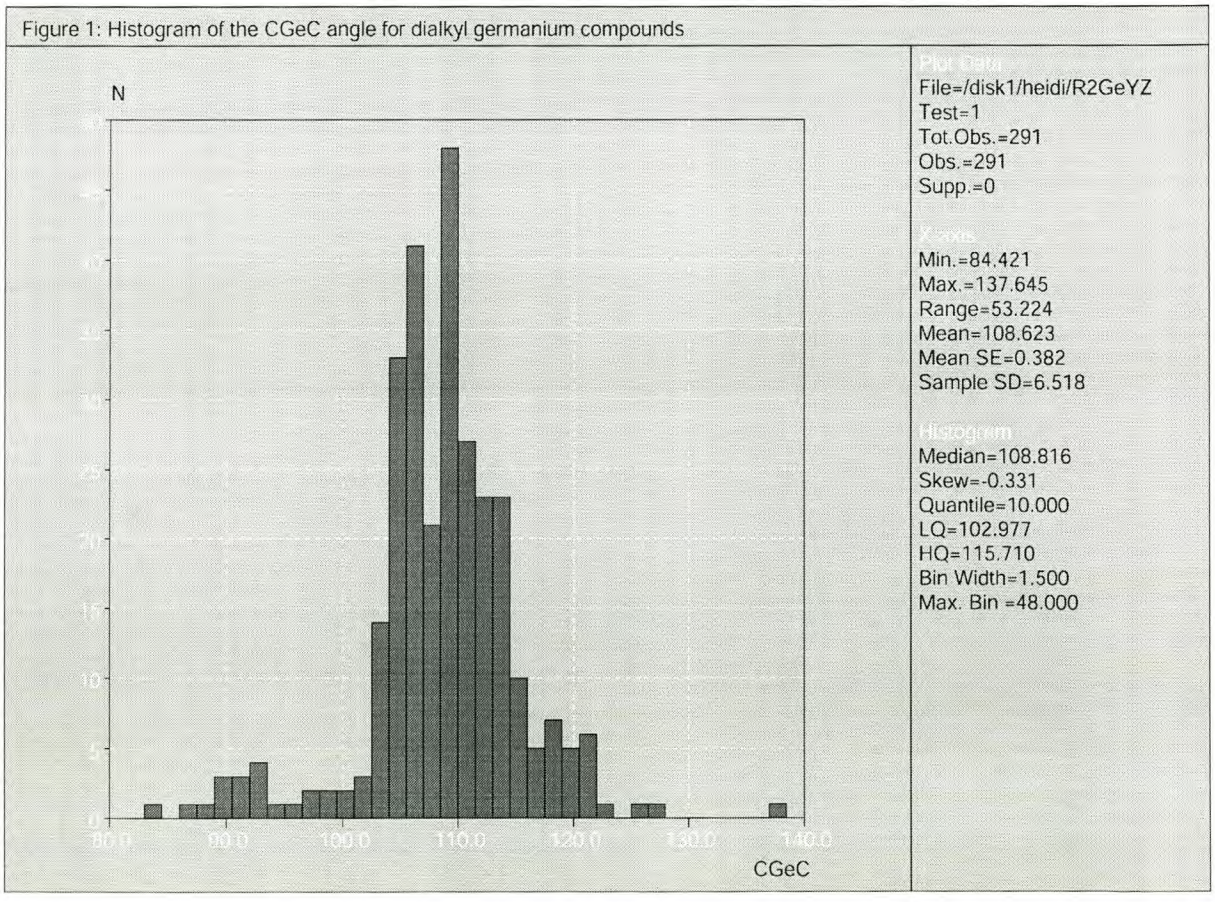

In the majority of these compounds however, either the C-Ge-C or Y-Ge-Z fragments formed part of a ring. Since this could have a potentially large

influence on the C-Ge-C angle, it is impossible to draw any conclusions from this average value. When the search was modified to include the restriction that there be no cyclicity present in the fragment, the number of compounds was reduced to only 16, too few to do a meaningful statistical analysis of.

In most of the 169 compounds found in the search the fragment formed only a small part of a much larger structure, many of them organometallic complexes with germanium either as the central atom or as part of one of the ligands. Cases where germanium was bonded to one or more metals were common and 39 compounds were found where both Y and Z were other germanium atoms. Other common substituents were oxygen and sulphur, with 19 compounds containing Y=Z=O and 20 with Y=Z=S.

2.10.2. Dihalogenated Germanium Compounds

Only five crystal structures of compounds containing germanium in its tetravalent state bonded to two carbon atoms and two halogens have been reported as of version 1.3. of the CSD. These are 1,1,4,4-tetrachloro-1,4-digermacyclohexa-2,5-diene (i), 1,1,4,4-Tetraiodo-1,4-digermacyclohexa-2,5-diene (ii), 10,10-dichloro-10-germa-9-oxa-9,10-dihydroanthracene (iii), Di-iodo-bis(pentachlorophenyl)-germanium (iv) and 1,1-dichloro-2,3,4,5-tetramethylgermole (v), the structures of which are shown in figure 2.2.

In all but one of the compounds germanium forms part of a six-membered ring, which restricts the C-Ge-C angle. In the other, non-cyclic compound, the substituents are two iodine atoms, which have a large molecular mass, and two pentachlorophenyl groups, which are large and bulky and have strong electronic properties. Both these factors can have potentially large effects on the C-Ge-C angle. There is thus no known crystal structure containing germanium bonded to two halogen and two carbon atoms, in which the size of the C-Ge-C angle can be directly correlated to the effect of the halogens, without the influence of other factors.

Figure 2.2: The structures of the dihalogenated germanes found on the Cambridge Crystallographic Database

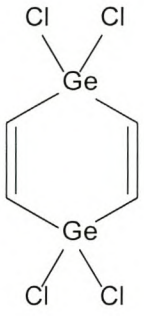

(i) 1,1,4,4-tetrachloro-1,4-digermacyclohexa-2,5-diene

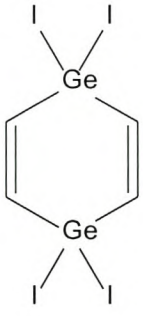

(ii) 1,1,4,4-tetraiodo-1,4-digermacyclohexa-2,5-diene

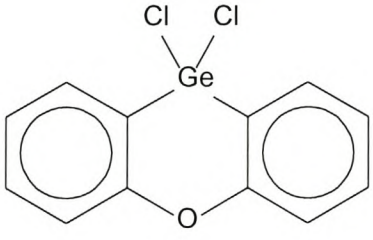

(iii) 10,10-dichloro-10-germa-9-oxa-9,10-dihydroanthracene

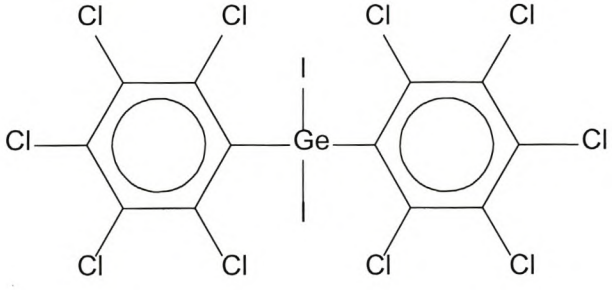

(iv) di-iodo-bis(pentachlorophenyl)-germanium

(v) 1,1-dichloro-2,3,4,5-tetramethylgermole

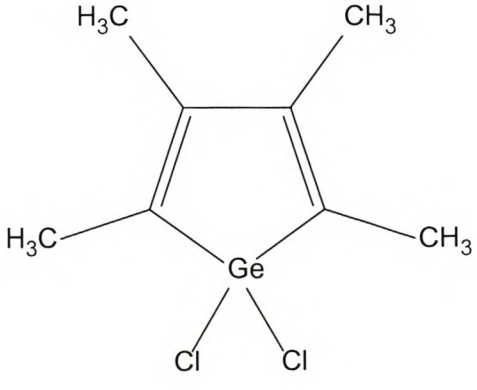

2.10.3. Dihalogenated Tin and Lead Compounds

A search was also performed for analogous tin and lead compounds, that is compounds of the form R'RAX$_2$, where A=Sn, Pb and X is a halogen. Only two dihalo-dialkyl lead compounds were found and in both the halogen was bromine. The two C-Pb-C angles in these compounds are both significantly larger than tetrahedral at 123.4° and 135.8° respectively. Dihalo-dialkyl tin compounds proved to be more abundant than both the germanium and lead analogs and 50 crystal structures containing a C_2SnX_2 fragment were found. A statistical analysis of these compounds gave an average C-Sn-C angle of 128.7° and the results are shown in figure 2.3. For both the tin and the lead compounds, the C-A-C angles are substantially larger than tetrahedral.

Figure 2.3: Histogram of the C-Sn-C angles for R_2SnX_2

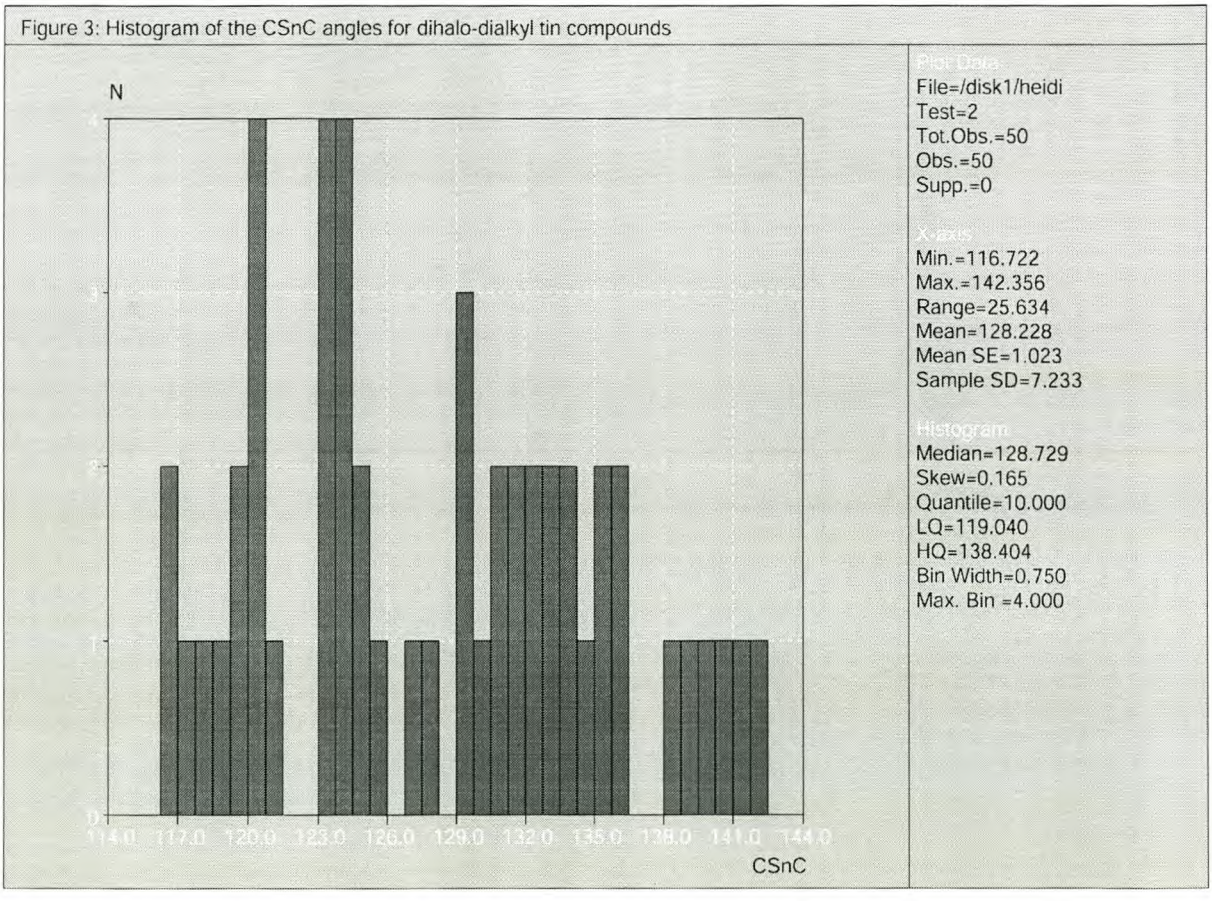

2.10.4. The role of electronegativity

When the original search was performed, it was noticed that the C-Ge-C angles seemed on the whole to be larger for the more electronegative substituents Y and Z. For the compounds with two oxygen or two sulphur substituents the medians of the C-Ge-C angle were 114.3° and 115.8° respectively. To determine whether electronegativity does in fact play a role in the size of the C-Ge-C angle, two searches were done, one restricting Y and Z to elements with electronegativity greater than 2.1 (excluding carbon) and the second restricting Y and Z to elements with electronegativity less than 2.1. Since no universally agreed upon scale for electronegativity exists, the Allred and Rochow scale of eletronegativity was used in the separation.

Figure 2.4: Histogram of the C-Ge-C angle for electronegative Y and Z

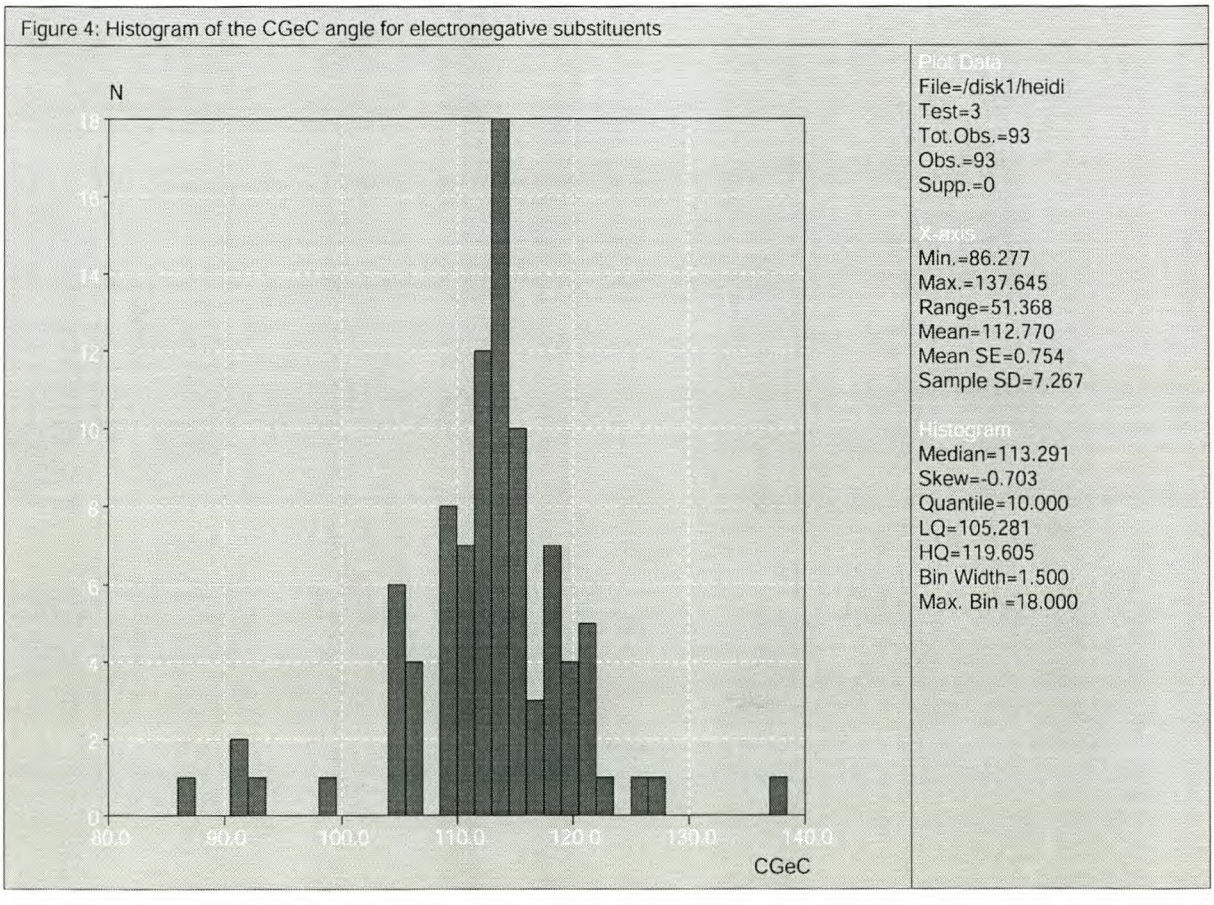

Figure 2.5: Histogram of C-Ge-C angle for electropositive Y and Z

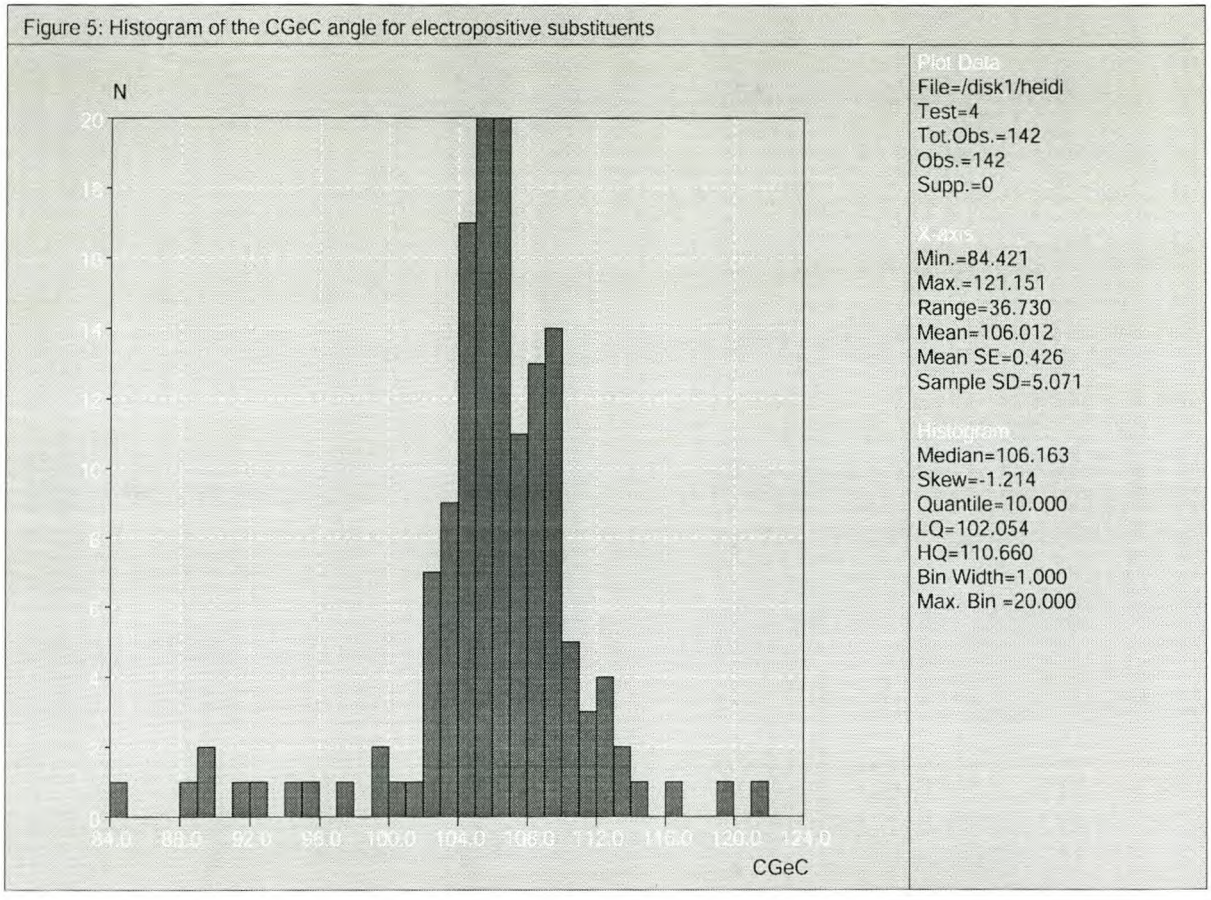

A statistical analysis of these two classes of compounds revealed the average C-Ge-C angle to be about 7° larger for the electronegative substituents than for the electropositive substituents. For χ (Y) and χ (Z) > 2.1 the median was 113.7° and for χ (Y) and χ (Z) < 2.1 it was 106.4°. This is in agreement with Bent's rule for electronegative substitution. It must be noted however, that since electronegativity is a subjective and qualitative property, these results merely provide a qualitative indication of the effect of electronegativity. There are several other factors, such as steric hindering and cyclicity, which could affect the size of the C-Ge-C angle and must therefore be taken into account before definite conclusions are drawn.

2.11. Conclusion

From studying the literature, a number of things become apparent. Firstly, there is insufficient structural information available for compounds of the form R_2GeX_2, where R is an alkyl group and X a halogen. The experimental structures that are available for the dihalo(dimethyl)germanes seem to indicate that the C-Ge-C angles in these compounds are exceptionally large in comparison with the analogous carbon and silicon compounds and the non-halogenated dimethylgermanes. The sources of this data are not always reliable however, and this cannot therefore be said with any certainty. There are also few known crystalline compounds of the form R_2GeX_2, from which reliable structural data could be obtained by X-ray diffraction.

Qualitatively, the structures obtained from computational studies for these compounds are in agreement with the experimental structures. However, the complete range of molecules Me_2AX_2, with A=C, Si=Ge and X=H, F, Cl and Br has not been calculated. Furthermore, no satisfactory explanation for these large angles has been put forward.

Although vibrational force fields have been developed for compounds of the form AH_nX_{4-n}, no traditional force fields exist which are able to predict the geometries of the dimethylated halogermanes. The generic force fields available for these compounds are also unable to correctly predict these large angles in the dihalo(dimethyl)germanes.

CHAPTER 3: ELECTRONIC STRUCTURE CALCULATIONS

3.1. Introduction

In order to verify the experimental results found by gas phase electron diffraction and microwave spectroscopy and provide a set of consistent and reliable data for the development of a force field, an *ab initio* study was initiated. Although the main focus of the study was to obtain optimized geometries and frequencies for the dihalo(dimethyl)germanes and the analogous carbon and silicon compounds (Me_2AX_2), for consistency the same calculations were also performed on a number of related compounds. Other compounds included in the study where dimethylgermane, dimethylsilane and propane (Me_2AH_2), the halogermanes, -silanes and –methanes (AH_nX_{4-n}) and compounds of the form Me_2AHX, $MeAH_2X$, $MeAHX_2$ and Me_2AI_2, where A=C, Si, Ge and X=H, F, Cl, Br. For further insight into the molecular structure and properties of the compounds partial atomic charges, electron densities and valence molecular orbitals were calculated.

The computational methods and programs used in the calculations and manipulation of the results are discussed in **Section 3.2.** This includes the building of input structures using Cerius2 [66], the *ab initio* calculations with Gaussian98 [83] and the visualization of the calculated molecular orbitals and electron densities using GOpenmol [84]. The results of the *ab initio* calculations are summarized in **Section 3.3.** The optimized geometric parameters, molecular vibrations, partial atomic charges, electron density and molecular orbitals are presented. This section also includes the MP2 and DFT optimized geometries and the geometries of the iodine series Me_2AI_2. A general discussion of the results is given in **Section 3.4.** and an attempt is made to explain the results of the calculations using three different theories of bonding, the VSEPR theory, Bent's Rule and a modified Ligand Close-Packing Model. **Section 3.5.** concludes this chapter.

3.2. Computational Methods

3.2.1. Building Input Structures using Cerius2

The input for the ab initio calculations was taken from molecules built with Cerius2 [66] and optimized using the Universal Force Field (UFF) [22]. For the simple halomethanes, -silanes and –germanes (molecules of the form AH_nX_{4-n} with A=C, Si, Ge and X=F, Cl, Br) an energy minimization was performed with no initial constraints on the molecules. The same was done for the dihalo(methyl)germanes ($MeAHX_2$) and the halo(methyl)germanes ($MeAH_2X$), for which the symmetric, open conformation was assumed to be the minimum energy structure.

For the dihalopropanes, dihalo(dimethyl)silanes and –germanes, propane, dimethylsilane and -germane, the situation is slightly more complex due to the addition of a number of torsion angles to the variables, increasing the number of possible low energy conformations. For each of the molecules in the series Me_2AX_2, with A=C, Si, Ge and X=H, F, Cl, Br, I a conformer analysis was done in Cerius2 to determine the local energy minima of the molecule. Five local energy minima, with energies quite close to each other, were found for each of the fifteen molecules in the series. For each of these minimum energy conformers, the molecule was built with the approximate torsion angles, given an element of disorder, and minimized. The energies were then calculated and compared to find the global minimum, which was found for all the structures to be the symmetric open conformation.

3.2.2. Calculations with Gaussian98

All the *ab initio* calculations were performed at the RHF level of theory using Gaussian98 [83]. For the fluorine, chlorine and bromine series, a 6-31G(d) basis set was used [57,85]. For the iodine series, for which the 6-31G(d) basis set has not been parameterized, the LANL2DZ basis set [57,85] was

substituted. The calculations were repeated for the dihalo(dimethyl)germanes at MP2 and DFT level using the same basis sets, mainly to ascertain the influence this would have on the geometry and whether this influence was large enough to make it necessary to repeat all the calculations at one of these higher levels of theory.

For each molecule a geometry optimization was performed, followed by a frequency calculation at optimized geometry. The geometry optimization was given extremely tight convergence criteria and molecular symmetry was included in the calculations. The symmetry requirements were kept loose, however, due to the sub-optimal geometries used as input.

For molecules of the form AH_nX_{4-n}, $MeAH_2X$ and $MeAHX_2$, the UFF optimized structures were used as input and no initial constraints where made on the molecules. For molecules of the form Me_2AX_2, all five of the local minimum energy structures obtained with UFF [22] were used separately as input, with constraints on the torsion angles, to verify that the symmetrical open conformation is in fact the global minimum, which was found to be the case. Partial geometry optimizations were therefore performed for these molecules instead of the full geometry optimizations of the other molecules.

In addition to the above, electron densities, molecular orbital coefficients and gross orbital populations, Mullikan charges and dipole, quadropole, octapole and hexadecapole moments were calculated for all the molecules.

3.2.3. Visualization of output

The electron densities and valence molecular orbitals of the molecules Me_2CF_2, Me_2GeH_2 and Me_2GeF_2 were visualized using a program called GOpenmol [84], which converts Gaussian output from a checkpoint file into three-dimensional images. The vibrations were animated and viewed with Weblab Viewer [86].

3.3. Results

3.3.1. Introduction

The optimized geometries computed at RHF level are reported for all the molecules calculated and discussed in detail. The frequency calculations at optimized geometry are given only for those groups of compounds used in the training set for the force field. The results of the calculation of partial atomic charges, electron density and valence molecular orbitals of the optimized structures are shown for selected representative compounds. The iodine compounds are discussed briefly and separately due to the different basis set used. The MP2 and DFT calculations are also reported only briefly, as they were performed only to check the results of the RHF calculations, which were found to be sufficient for the purposes of this work.

3.3.2. Geometry Optimization

The calculated geometric parameters are summarized in tables 3.1 to 3.8. The parameters are named according to the element symbols of the atoms involved. For the molecules containing methyl groups, where parameters containing the same elements are not necessarily identical in value, the atoms are numbered as shown in figure 3.1. and the parameters named accordingly. All the bond lengths are in angstrom (Å) and all angles in degrees (°).

Table 3.1: Geometric Parameters of molecules of the form AX_4

X	H			F			Cl			Br		
A	C	Si	Ge	C	Si	Ge	C	Si	Ge	C	Si	Ge
A-X	1.084	1.475	1.535	1.302	1.557	1.677	1.766	2.029	2.116	1.933	2.188	2.272
X-A-X	109.5	109.5	109.5	109.5	109.5	109.5	109.5	109.5	109.5	109.5	109.5	109.5

In the monohalogermanes, -silanes and -methanes (AH_3X), both the A-H and the A-X bond lengths increase along the series A=C, Si, Ge, as is to be expected from the increasing size of the central atom. The H-A-H angles increase from A=C to A=Ge for X=F and Cl, while for X=Br there is a slight decrease from 111.2° for A=C to 110.6° for A=Si, followed by an increase to 111.5° for A=Ge. The trend in the H-A-X angles is exactly the opposite, decreasing from A=C to A=Ge for X=F and Cl and increasing from A=C to A=Si only to decrease again from A=Si to A=Ge for X=Br.

Table 3.2: Geometric parameters of molecules of the form AH_3X

X	H			F			Cl			Br		
A	C	Si	Ge	C	Si	Ge	C	Si	Ge	C	Si	Ge
A-H	1.084	1.475	1.535	1.082	1.470	1.531	1.078	1.468	1.529	1.076	1.467	1.530
A-X	1.084	1.475	1.535	1.365	1.594	1.727	1.785	2.067	2.168	1.948	2.222	2.309
H-A-H	109.5	109.5	109.5	109.8	110.2	111.8	110.5	110.6	111.8	111.2	110.6	111.5
H-A-X	109.5	109.5	109.5	109.1	108.8	107.0	108.5	108.3	107.1	107.7	108.4	107.4

All the bond lengths in the dihalogermanes, -silanes and –methanes (AH_2X_2) are, without exception, smaller than the corresponding bond lengths in the monohalogermanes. The H-A-H angles show a marked increase of between 1° and 5° from those of the corresponding monohalogermanes, but the trend from A=C to A=Ge is the same, namely that the angles increase along the series. As well as the increase relative to the monohalogenated analogs, the increase in the H-A-H angle from A=C to A=Si is only 1° to 1.5°, while the increase from A=Si to A=Ge is much larger, between 1.5° and 3.5°. The X-A-X angles show a gradual decrease from A=C to A=Ge, which corresponds roughly to the increase in the H-A-H angles. The H-A-X angles do not seem to be much affected by the central atom and remain fairly constant along the series, with an average value of 108°.

Table 3.3: Geometric parameters of molecules of the form AH_2X_2

X	H			F			Cl			Br		
A	C	Si	Ge	C	Si	Ge	C	Si	Ge	C	Si	Ge
AH	1.084	1.475	1.535	1.078	1.462	1.523	1.074	1.460	1.523	1.072	1.460	1.526
AX	1.084	1.475	1.535	1.338	1.581	1.710	1.768	2.050	2.146	1.930	2.206	2.292
HAH	109.5	109.5	109.5	112.5	113.4	117.3	111.1	112.9	115.4	112.2	113.0	114.8
HAX	109.5	109.5	109.5	108.9	108.9	108.7	108.2	108.4	108.2	107.9	108.0	108.0
XAX	109.5	109.5	109.5	108.6	107.6	103.9	112.9	110.2	108.3	113.1	111.9	110.0

The substitution of yet another halogen in the place of a hydrogen in the trihalogermanes, -silanes and –methanes (AHX_3) leads again to a general decrease in the A-H and A-X bond lengths, contrary to what one might expect from the relative radii of the halogen and hydrogen atoms. There is once again the expected increase in bond length along the series from X=F to X=Br, as was the case for the mono- and dihalogermanes. Where the H-A-X angles decreased from A=C to A=Ge in the monohalogenated compounds, there is in the trihalogenated compounds an increase of 1° to 2° along the series from A=C to A=Ge. The X-A-X angles decrease from A=C to A=Ge, qualitatively much the same as they did in the dihalogermanes, -silanes and –methanes. For X=F, the X-A-X angles are larger in AHX_3 than in AH_2X_2, whereas for X=Cl and Br they are smaller.

Table 3.4: Geometric parameters of molecules of the form AHX_3

X	H			F			Cl			Br		
A	C	Si	Ge	C	Si	Ge	C	Si	Ge	C	Si	Ge
AH	1.084	1.475	1.535	1.074	1.449	1.510	1.071	1.454	1.517	1.069	1.454	1.523
AX	1.084	1.475	1.535	1.317	1.569	1.693	1.763	2.038	2.129	1.926	2.195	2.280
HAX	109.5	109.5	109.5	108.5	110.9	112.9	107.6	109.4	110.4	107.5	108.7	110.1
XAX	109.5	109.5	109.5	110.4	108.0	105.9	111.3	109.6	108.5	111.4	110.2	108.8

For the monohalo(methyl)germanes, -silanes and -methanes (CH_3AH_2X), the A-C, A-H and A-X bond lengths increase with the increasing size of atom A for X=H, F, Cl and Br. The C-H bond distances in the methyl group however, increase from A=C to A=Si and then decrease again for A=Ge. The C-H bond lengths in CH_3GeH_2X are on the whole even shorter than those found in the unsubstituted methyl group of CH_3CH_2F. The C-A-H angles decrease from A=C to A=Si and increase again for A=Ge, both for X=H and X=F, Cl and Br, but the C-A-H angle is smaller in CH_3GeH_3 than in CH_3CH_3 whereas it is larger in CH_3GeH_2X than in CH_3CH_2X. The C-A-X angle decreases down group IV for all three halogens and the decrease is slightly larger from A=Si to A=Ge than from A=C to A=Si. The H-A-H angles increase systematically by 0.5° to 1° from A=C to A=Ge and the H-A-X angles once again show an increase from A=C to A=Si followed by a decrease from A=Si to A=Ge.

All the bond lengths in the dihalo(methyl)germanes, -silanes and -methanes (CH_3AHX_2) are shorter than the corresponding bond lengths in their mono-halogenated counterparts. For the A-C, A-H and A-X bond lengths this decrease is in the order of 0.002 to 0.02 Å and for the C-H bond lengths around 0.001 Å. Otherwise, the trends are the same, with the expected increase in bond length with increasing size of the central atom. What is interesting to note however, is that in many cases corresponding bond lengths actually decrease from X=F to X=Br, contrary to what one might expect from the relative size of the substituents. The same effect is found in the monohalo(methyl)germanes, -silanes and –methanes. The C-A-H angles increase from A=C to A=Si and decrease from A=Si to A=Ge, but the value for A=Ge is still larger than for A=C. The same trend is apparent in the C-A-X angle, except that for X=Br the angle does not decrease between A=Si and A=Ge but increases further, although not by much. The H-A-X and X-A-X angles are very close in value and undergo similar changes with the change on the central atom, decreasing from A=C to A=Si and increasing again from A=Si to A=Ge. The angles are smaller for germanium than for carbon.

Table 3.5: Geometric parameters of molecules of the form $MeAH_2X$

X	H			F			Cl			Br		
A	C	Si	Ge	C	Si	Ge	C	Si	Ge	C	Si	Ge
A-C	1.527	1.888	1.949	1.512	1.871	1.933	1.517	1.874	1.935	1.516	1.875	1.936
C-H3	1.086	1.086	1.084	1.084	1.086	1.084	1.083	1.085	1.084	1.083	1.085	1.083
C-H5	1.086	1.086	1.084	1.086	1.087	1.085	1.086	1.087	1.085	1.087	1.087	1.085
A-H	1.086	1.478	1.542	1.083	1.473	1.537	1.079	1.470	1.535	1.077	1.470	1.537
A-X	1.086	1.478	1.542	1.373	1.599	1.732	1.799	2.076	2.180	1.965	2.231	2.322
C-A-H	111.2	110.6	110.7	111.6	111.1	113.2	111.8	111.6	113.1	112.5	111.5	112.8
C-A-X	111.2	110.6	110.7	109.5	109.4	107.2	111.5	109.6	107.7	111.2	110.1	108.1
H-A-H	107.7	108.3	108.2	108.7	109.6	110.5	109.0	109.7	110.5	109.6	109.8	110.4
H-A-X	107.7	108.3	108.2	107.7	107.8	106.1	106.2	107.1	105.9	105.3	106.9	106.1
A-C-H3	111.2	111.1	110.6	110.5	111.4	110.6	111.0	111.2	110.2	111.1	111.2	110.1
A-C-H5	111.2	111.1	110.6	110.3	110.5	110.3	109.2	110.2	110.3	109.3	110.0	110.3
H3-C-H4	107.7	107.8	108.3	108.4	107.8	108.5	108.5	108.0	108.7	108.5	108.2	108.9
H3-C-H5	107.7	107.8	108.3	108.5	107.8	108.4	108.5	108.0	108.6	108.4	108.0	108.7

Table 3.6: Geometric parameters of molecules of the form $MeAHX_2$

X	H			F			Cl			Br		
A	C	Si	Ge	C	Si	Ge	C	Si	Ge	C	Si	Ge
A-C	1.527	1.888	1.949	1.502	1.857	1.919	1.516	1.864	1.924	1.515	1.865	1.927
C-H3	1.086	1.086	1.084	1.083	1.086	1.084	1.082	1.085	1.083	1.081	1.085	1.083
C-H4	1.086	1.086	1.084	1.083	1.086	1.084	1.083	1.086	1.084	1.084	1.086	1.084
A-H	1.086	1.478	1.542	1.079	1.464	1.527	1.075	1.462	1.527	1.073	1.462	1.529
A-X	1.086	1.478	1.542	1.346	1.586	1.715	1.782	2.060	2.158	1.946	2.214	2.304
C-A-H	111.2	110.6	110.7	109.3	111.1	109.8	110.7	111.1	109.2	110.8	110.7	107.9
C-A-X	111.2	110.6	110.7	110.1	111.0	110.5	109.5	110.5	110.2	109.6	110.4	110.5
H-A-X	107.7	108.3	108.2	109.1	107.9	108.7	109.1	108.2	109.1	108.9	108.4	109.3
X-A-X	107.7	108.3	108.2	109.1	107.9	108.7	109.1	108.3	109.1	109.1	108.5	109.4
A-C-H3	111.2	111.1	110.6	113.8	114.1	119.0	111.9	113.7	117.4	113.0	113.8	117.6
A-C-H4	111.2	111.1	110.6	110.0	109.8	109.2	110.9	109.7	108.8	110.9	109.4	107.8
H3-C-H4	107.7	107.8	108.3	107.8	108.1	107.5	106.2	107.3	107.1	105.7	106.9	107.5
H4-C-H5	107.7	107.8	108.3	107.2	106.6	103.2	110.5	108.9	107.1	110.4	110.4	108.4

Figure 3.1: Atom numbering scheme for the methylated compounds

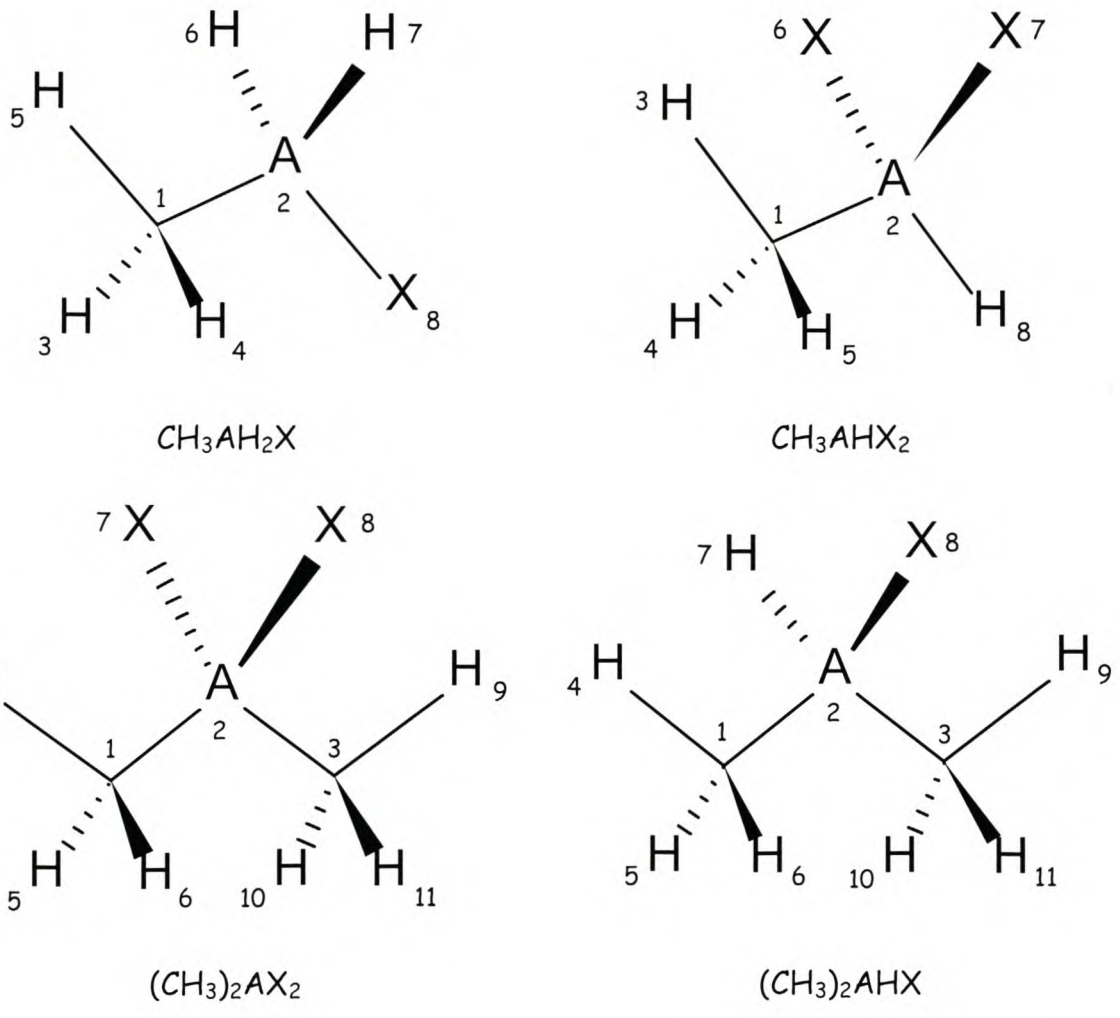

In the dihalo(dimethyl)germanes, -silanes and –propanes (Me_2AX_2), the main focus of the study, the A-C and A-X bond distances increase as the size of both the central atom A and the substituents X increases. For the previous two groups of compounds containing only one methyl substituent, this was not the case for the A-X distance. The C-H bond lengths increase from A=C to A=Ge, but for a specific central atom, they decrease from X=F to X=Br. The C-A-C angles of the molecules Me_2AX_2 for the series C, Si, Ge are shown in figure 3.2. for X=H, F, Cl, Br. Where the angles decrease slightly from A=C to A=Ge for X=H, the C-A-C angle is much larger for A=Ge than for A=C where X=F, Cl and Br. For X=F the angle decreases from A=C to A=Si and then increases dramatically between A=Si and A=Ge, for X=Cl there is an

almost linear increase along the series and for X=Br, the angle increases only very slightly from A=C to A=Si and then there is a large increase between A=Si and A=Ge. The C-A-X angle seems to be largely independent of the central atom A and remains at roughly 108.5° for X=F, Cl and Br. The angle for X=H also remains fairly constant along the series, but has a higher average value of about 109.5°. The X-A-X angles show a decrease along the series A=C to A=Ge that is roughly proportional to the increase in the C-A-C angle but not as dramatic. This is similar to what was seen for the dihalogermanes, -silanes and –methanes (AH_2X_2), although the effect was not as pronounced as it is in the dimethylated compounds.

Fig 3.2 : The C-A-C angle in the molecules of the form Me_2AX_2 with A=C, Si Ge and X=H, F, Cl, Br

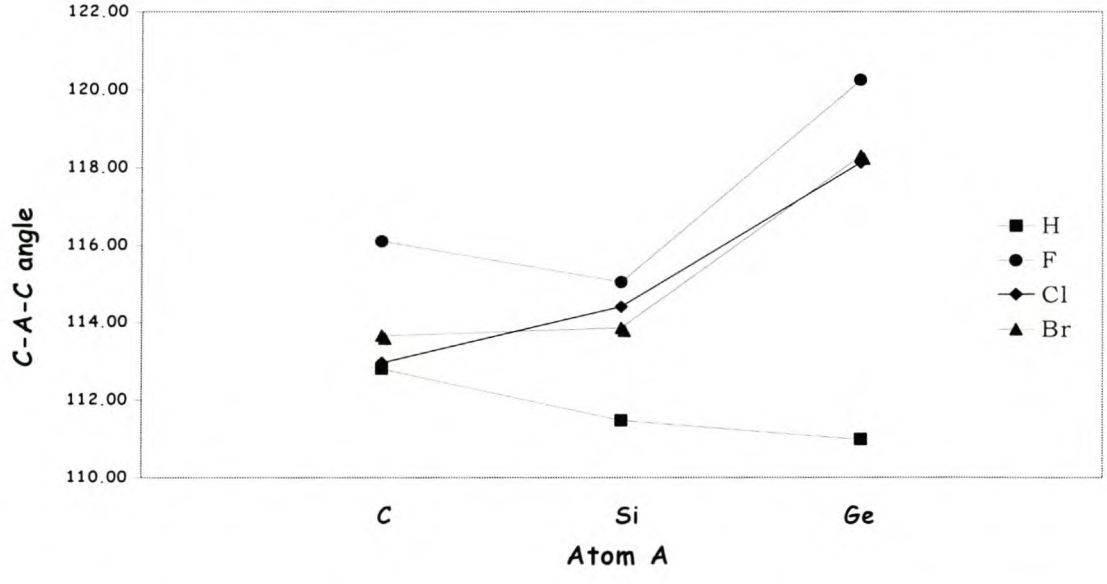

In the monohalo(dimethyl)germanes, -silanes and –propanes (Me_2AHX) both the A-C and A-X bond distances increase with increasing size of the central atom A and the substituents X, as was seen for the dihalogenated molecules. The A-H bond distances increase from A=C to A=Ge but decrease or remain constant for a fixed central atom from X=F to X=Br. All the C-H bond lengths increase from carbon to silicon but decrease again between silicon and germanium to values similar to those found for carbon.

Table 3.7: Geometric parameters of molecules of the form Me_2AX_2

X	H			F			Cl			Br		
A	C	Si	Ge	C	Si	Ge	C	Si	Ge	C	Si	Ge
A-C	1.528	1.890	1.951	1.509	1.861	1.921	1.521	1.867	1.926	1.519	1.867	1.927
A-X	1.087	1.481	1.549	1.354	1.592	1.721	1.798	2.069	2.170	1.964	2.222	2.317
C-H4	1.086	1.086	1.084	1.083	1.086	1.084	1.081	1.085	1.083	1.081	1.084	1.082
C-H5	1.087	1.087	1.085	1.083	1.086	1.085	1.084	1.086	1.084	1.084	1.086	1.084
C-A-C	112.8	111.5	111.0	116.1	115.0	120.2	112.9	114.4	118.1	113.7	113.8	118.3
C-A-X	109.4	109.5	109.6	108.6	108.9	108.2	108.9	108.6	108.0	108.7	108.5	107.6
X-A-X	106.3	107.5	107.4	105.9	105.8	102.5	108.4	107.8	106.3	108.1	109.1	107.6
A-C-H4	111.3	111.2	111.1	109.1	111.0	110.1	110.9	111.2	109.8	111.2	111.2	108.8
A-C-H5	111.1	111.2	110.5	110.3	111.2	110.4	109.5	110.6	110.0	109.5	110.3	110.0
H4-C-H5	107.8	107.6	108.1	109.0	107.8	108.6	109.0	108.1	109.0	108.9	108.4	109.3
H5-C-H6	107.6	107.7	108.3	109.2	107.8	108.7	109.1	108.2	109.2	109.0	108.3	109.5

Table 3.8: Geometric parameters of molecules of the form Me_2AHX

X	H			F			Cl			Br		
A	C	Si	Ge	C	Si	Ge	C	Si	Ge	C	Si	Ge
A-C	1.528	1.890	1.951	1.516	1.874	1.935	1.520	1.876	1.937	1.519	1.876	1.938
A-H	1.087	1.481	1.549	1.084	1.476	1.543	1.080	1.472	1.540	1.078	1.472	1.541
A-X	1.087	1.481	1.549	1.381	1.604	1.738	1.815	2.085	2.193	1.984	2.239	2.335
C-H4	1.086	1.086	1.084	1.084	1.086	1.084	1.083	1.085	1.083	1.082	1.085	1.083
C-H5	1.087	1.087	1.085	1.085	1.088	1.086	1.086	1.088	1.086	1.087	1.088	1.086
C-H6	1.087	1.087	1.085	1.085	1.087	1.085	1.084	1.086	1.084	1.084	1.086	1.084
C-A-C	112.8	111.5	111.0	114.0	112.2	113.9	113.3	112.5	113.2	113.7	112.0	112.2
C-A-H	109.4	109.5	109.6	110.1	110.4	112.0	110.1	110.7	112.5	110.8	110.8	112.7
C-A-X	109.4	109.5	109.6	108.0	108.4	106.5	109.3	108.4	106.4	108.9	108.7	106.5
HAX	106.3	107.5	107.4	106.4	106.9	105.3	104.3	106.0	105.1	103.2	105.6	105.5
A-C-H4	111.3	111.2	111.1	110.3	111.4	111.0	111.2	111.3	110.9	111.3	111.5	111.0
A-C-H5	111.1	111.2	110.5	110.7	110.8	110.3	109.3	110.4	110.5	109.2	110.1	110.6
A-C-H6	111.1	111.2	110.5	110.4	111.4	110.5	110.9	111.3	109.6	110.9	111.1	109.0
H4-C-H5	107.8	107.6	108.1	108.5	107.6	108.2	108.4	107.9	108.5	108.4	107.9	108.6
H4-C-H6	107.8	107.6	108.1	108.4	107.7	108.3	108.5	107.9	108.6	108.5	108.1	108.8
H5-C-H6	107.6	107.7	108.3	108.6	107.7	108.4	108.4	107.9	108.7	108.4	107.9	108.7

The C-A-C angles are interesting, since they do not show the same large increase from A=C to A=Ge that was found with two halogen substituents. The angles are 1° to 2° larger than those of the dimethylgermanes, -silanes and –methanes but the values for A=Ge are almost identical to those for A=C and for X=Br there is even a slight decrease. The C-A-H angles on the other hand, which are very nearly tetrahedral in molecules of the form Me_2AH_2, are similar for A=C and A=Si but increase from an average of 110.5° to one of 112.5° for A=Ge. Although this is still fairly close to tetrahedral, there is a significant difference between the values for A=C and Si and those for A=Ge. The C-A-X angles are also similar for A=C and Si, but they decrease by about 2° for A=Ge. The H-A-X angles increase slightly from A=C to A=Si and then decrease again from A=Si to A=Ge and all of them are smaller than the tetrahedral angle. For X=F, the C-Ge-C angle is smaller than the C-C-C angle but for the other two halogens the C-C-C angle is the smallest.

3.3.3. Symmetry Classification and Vibrations

The vibrational frequencies of the halomethanes, -silanes and –germanes and the 2,2-dihalopropanes, dihalo(dimethyl)silanes and dihalo(dimethyl)-germanes at their optimized geometries are listed in **Addendum B**, together with symmetry and assignment of each vibrational mode. The frequencies calculated with the force field are also included, but these will be discussed in **Chapter 5**. A point group analysis of the vibrational modes of molecules of the form AH_2X_2, AH_3X, AHX_3 and Me_2AX_2 is given in **Addendum C**.

Frequencies computed at HF level are known to contain systematic errors due to the neglect of electron correlation and are consistently overestimated by about 10%-12% [57]. It is therefore usual to scale frequencies by an empirical factor, the value of which differs slightly for different basis sets. For a 6-31G(d) basis set the scaling factor is 0.8929 [57] and the frequencies shown in **Addendum B** are the scaled frequencies.

For molecules of the form AH_nX_{4-n} there are 9 normal modes of vibration. For those molecules of the form AX_4, they are divided into 3 degenerate T_2 bend deformations, 2 degenerate E bend deformations, 3 degenerate T_2 stretches and one A_1 symmetrical stretch. The bending modes are generally lower in energy than the stretching modes but the exact order of the individual vibrations differs with changes in A and X.

Molecules of the form AH_3X all have one A_1 symmetric A-X stretching mode, two degenerate E asymmetric H-A-X bending modes, an A_1 symmetric H-A-X bending mode, two degenerate E H-A-H bending modes, a symmetric A_1 A-H stretching mode and two degenerate E A-H asymmetric stretching modes. In general the energy of the vibrations increases in the order A-X stretch < H-A-X bend < H-A-H bend < A-H stretch, but in some cases the H-A-X and H-A-H bending modes are interchanged and for some molecules the H-A-X bending mode is lower in energy than the A-X stretching mode.

Molecules of the form AHX_3 belong to the same point group as molecules of the form AH_3X and the number, symmetry and description of the vibrations is therefore identical, if H and X are interchanged in the assignment. The frequencies of the modes differ however, and the energy of the vibration increases in the order X-A-X bend < symmetric H-A-X bend < symmetric A-X stretch < asymmetric A-X stretch < asymmetric H-A-X bend < symmetric A-H stretch for all the molecules except in $GeHF_3$, where the asymmetric H-Ge-F bending modes are lower in energy than the symmetric Ge-F stretch.

In molecules of the form AH_2X_2 there are no degenerate modes and the vibrations consist of 4 A_1, one A_2, 2 B_1 and 2 B_2 modes. For all molecules of this form the lowest energy mode is the A_1 symmetric X-A-X bend and the highest energy modes are the A_1 symmetric and B_1 asymmetric C-H stretches, but the order of the in-between modes, which include the H-A-H rocking, twisting and wagging modes, the symmetric and asymmetric A-X stretching modes and a symmetric H-A-H bending mode, changes as A and X change.

For molecules of the form Me_2AX_2 there are 27 normal vibrational modes, of which 9 have A1 symmetry, 5 have A_2 symmetry, 6 have B_1 symmetry and 7 have B_2 symmetry. These consist of two A-X, two A-C and six C-H stretching modes, one X-A-X and one C-A-C bending mode, three C-A-X bending modes (the X-A-X rocking, twisting and wagging modes), six H-C-H and four A-C-H bending modes and two torsional modes. The vibrations of the methyl groups (the H-C-H bending and C-H stretching modes) have the highest energy, while the order of the other vibrations differs greatly from one molecule to another.

3.3.4. Partial Atomic Charges

The calculated partial atomic charges are summarized in tables 3.9 to 3.16. The numbering of the atoms is the same as for the geometric parameters and is shown in figure 3.1. Only the results for the dihalo(dimethyl)germanes are discussed.

For molecules of the form Me_2AX_2, the partial charge on the central atom decreases in the order Si > Ge > C, regardless of the X substituent. For A=Si and Ge the partial charge is a positive while for A=C it is slightly negative for X=H, Cl, Br but positive for X=F. The charge on X is negative throughout, except for propane, as is to be expected. The charges on the carbon atoms of the methyl groups are all negative with the carbon atoms bonded to silicon being the most negative, followed by those bonded to germanium and then those bonded to carbon. The charges on the hydrogen atoms of the methyl groups are positive and all in the region of 0.15 to 0.20, slightly larger for the halogenated compounds than for X=H.

The charges on atoms A and X are considerably larger for X = F, Cl, Br than for X=H, while the charges on the C atoms are comparable throughout with a slight increase for X=F. For a constant value of X, the partial charges on all the heavy atoms decrease in the order Si > Ge > C, regardless of whether X is

Table 3.9: Partial atomic charges for AX_4

X	H			F			Cl			Br		
A	C	Si	Ge	C	Si	Ge	C	Si	Ge	C	Si	Ge
Q_A	-0.660	0.545	-0.001	1.313	1.855	2.066	-0.364	0.931	0.604	-0.095	0.987	0.696
Q_X	0.165	-0.136	0.000	-0.328	-0.464	-0.516	0.091	-0.233	-0.174	0.024	-0.247	-0.174

Table 3.10: Partial atomic charges for AH_3X

X	H			F			Cl			Br		
A	C	Si	Ge	C	Si	Ge	C	Si	Ge	C	Si	Ge
Q_A	-0.660	0.545	-0.001	-0.063	0.993	0.572	-0.536	0.727	0.224	-0.475	0.724	0.231
Q_X	0.165	-0.136	0.000	-0.401	-0.514	-0.561	-0.176	-0.367	-0.290	-0.176	-0.364	-0.284
Q_H	0.165	-0.136	0.000	0.155	-0.160	-0.004	0.215	-0.120	0.022	0.217	-0.120	0.018

Table 3.11: Partial atomic charges for AH_2X_2

X	H			F			Cl			Br		
A	C	Si	Ge	C	Si	Ge	C	Si	Ge	C	Si	Ge
Q_A	-0.660	0.545	-0.001	0.452	1.326	1.081	-0.452	0.841	0.392	-0.320	0.849	0.420
Q_X	0.165	-0.136	0.000	-0.374	-0.498	-0.550	-0.033	-0.320	-0.241	-0.099	-0.322	-0.244
Q_H	0.165	-0.136	0.000	0.148	-0.165	0.010	0.259	-0.100	0.045	0.259	-0.102	0.034

Table 3.11: Partial atomic charges for AHX_3

X	H			F			Cl			Br		
A	C	Si	Ge	C	Si	Ge	C	Si	Ge	C	Si	Ge
Q_A	-0.660	0.545	-0.001	0.883	1.593	1.560	-0.400	0.903	0.512	-0.195	0.933	0.570
Q_X	0.165	-0.136	0.000	-0.346	-0.481	-0.536	0.034	-0.276	-0.194	-0.034	-0.283	-0.207
Q_H	0.165	-0.136	0.000	0.154	-0.148	0.049	0.299	-0.076	0.070	0.296	-0.083	0.052

Table 3.12: Partial atomic charges for $MeAH_2X$

X	H			F			Cl			Br		
A	C	Si	Ge	C	Si	Ge	C	Si	Ge	C	Si	Ge
Q_A	-0.476	0.683	0.207	0.115	1.094	0.747	-0.375	0.846	0.416	-0.307	0.843	0.423
Q_C	-0.476	-0.783	-0.710	-0.522	-0.807	-0.732	-0.483	-0.789	-0.712	-0.482	-0.787	-0.714
Q_X	0.159	-0.150	-0.019	-0.412	-0.513	-0.562	-0.119	-0.384	-0.319	-0.192	-0.381	-0.312
Q_{H6}	0.159	-0.150	-0.019	0.150	-0.172	-0.024	0.214	-0.130	0.006	0.216	-0.131	0.001
Q_{H5}	0.159	0.183	0.187	0.161	0.184	0.191	0.173	0.189	0.194	0.172	0.188	0.193
Q_{H4}	0.159	0.183	0.187	0.179	0.193	0.202	0.187	0.200	0.205	0.188	0.199	0.204

Table 3.13: Partial atomic charges for $MeAHX_2$

X	H			F			Cl			Br		
A	C	Si	Ge	C	Si	Ge	C	Si	Ge	C	Si	Ge
Q_A	-0.476	0.683	0.207	0.627	1.394	1.222	-0.316	0.941	0.569	-0.174	0.948	0.593
Q_C	-0.476	-0.783	-0.710	-0.560	-0.821	-0.746	-0.477	-0.788	-0.709	-0.472	-0.784	-0.710
Q_X	0.159	-0.150	-0.019	-0.388	-0.498	-0.553	-0.036	-0.335	-0.268	-0.107	-0.337	-0.271
Q_{H8}	0.159	-0.150	-0.019	0.147	-0.174	-0.010	0.262	-0.106	-0.106	0.262	-0.110	0.025
Q_{H3}	0.159	0.183	0.187	0.197	0.205	0.221	0.208	0.214	0.219	0.207	0.213	0.216
Q_{H4}	0.159	0.183	0.187	0.182	0.196	0.209	0.198	0.204	0.210	0.195	0.203	0.208

Table 3.14: Partial atomic charges for Me_2AHX

X	H			F			Cl			Br		
A	C	Si	Ge	C	Si	Ge	C	Si	Ge	C	Si	Ge
Q_A	-0.302	0.824	0.417	0.278	1.194	0.926	-0.232	0.907	0.609	-0.156	0.962	0.613
Q_C	-0.476	-0.784	-0.715	-0.515	-0.808	-0.739	-0.472	-0.789	-0.716	-0.472	-0.788	-0.718
Q_x	0.155	-0.162	-0.037	-0.426	-0.509	-0.563	-0.124	-0.399	-0.345	-0.203	-0.394	-0.337
Q_{H7}	0.155	-0.162	-0.037	0.150	-0.181	-0.043	0.216	-0.138	-0.006	0.217	-0.140	-0.010
Q_{H4}	0.160	0.181	0.185	0.181	0.191	0.200	0.190	0.198	0.203	0.191	0.198	0.202
Q_{H5}	0.156	0.177	0.179	0.159	0.180	0.185	0.170	0.183	0.187	0.168	0.182	0.186
Q_{H6}	0.156	0.177	0.179	0.173	0.186	0.194	0.183	0.194	0.197	0.184	0.194	0.196

Table 3.15: Partial atomic charges for Me_2AX_2

X	H			F			Cl			Br		
A	C	Si	Ge	C	Si	Ge	C	Si	Ge	C	Si	Ge
Q_A	-0.302	0.824	0.417	0.792	1.463	1.371	-0.203	1.041	0.747	-0.052	1.045	0.768
Q_C	-0.476	-0.784	-0.715	-0.546	-0.821	-0.752	-0.458	-0.786	-0.709	-0.454	-0.783	-0.713
Q_X	0.155	-0.162	-0.037	-0.403	-0.494	-0.554	-0.036	-0.346	-0.289	-0.110	-0.346	-0.291
Q_{H4}	0.160	0.181	0.185	0.198	0.203	0.217	0.210	0.213	0.218	0.209	0.212	0.215
Q_{H5}	0.156	0.177	0.179	0.178	0.191	0.202	0.193	0.199	0.204	0.191	0.198	0.203

a halogen or hydrogen. The bonding in the Si and Ge compounds is clearly more ionic than in the C compounds and the ionic character of the bonding increases when halogen substituents are present. However, although the bonding in the dihalo(dimethyl)germanes is a great deal more ionic than that of the dimethylgermanes or the 2,2-dihalopropanes, the bonding in the dihalo(dimethyl)silanes is even more so. While the degree of ionic or covalent bonding in these compounds may be a factor in the size of the C-A-C angle, a comparison of the partial charges for and the C-A-C angles for A=Si and A=Ge, shows that it cannot be the only factor.

3.3.5. Electron Density

The total electron density distributions of Me_2GeH_2, Me_2GeF_2 and Me_2CF_2 are shown in figure 3.3. In the case of 2,2-difluoropropane, the electron density is diffuse and evenly distributed over the whole molecule. There is clearly much delocalisation of electrons, indicating a high degree of covalency in the bonds between the atoms despite the presence of the highly electronegative fluorine substituents.

In contrast, the electron density of difluoro(dimethyl)germane is very much localised on individual atoms, except between the carbon and hydrogen

Figure 3.3: Total electron density distributions

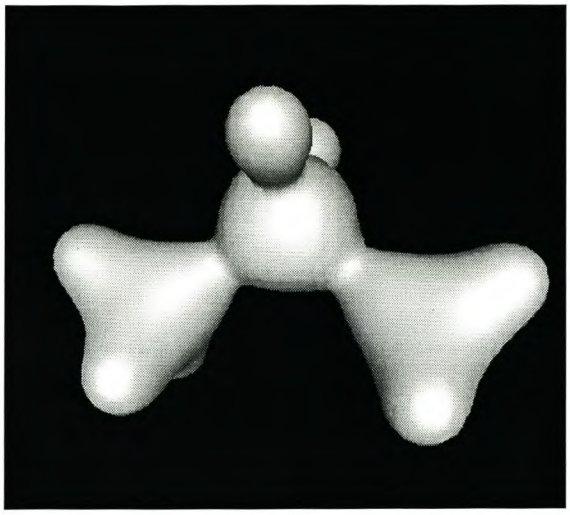

$(CH_3)_2GeH_2$

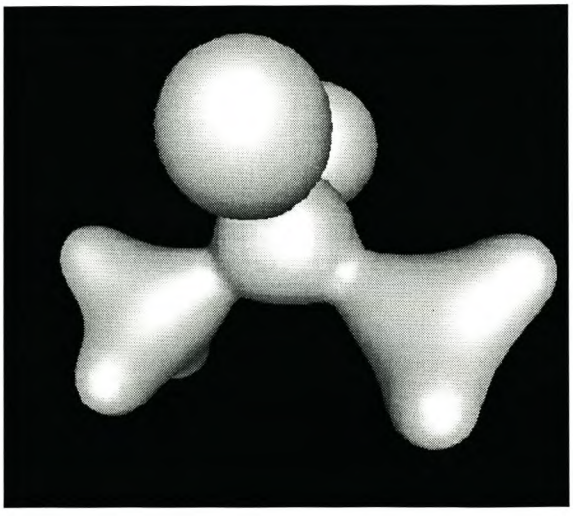

$(CH_3)_2GeF_2$

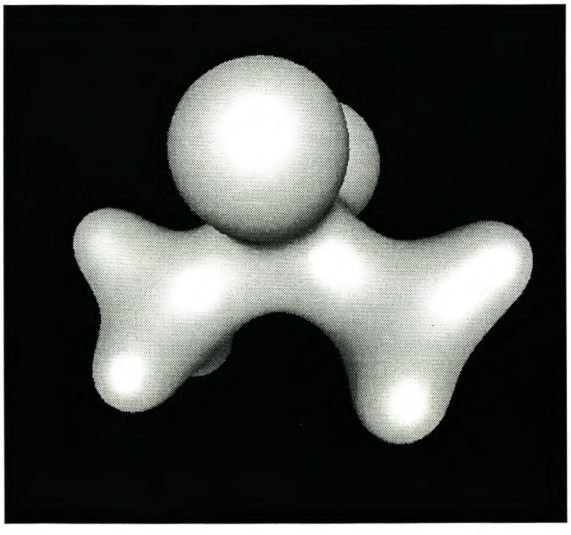

$(CH_3)_2CF_2$

atoms of the two methyl substituents. There is clear definition between the electrons belonging to the central atom and those of the substituents. This indicates that the bonding in this molecule is much more ionic in nature than that of the corresponding carbon compound. This can be attributed partly to the larger difference in electronegativity between germanium and fluorine ($\Delta\chi$=2.08 on the Allred and Rochow scale) than between carbon and fluorine ($\Delta\chi$=1.60) and to the fact that the C-C bond is homonuclear ($\Delta\chi$=0) while the C-Ge bond is heteronuclear ($\Delta\chi$=0.48).

The general shape of the electron density of dimethylgermane is similar to that of difluoro(dimethyl)germane, except for the much smaller electron cloud surrounding the H atoms attached to germanium. Hydrogen is only slightly more electronegative than germanium and the difference is much less than for fluorine, but the small size of the hydrogen atom could be a contributing factor in the ionicity of this compound.

Although the differences in the total electron distribution of these three molecules are interesting, they provide little insight into possible reasons for the large C-Ge-C angles in the dihalo(dimethyl)germanes as opposed to the corresponding angles in dimethylgermane or the 2,2-dihalopropanes.

3.3.6. Valence Molecular Orbitals

The outer valence molecular orbitals of dimethylgermane, difluoro(dimethyl)-germane and 2,2-difluoropropane are shown in **Addendum A**. They are named in the manner AXn, where A is the central atom, X is the substituent and n the number of the molecular orbital according to the Gaussian98, where they are numbered from lowest to highest energy. The diagrams are arranged so that orbitals with the same symmetry and similar distribution for the three molecules are shown next to each other.

There are both some interesting similarities and differences between the orbitals of dimethylgermane and difluoro(dimethyl)germane and between

those of difluoro(dimethyl)germane and 22-difluoropropane, but these are much to be expected on the grounds of the respective atomic orbitals involved in the hybridization and once again they do not contribute anything to the question of the large C-Ge-C angle of the dihalo(dimethyl)germanes.

3.3.7. Calculations at Higher Levels of Theory

A complete list of the geometric parameters calculated at MP2 and DFT levels of theory for molecules of the form Me_2AX_2 (A=C, Si, Ge and X=H, F, Cl, Br) is given in tables 3.16. and 3.17. The heavy atom parameters are compared to those obtained with the RHF method in **Addendum D**. It is clear that the only parameter that is significantly affected by the change to a higher level of theory (taken as a percentage difference of more than 1%) is the A-X bond distance. For all the other heavy atom parameters, including the C-A-C angle that is the focus of our study, the percentage difference between both the RHF and MP2 values and the RHF and DFT values remains below 1%.

Since the A-X bond length is not the focal point of the study and since the C-A-C angle is not significantly affected, it was decided that a change to a higher level of theory was unnecessary for the purposes of this work. The large group of molecules being studied and the increase in computational time this would require did not seem worth the small increase in accuracy that would result.

This is in agreement with the findings of Jonas, Boehme and Frenking [18] in their *ab initio* study of molecules Me_2ACl_2, with A=C, Si, Ge, Sn, Pb, Ti, Zr, Hf, namely that the angles calculated at HF and MP2 levels of theory do not differ significantly from each other. The bond lengths are not mentioned, but it can be assumed that they too found any changes in bond length between the two methods insignificant for their purposes, which was the investigation of the changes in bond angles along the series.

Table 3.16: MP2 Geometric parameters of molecules of the form Me_2AX_2

X	H			F			Cl			Br		
A	C	Si	Ge	C	Si	Ge	C	Si	Ge	C	Si	Ge
A-C	1.526	1.885	1.950	1.506	1.855	1.919	1.517	1.862	1.925	1.516	1.861	1.925
A-X	1.096	1.491	1.561	1.384	1.617	1.762	1.795	2.064	2.168	1.974	2.226	2.326
C-H4	1.094	1.093	1.092	1.091	1.093	1.092	1.091	1.093	1.092	1.091	1.093	1.091
C-H5	1.095	1.094	1.093	1.092	1.094	1.093	1.093	1.094	1.093	1.094	1.094	1.093
C-A-C	112.4	111.0	110.9	116.7	114.6	121.1	113.1	114.2	118.2	114.1	114.2	119.4
C-A-X	109.5	109.6	109.7	108.4	108.9	107.9	108.7	108.6	107.9	108.7	108.4	107.3
X-A-X	106.3	107.5	107.2	106.0	106.1	102.6	108.7	108.2	106.5	107.9	109.1	107.6
A-C-H4	111.5	111.4	110.9	108.7	111.1	109.8	110.7	110.9	109.2	110.9	110.8	108.0
A-C-H5	110.8	111.0	110.3	110.1	110.9	110.2	109.4	110.5	109.8	109.3	110.1	109.8
H4-C-H5	107.9	107.8	108.4	109.3	107.9	108.8	109.1	108.2	109.2	109.0	108.6	109.7
H5-C-H6	107.7	107.8	108.5	109.4	107.9	108.9	109.2	108.4	109.5	109.3	108.7	110.0

Table 3.17: DFT Geometric parameters of molecules of the form Me_2AX_2

X	H			F			Cl			Br		
A	C	Si	Ge	C	Si	Ge	C	Si	Ge	C	Si	Ge
A-C	1.532	1.891	1.954	1.516	1.862	1.927	1.522	1.870	1.934	1.519	1.870	1.935
A-X	1.099	1.493	1.555	1.381	1.613	1.751	1.828	2.087	2.194	1.993	2.234	2.337
C-H4	1.096	1.096	1.094	1.093	1.095	1.093	1.092	1.094	1.092	1.092	1.094	1.092
C-H5	1.097	1.096	1.095	1.094	1.096	1.094	1.095	1.096	1.094	1.096	1.096	1.094
C-A-C	112.9	111.9	111.1	116.4	114.9	121.0	113.8	114.7	118.7	114.7	113.9	118.6
C-A-X	109.4	109.4	109.6	108.4	108.9	107.9	108.7	108.5	107.7	108.6	108.4	107.5
X-A-X	106.1	107.1	107.2	106.2	106.0	102.9	108.3	108.0	106.6	107.7	109.4	108.0
A-C-H4	111.5	111.1	110.9	109.1	111.0	109.8	111.0	110.9	109.4	111.3	110.9	108.4
A-C-H5	111.1	111.2	110.4	110.4	111.0	110.1	109.5	110.4	109.6	109.6	110.1	109.6
H4-C-H5	107.7	107.7	108.3	109.0	107.9	108.9	108.9	108.3	109.3	108.7	108.5	109.7
H5-C-H6	107.5	107.8	108.5	109.0	107.9	109.0	109.0	108.4	109.6	108.9	108.5	109.9

3.3.8. Iodine Containing Compounds

Table 3.18. contains the geometric parameters of 2,2-diiodopropane, diiodo-(dimethyl)silane and diiodo(dimethyl)germanes as calculated at RHF, MP2 and DFT level. It is clear that, although the C-Ge-C angle still increases in the order A=C, Si, Ge, the effect is a great deal less pronounced in the iodine compounds than for the other halogens. This is in keeping with the general trend, namely that the increase in size of the C-A-C angle due to halogen substitution decreases with increasing molecular mass of the halogen.

Table 3.18: Geometric parameters of molecules of the form Me_2AI_2

Theory	RHF			MP2			DFT		
A	C	Si	Ge	C	Si	Ge	C	Si	Ge
A-C	1.535	1.880	1.952	1.557	1.898	1.971	1.536	1.884	1.961
A-X	2.215	2.546	2.600	2.227	2.556	2.613	2.242	2.566	2.626
C-H4	1.080	1.082	1.082	1.102	1.104	1.103	1.093	1.095	1.094
C-H5	1.084	1.084	1.084	1.106	1.106	1.105	1.098	1.097	1.097
C-A-C	112.2	114.6	115.7	112.4	113.5	114.2	113.4	115.1	116.0
C-A-X	108.8	108.2	108.0	108.6	108.3	108.1	108.6	108.1	107.8
X-A-X	109.4	109.1	109.0	110.1	110.2	110.2	109.2	109.4	109.5
A-C-H4	112.0	111.2	110.6	111.8	111.4	110.8	112.1	111.1	110.3
A-C-H5	109.6	110.3	109.8	109.5	110.4	110.0	109.6	110.3	109.7
H4-C-H5	108.5	108.2	108.7	108.5	108.0	108.4	108.5	108.8	108.8
H5-C-H6	108.6	108.7	109.2	109.0	108.7	109.2	108.6	109.4	109.4

3.4. Discussion

The results show clearly that the C-Ge-C angles in the dihalo(dimethyl)-germanes are exceptionally large. It is also clear that this is not the case for analogous carbon compounds or for compounds where the halogens have been replace by hydrogen atoms. The other two group IV elements, tin and

lead, were excluded from this study mainly due to the computational time factor. However, this makes it impossible to state with any certainty that the large C-Ge-C angles in the dihalo(dimethyl)germanes are, in fact, anything out of the ordinary. It can also be argued that it is the C-Si-C angle in the dihalo(dimethyl)silanes that is abnormally small, while the group trend is towards an increase in the C-A-C angle. This view is supported by a previous study [20] in which Me_2PbF_2 was optimized by HF methods and was shown to have a C-Pb-C angle of 134.8°, as opposed to angles of 116.4° and 109.5° in Me_3PbF and Me_4Pb respectively.

Another possibility is that there is an increase in C-A-C angles as one moves down group IV, but that the trend is of a higher order than linear, so that increases that initially seem abnormally large on a linear scale are not out of the ordinary when a higher order fitting is done. Figure 3.4. shows a plot of the C-A-C angles for molecules of the form Me_2AF_2 and Me_2ACl_2, where A is a group IV element, for which second order polynomial functions have been fitted to the calculated values. For Me_2AF_2 the first three values are those that have been calculated in this study and the value for A=Pb is taken from the study mentioned above [20]. For Me_2ACl_2 the values have been taken from calculations by Jonas, Boehme and Frenking [18], which give C-A-C angles of 113.0°, 114.5°, 118.6°, 122.1° and 128.6° for A=C, Si, Ge, Sn and Pb respectively.

The fit of the polinomial function is good for both groups of compounds, with R^2 values of 0.9922 for Me_2AF_2 and 0.9957 for Me_2ACl_2. Although calculated data for Me_2SnF_2 is not available, interpolation of the fitted function would lead to a value of around 127° for the C-Sn-C angle, which is remarkably similar to the average C-Sn-C angle of 128.7° found for crystal structures of the form R_2SnX_2 in the CSD. The second order polynomial function seems to be a good starting approximation for the trend in C-A-C angles in Me_2AX_2.

Figure 3.4 : The C-A-C angles for Me_2AF_2 and Me_2ACl_2 fitted with second order polinomial functions

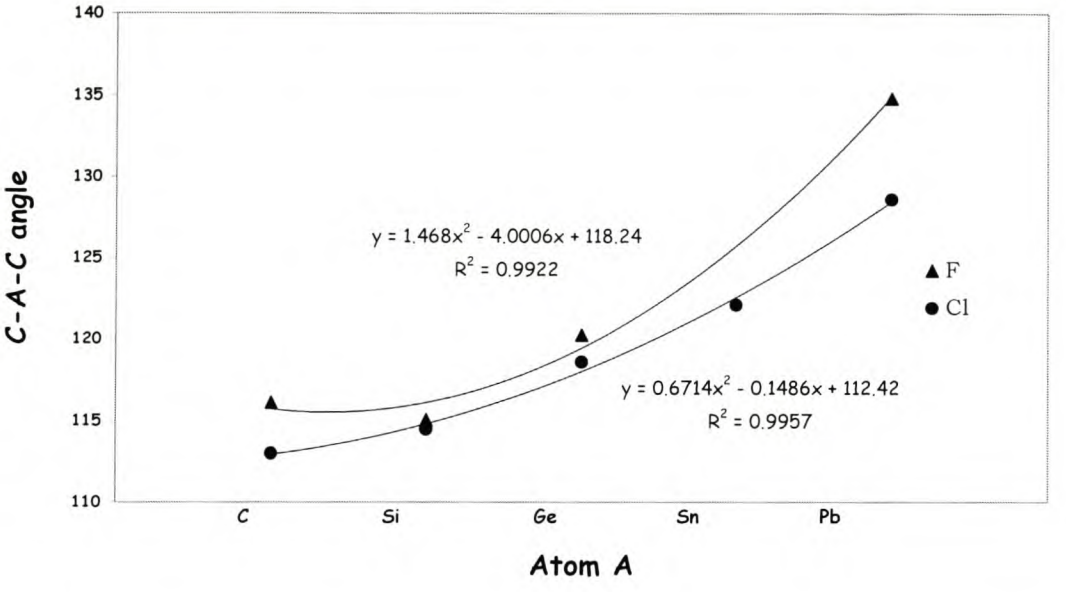

Qualitatively, some of the results can be explained in terms of three bonding models, the VSEPR theory [50], Bent's Rule [51] and a modification of the LCP model [52]. For a general discussion of these theories, see **Chapter 2**.

In terms of the VSEPR theory, the geometry of the dihalo(dimethyl)germanes can be explained as follows. Firstly, the repulsions exerted by the bonding electron-pairs decrease with increasing electronegativity of the ligand. Since $\chi(X) > \chi(C)$ for X = F, Cl and Br, for the dihalo(dimethyl)germanes this implies that the X-A-X angle should decrease below and the C-A-C angle increase above the tetrahedral value of 109.47°, which is exactly the effect that is seen. Furthermore, as the electronegativity of the ligand X decreases in the order F > Cl > Br, one would expect deviations in the X-A-X and C-A-C angles to decrease accordingly, which is also found to be the case.

The second postulate states that the repulsions between electron-pairs in filled shells are larger than those between electron-pairs in incompletely filled shells. The resistance to factors that tend to decrease the bond angles will therefore be greater in the filled valence shell of carbon than it is for germanium or any of the other group IV elements. For Me_2AX_2 the decrease

in the X-A-X angle and the subsequent increase in the C-A-C angle due to electronegativity differences will therefore not be as dramatic for carbon and should increase down group IV as more space becomes available in the valence shells of the central atom. This would explain the observed increase in the deviations of the bond angles from A=C to A=Ge.

Bent's rule states that atomic s character concentrates in orbitals directed towards more electropositive substituents. For the dihalo(dimethyl)germanes this will cause a decrease in the X-A-X angle and an increase in the C-A-C angle as the s-character of the bonding orbitals directed towards the carbon atoms increases and the p-character of the bonding orbitals directed towards the halogens increases. The effective electronegativity of a methyl group is very close to the electronegativity of hydrogen [20] and the same effect is therefore not seen in the dimethylgermanes.

Furthermore, Bent's rule also says that if the electronegativity of X remains fixed, a decrease in the electronegativity of the central atom A has the same effect as an increase in the electronegativity of X. Although this rule is only stated for molecules where the other two substituents are unshared electron pairs, if it is extended to include electron-pairs bonded to atoms that are more electropositive than X, this would imply that the increase in the C-A-C angle and decrease in X-A-X angle would become more pronounced as the electronegativity of A decreases in the order C > Si > Ge.

If one assumes that bonding in Me_2AX_2 is predominantly covalent for A=C and becomes increasingly more ionic as one moves down group IV, as the electron density and partial atomic charges suggest, the LCP model would gain increasing importance with the increased ionic nature of the molecule. If the ligand close-packing of the halogens were taken as the predominant factor in determining geometry, the X-A-X angle would decrease as the size of the central atom A increases in order to maintain the proposed constant non-bonded distance between the halogen substituents. The LCP model on its own however, is unable to explain the increase in C-A-C angle that goes

with this decrease in X-A-X angle. A mixed ionic and covalent model, where the geometry of the X-A-X fragment is based on the LCP model while the geometry of the Me-A-Me fragment is based on the hybridization of atomic orbitals, would lead to much the same geometry as that predicted by Bent's Rule and would be in accordance with the results of this study.

3.5. Conclusion

The results of the *ab initio* calculations are in agreement with experimental geometric parameters obtained from gas phase electron diffraction, within the experimental errors quoted. However, the calculated C-Ge-C angles are consistently lower than the electron diffraction values and it is likely that experimental errors in the ED results lead to quoted values that are larger than what is actually the case.

It is clear that electronegativity does play a role in opening up the C-Ge-C angle in the dihalo(dimethyl)germanes. It is unlikely however, that this is the only factor at play here, or even the most important factor. The more likely scenario is that it is the combination and interaction of the electronegative substituents and some property of germanium, which is not found in carbon or silicon, which causes the increase.

We have seen that the C-Pb-C angle in Me_2PbF_2 is also exceptionally large and the C-Sn-C angles found in the dihalo-dialkyl tin compounds on the CCDB are also in the region of 120° to 130°. Since germanium, tin and lead all have filled d-orbitals in their outer valence shells, which carbon and silicon do not, it is possible that the d-orbitals play a role in opening up the C-A-C angle.

The VSEPR theory, Bent's Rule and a modification of the LCP model are able to qualitatively explain some aspects of the molecular geometry of the dihalo-(dimethyl)germanes. However, none of these theories is able to sufficiently explain all the aspects of their geometry.

CHAPTER 4: SYNTHESIS OF $(PhCH_2CH_2)_2GeCl_2$ AS REPRESENTATIVE COMPOUND

4.1. Introduction

Due to the lack of reliable and appropriate experimental data on the geometry of compounds of the form R_2GeX_2, where R is an alkyl group and X a halogen, it was decided to synthesize a structure representative of this type of molecule. This was done to obtain experimental verification of the results of previous experimental studies and the *ab initio* calculations reported in **Chapter 3**.

In choosing an appropriate compound for the synthesis, there were a number of factors to be considered. Firstly, the compound had to be bulky enough to crystallize at room temperature so that reliable crystal structure data of the molecule could be obtained. Since the X-Ge-X fragment is fixed, this meant that the size of the alkyl chain R had to be varied. Secondly, it was important to choose the alkyl group so that the properties of the carbon atom attached to the central Ge were as close to those of a methyl group as possible. This meant that any substituents on the alkyl chains had to be far enough away from the central atom so as not to cause any steric hindrance or electronic effects that could influence the C-Ge-C angle.

Since these two requirements can be conflicting, a compromise had to be reached. The compound that was finally decided upon was dichlorobis-(phenethyl)germane ($(PhCH_2CH_2)_2GeCl_2$), containing two phenyl groups to provide the bulk needed for crystallization, but far enough away from the central atom not to influence the C-Ge-C angle.

The experimental details of the synthesis, including the materials and physical methods used, as well as the reactions, is contained in **Section 4.2.** In **Section 4.3.** the product is characterised by means of electron-spray mass spectroscopy, NMR and crystal structure determination by X-ray diffraction. The results are summarized in **Section 4.4.** and the chapter is concluded in **Section 4.5.**

4.2. Experimental

4.2.1. Materials

Magnesium turnings were obtained from Saarchem and dried overnight in an oven at 80-100° before use. Tetrachlorogermane and phenethyl chloride were purchased from Aldrich and used without further purification. Phenethylmagnesium chloride was prepared according to standard literature methods for Grignard reactions [87,88]. Diethylether, benzene and tetrahydrofuran were dried over sodium wire and distilled under nitrogen shortly before use. Dichloromethane was dried over CaH_2 and also distilled under nitrogen shortly before use.

4.2.2. Physical methods

All the reactions and manipulations of the product were performed under nitrogen atmosphere using standard vacuum and Schlenk techniques [87,88]. NMR spectra (^1H at 300 MHz, $^{13}C\{^1H\}$ at 75 MHz) were recorded on a Varian VXR 300FT spectrometer with Me_4Si as an internal standard. The electron-spray mass spectrum (ESMS) was recorded on a VG Quattro mass spectrometer with an electron spray ionization source. The crystal structure data was collected on a Nonius Kappa CCD diffractometer [89] by Dr. John Bacsa of the University of Cape Town, South Africa and the crystal structure was solved by Prof. Jan Dillen of the University of Stellenbosch.

4.2.3. Reactions

Preparation of $PhCH_2CH_2MgCl$:

Diethylether (25 ml; 17 g; 0.238 mol) was added to dry magnesium turnings (1.823 g; 0.075 mol) and the resulting solution stirred. To this was added 5ml of a mixture of phenethyl chloride (6.577 ml; 7.031 g; 0.05 mol) and diethylether (25 ml; 17 g; 0.238 mol) and the solution warmed slightly to initiate the reaction while continuing the stirring throughout. Once the reaction was sufficiently underway (indicated by a slight milkyness of the solution) the rest of the phenethyl chloride and ether mixture was added dropwise to the reaction flask and the solution refluxed for a further 2 hours.

Preparation of $(PhCH_2CH_2)_2GeCl_2$:

Phenethylmagnesium chloride from the previous reaction was added dropwise to a solution of tetrachlorogermane (5.360 g; 0.025 mol) in THF (20 ml; 17.78 g; 0.2218 mol) and the reaction mixture stirred at ambient temperature for 16 hours. The solvent was then distilled off under vacuum, benzene (75 ml; 65.55 g; 0.7797 mol) was added and the solution heated under reflux for a further hour. The product was left to cool and precipitate at room temperature and the solution was evaporated to dryness.

Re-crystallization of the product:

Enough hexane was added to the product of the previous reaction to dissolve it and the resulting solution filtered. The filtered solution was then distilled to half its original volume and left to stand for crystallisation. The crystals obtained were evaporated to dryness, dissolved in hexane, separated into three parts and layered with THF, dichloromethane and ether for the final recrystallization.

4.3. Characterization

4.3.1. ESMS

The ESMS of the product is shown in figure 4.1. and enlargements of the spectrum are shown in figures I-IV of **Addendum E**. Electronspray mass spectrometry makes use of a non-fragmental ionisation method called electronspray ionization. The sample is introduced onto the machine as a high-pressure stream of a mixture of an aqueous solution of the sample and an organic solvent, in this case 50% acetonitrile. In the inlet of the mass spectrometer the liquid is broken up into highly charged droplets to form an electron spray, which is gradually broken up into smaller droplets, clusters and ionic species and finally the constituent ions. The recorded peaks are therefore not simple fragments of the parent ion, but aggregates of water, acetonitrile, the product and its fragments and any impurities found in the sample.

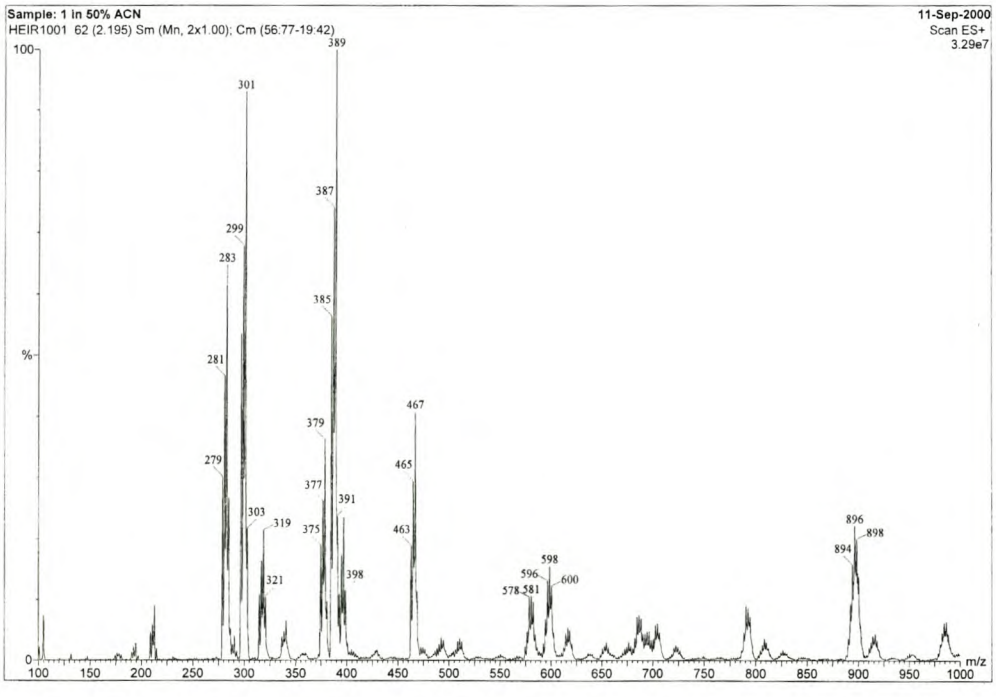

Figure 4.1: ESMS of the product

The peak assignments are given in table 4.1. The fragments containing germanium can be clearly distinguished by the fine structure caused by the five isotopic species of germanium. From the spectrum it is clear that the main product is in fact dichlorobis(phenethyl)germane and the molecular ion is present in a number of the fragments. There seems also to be some of the tri-chlorinated species present, although in much smaller quantities. There is a possibility of slight traces of the mono-chlorinated species being present, but this is only evident in peaks 12,13 and 14 and it is more likely that the peaks are due to the main product. The peaks with m/z > 800 have not been assigned as ESMS becomes unreliable at high m/z ratios.

Table 4.1: Peak analysis of the ESMS

Peak	m/z	Assignment
1	105	$PhCH_2CH_2$
2	177, 178, 181	$PhCH_2CH_2Ge$
3	191, 193, 195	$PhCH_2CH_2Ge + H_2O$
4	209, 211, 213, 215	$PhCH_2CH_2Ge + 2H_2O$
5	279, 281, 283, 285	$(PhCH_2CH_2)_2Ge$
6	297, 299, 301	$(PhCH_2CH_2)_2Ge + H_2O$
7	315, 317, 319, 321	$(PhCH_2CH_2)_2Ge + 2H_2O$
8	375, 377, 379	$PhCH_2CH_2GeCl_3 + CH_3CN + 3H_2O$
9	385, 387, 389	$(PhCH_2CH_2)_2GeCl_2 + 2H_2O$
10	397, 398	$PhCH_2CH_2GeCl_3 + CH_3CN + 4H_2O$
11	463, 465, 467, 469	$(PhCH_2CH_2)_2GeCl_2 + CH_3CN + 4H_2O$
12	576, 578, 581, 582	$(PhCH_2CH_2)_2GeCl_2 + 2CH_3CN + 8H_2O$ / $(PhCH_2CH_2)_3GeCl + 3CH_3CN + 2H_2O$
13	595, 596, 598, 600	$(PhCH_2CH_2)_2GeCl_2 + 2CH_3CN + 9H_2O$ / $(PhCH_2CH_2)_3GeCl + 3CH_3CN + 3H_2O$
14	614, 616, 618	$(PhCH_2CH_2)_2GeCl_2 + 2CH_3CN + 10H_2O$ / $(PhCH_2CH_2)_3GeCl + 3CH_3CN + 4H_2O$
15	683, 685, 686, 688	$2PhCH_2CH_2GeCl_3 + 2CH_3CN + 2H_2O$
16	702, 705, 707	$2(PhCH_2CH_2)_2GeCl_2$
17	722	$2(PhCH_2CH_2)_2GeCl_2 + H_2O$
18	788, 790, 792, 794	$(PhCH_2CH_2)_2GeCl_2 + C_6H_{14}$

4.3.2. NMR

Data from the ^{1}H and $^{13}C\{^{1}H\}$ spectra of the product are given in tables 4.2. and 4.3, the spectra are shown in figures 4.2 and 4.3 and the enlargements in figures V-X of **Addendum E**.

Table 4.2: Peak analysis of the ^{1}H NMR

Peak	Frequency	ppm	Intensity	Assignment
1	2204.03	7.36	0.272	
2	2197.29	7.33	0.613	
3	2195.66	7.33	0.379	H5
4	2191.24	7.31	0.263	
5	2189.83	7.31	0.684	
6	2184.69	7.29	0.541	Chloroform
7	2179.28	7.27	0.319	
8	2177.88	7.27	0.206	H6
9	2172.13	7.25	0.363	
10	2156.13	7.2	0.536	
11	2154.52	7.19	0.640	H4
12	2149.23	7.17	0.251	
13	2147.69	7.17	0.420	
14	861.58	2.88	0.421	
15	853.55	2.85	0.431	H2
16	851.41	2.84	0.230	
17	845.24	2.82	0.461	
18	650.95	2.17	10.756	Acetone
19	523.06	1.75	0.917	
20	516.78	1.72	0.351	
21	514.77	1.72	0.806	H1
22	513.13	1.71	0.353	
23	506.74	1.69	0.804	
26	-0.17	0.00	138.333	TMS

Figure 4.2: ^{1}H NMR spectrum of the product

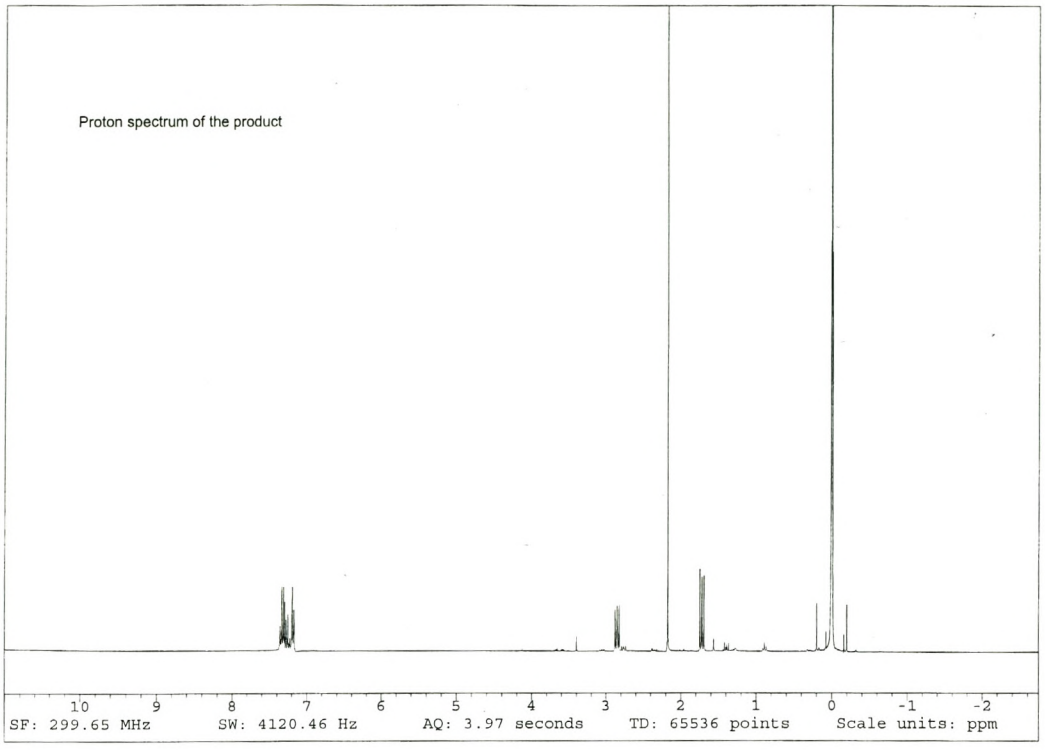

Figure 4.3: $^{13}C\{^{1}H\}$ NMR spectrum of the product

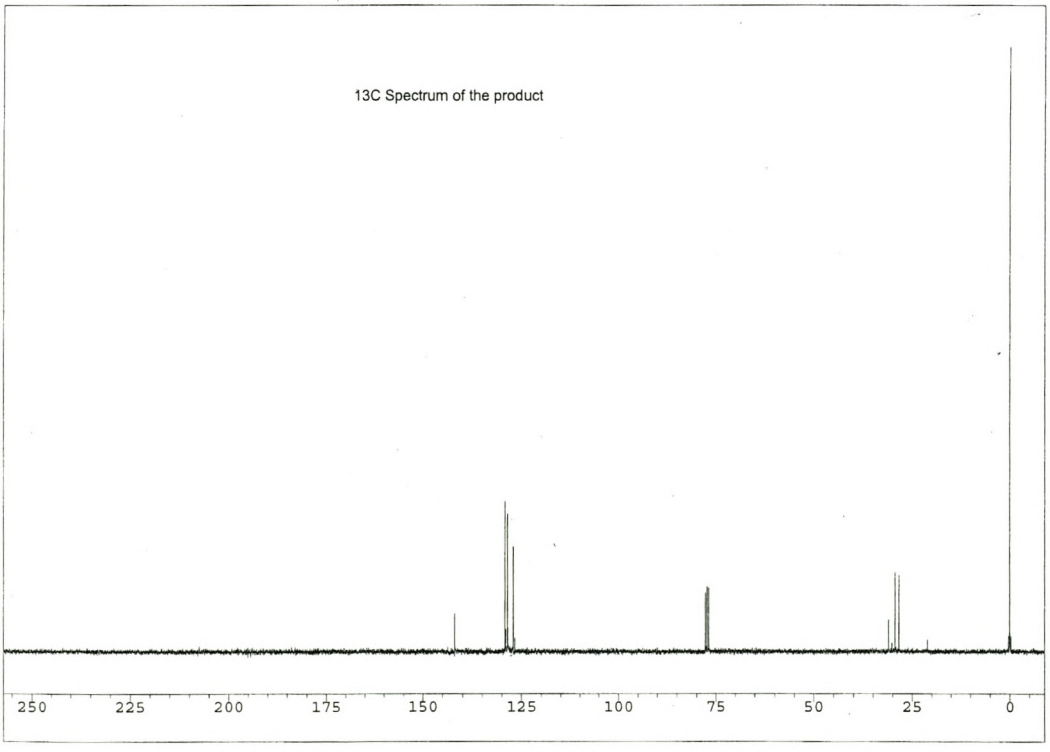

The numbering scheme for the carbon atoms in the $^{13}C\{^1H\}$ NMR spectrum is shown in figure 4.4. Atoms that are equivalent in NMR terms are given the same numbering. The hydrogen atoms are not shown, but numbering is such that a hydrogen atom attached to C_n is numbered H_n .

Table 4.3: Peak analysis of the ^{13}C $\{^1H\}$ NMR

Peak	Frequency	ppm	Intensity	Assignment
1	10702.23	141.91	6.682	C3
2	9741.81	129.18	34.976	C5
3	9727.34	128.99	4.056	
4	9694.13	128.55	30.075	C4
5	9684.35	128.42	4.911	
6	9580.32	127.04	21.047	C6
7	5859.41	77.70	12.762	Chloroform
8	5827.12	77.27	13.022	
9	5795.3	76.85	12.36	
10	2337.24	30.99	6.809	C2
11	2213.07	29.35	13.770	Acetone
12	2137.62	28.35	15.998	C1
15	-0.21	0.00	137.787	TMS

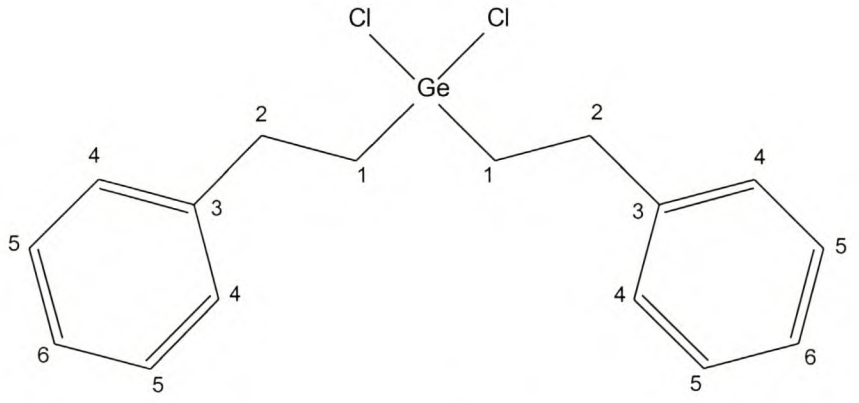

Figure 4.4: Numbering scheme for the NMR spectra

The spectra show the presence of only one species and some impurities (acetone and chloroform). The species has been identified as the desired product, dichlorobis(phenethyl)germane.

4.3.3. X-ray crystal structure

The molecular structure of dichlorobis(phenethyl)germane as determined by X-ray diffraction methods is shown in figure 4.5, along with the numbering scheme used to describe the parameters. Bond lengths and bond angles are listed in tables 4.4. and 4.5. respectively, with the s.u.s in parenthesis. The hydrogen atoms were placed at calculated positions with C-H bond lengths of 0.990 Å for aliphatic H atoms and 0.950 Å for aromatic H atoms. The C-H bond lengths are therefore not listed in table 4.4. The hydrogen containing bond angles are also not given in table 4.5, since they were calculated and are therefore not meaningful.

The crystal data and the collection and refinement details are given in table 4.6. The structure was solved using SHELXS97 and refined using SHELXL97 [90] within the WINGX package [91]. The figure of the molecular structure was generated using Ortep3 for Windows, with the displacement ellipsoids at 50% probability level [92]. In the crystal structure determination, only the heavy atom parameters were determined.

The equivalent isotropic displacement parameters are low for all anisotropic atoms except C5, for which U=0.120. For the diagonal elements of the tension matrix for this atom, the ratios U_{11}/U_{22} and U_{33}/U_{22} are both greater than 3, which is a fairly significant difference. This can be seen clearly in the Ortep plot, which shows a very elongated ellipsoid for C5. Also, the C4-C5 bond length is 1.422 Å, which is abnormally small for a carbon-carbon bond and a great deal smaller than the equivalent C12-C13 bond length in the other alkyl chain. The possibility that the disorder is static rather than dynamic was investigated and an attempt was made to model the disorder using two atom positions with a 50% probability each for C5 instead of the

single atom position. This improved the temperature factor U and the ratios U_{11}/U_{22} and U_{33}/U_{22} but lead to abnormal C7-C6-C5 and C11-C6-C5 angles and a general worsening of the geometry. It was eventually concluded that the disorder is in fact dynamic, rather than static.

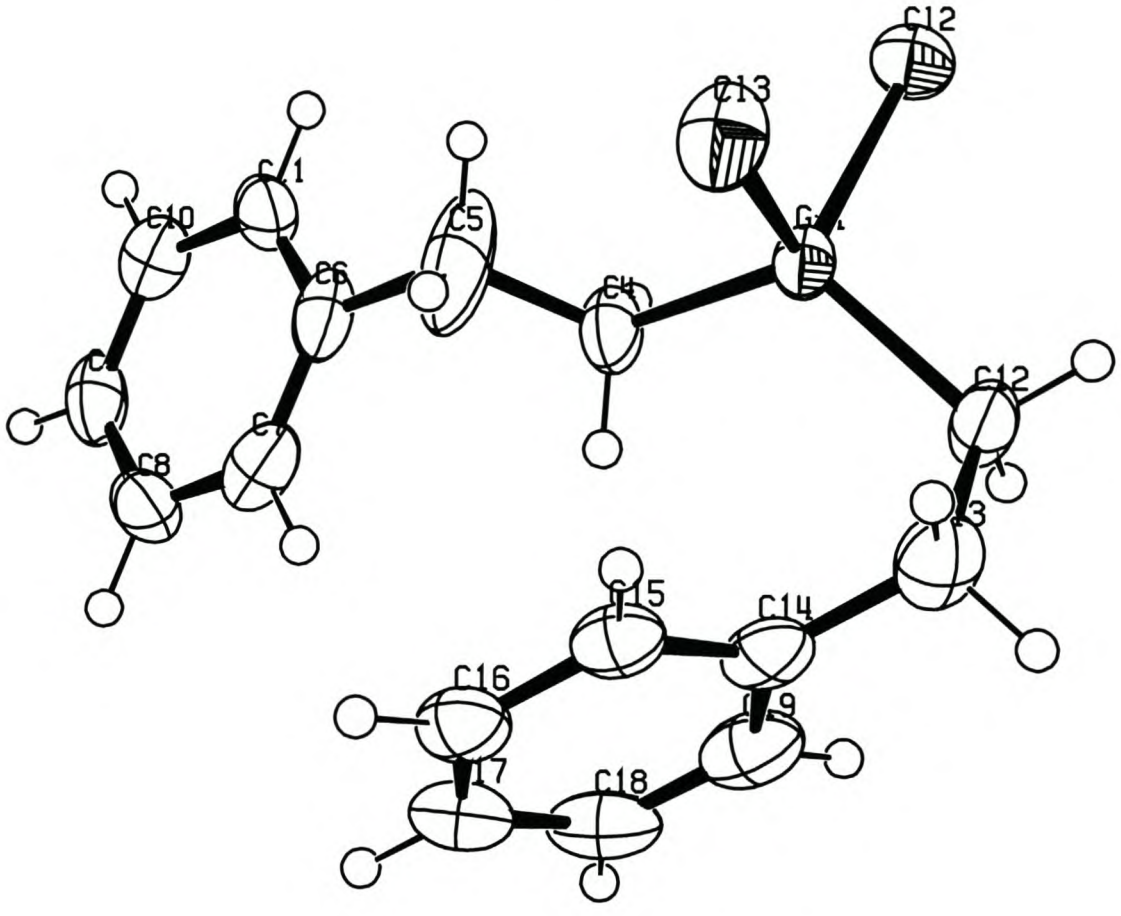

Figure 4.5: Ortep plot of the molecular structure of dichlorobis(phenethyl)germane at 50% ellipsiod probability

Another noticeable feature of the crystal structure is the difference in the orientation of the R groups. One of the chains is folded back under the Cl-Ge-Cl fragment so that the planes in which the phenyl groups lie are perpendicular to each other. Corresponding parameters of the two groups are in general not equal and the differences between them are sometimes quite large. Where the valence angles around the central germanium atom are concerned, the C-Ge-C angle is significantly larger (121.2°) and the Cl-Ge-Cl angle significantly smaller (103.2°) than the tetrahedral value.

Table 4.4: List of bond lengths (Å) with e.s.d.s. in parenthesis

C(4) - C(5)	1.422(7)	C(15) - C(16)	1.381(5)
C(5) - C(6)	1.510(6)	C(16) - C(17)	1.379(5)
C(6) - C(11)	1.378(5)	C(17) - C(18)	1.365(6)
C(7) - C(8)	1.381(6)	C(18) - C(19)	1.384(6)
C(8) - C(9)	1.369(6)	Cl(2) - Ge(1)	2.160(1)
C(9) - C(10)	1.363(6)	C(4) - Ge(1)	1.942(4)
C(10) - C(11)	1.375(5)	C(6) - C(7)	1.376(6)
C(12) - C(13)	1.539(5)	C(12) - Ge(1)	1.935(4)
C(13) - C(14)	1.504(5)	C(14) - C(15)	1.387(5)
C(14) - C(19)	1.408(5)	Cl(3) - Ge(1)	2.167(1)

Table 4.5: List of bond angles (°) with e.s.d.s. in parenthesis

C(4)-C(5)-C(6)	116.5(5)	C(5)-C(4)-GE(1)	117.5(3)
C(5)-C(6)-C(7)	121.8(4)	C(5)-C(6)-C(11)	120.1(4)
C(7)-C(6)-C(11)	118.1(4)	C(7)-C(8)-C(9)	119.9(4)
C(6)-C(7)-C(8)	121.0(4)	C(9)-C(10)-C(11)	120.4(4)
C(8)-C(9)-C(10)	119.7(4)	C(6)-C(11)-C(10)	120.9(4)
C(12)-C(13)-C(14)	113.9(3)	C(13)-C(12)-Ge(1)	113.0(3)
C(13)-C(14)-C(15)	121.0(3)	C(13)-C(14)-C(19)	121.6(3)
C(15)-C(14)-C(19)	117.4(3)	C(15)-C(16)-C(17)	120.8(4)
C(14)-C(15)-C(16)	121.0(3)	C(17)-C(18)-C(19)	120.7(4)
C(16)-C(17)-C(18)	119.3(4)	C(14)-C(19)-C(18)	120.8(4)
C(4)-Ge(1)-C(12)	121.2(2)	C(4)-Ge(1)-Cl(2)	107.2(2)
C(4)-Ge(1)-Cl(3)	108.7(2)	C(12)-Ge(1)-Cl(2)	107.8(1)
C(12)-Ge(1)-Cl(3)	107.2(1)	Cl(2)-Ge(1)-Cl(3)	103.2(1)

4.4. Results

Dichlorobis(phenethyl)germane was readily prepared by the treatment of tetrachlorogermane with phenethyl chloride and characterized by means of ESMS, ^{1}H NMR and $^{13}C\{^{1}H\}$ NMR spectra. The molecular structure was determined by means of X-ray diffraction techniques.

Table 4.6: Crystal data, collection and refinement details for Dichlorobis(phenethyl)germane

Empirical formula	$C_{16}H_{18}Cl_2Ge$
Formula weight	353.81 g/mol
Unit cell weight	1415.26 g/mol
Crystal system	Monoclinic
Crystal size	0.5 mm, 0.2 mm, 0.15 mm
Color	Colourless
Space group	$P2_1/c$
a	9.208 Å
b	9.785 Å
c	19.54 Å
α	90.00 °
β	90.00 °
γ	114.22 °
Z	4
V	1605.5 $Å^3$
Calculated density	1.4638 g/cm^3
Radiation, wavelength	Mo Kα, 0.71073 Å
Monochromator	Graphite
Absorption coefficient μ	22.25 cm^{-1}
T	173 K
F (000)	720.0 (721.93)
Diffractometer	Nonius Kappa CCD
Scan type	Area detector
Scan range θ	1.02 ° < θ < 25.68 °
h range	-11 < h < 11
k range	-23 < k < 23
l range	-11 < l < 11
Reflections measured	12049
Unique reflections used to refine	3056
Number of parameters refined	173
Δρ, min, max	-0.50 $eÅ^{-3}$, 0.48 $eÅ^{-3}$
R (internal)	0.028
R, R_w	0.032, 0.077

4.5. Conclusion

The crystal structure determination of dichlorobis(phenethyl)germane verifies the results of both the gas phase electron diffraction and *ab initio* studies, namely that the C-Ge-C angle is significantly larger and the X-Ge-X angle significantly smaller than the tetrahedral value of 109.47° in compounds of the general form R_2GeX_2, where R is an alkyl group and X a halogen.

CHAPTER 5: FORCE FIELD DEVELOPMENT

5.1. Introduction

One of the problems with the development of a force field for halogenated organogermanium compounds has always been the lack of experimental data for the training set. Although the vibrations of these molecules are well characterized [24-35] and vibrational force fields have been developed for a number of the non-methylated halogermanes, these all assume an idealized tetrahedral geometry, which has been shown not to be the case. Generic force fields containing germanium as an atom type are available but are also unable to correctly predict the trends in the C-Ge-C bond angles of the dihalo(dimethyl)germanes.

A force field based entirely on *ab initio* calculations has been developed here which is able to correctly predict the trends in the C-A-C angles in compounds of the form Me_2AX_2, for A=C, Si, Ge and X=H, F, Cl, Br, and provide good estimates of the geometry and vibrational frequencies of other halogenated organogermanes, -silanes and methanes.

The computational methods and programs used in the development of the force field and the animation of the vibrations to determine their symmetry, are discussed in **Section 5.2.** The force field is defined in **Section 5.3.** in terms of the training set, parameters, interactions and atom types used and a general description of the development of the force field is given. **Section 5.4.** contains the results of the optimization and is subdivided into sections on the geometry and vibrational frequencies of the training set, optimized parameters and interactions. The parameters are also compared to those of previously developed force fields. The results are discussed in **Section 5.5.** and **Section 5.6.** concludes the chapter.

5.2. Computational Methods

The optimization of the force field was done using the Program for the Development of Empirical Force Fields (PEFF) [93]. This program differs from many other molecular mechanics programs in that it uses external force fields that are read in from a file [94]. This enables the user to modify not only the force constants, but the number and nature of the interactions as well. PEFF recognizes 24 different interaction types and for each interaction type different functions are available, including functions for several force fields in common use. Within limits, additional interactions can also be defined.

PEFF minimizes the steric energy of a molecule using one of three methods, the steepest descent method and the diagonal- and full-matrix Newton-Raphson methods. The steepest descent method is the simplest and fastest of the three. It uses only first derivatives and has a big convergence radius, allowing for a poor starting geometry. However, since no second derivatives are calculated, convergence slows progressively and the true minimum of the potential function is not reached. In the diagonal-matrix Newton-Raphson method, some second derivatives are calculated and the minimum can be approached more closely. The method is less tolerant to a bad starting geometry and convergence is slower. In the full-matrix Newton–Raphson method, all the second derivatives are calculated and the minimum of the potential energy function can be found with extreme accuracy. PEFF is able to refine a structure using various combinations of the above methods.

For this force field the steepest descent method was used to approach the minimum and the true minimum was then calculated with the full-matrix method. The interaction types, as well as the mathematical functions that describe them, are discussed below. The symmetry of each vibrational mode calculated by the force field was determined and an assignment was made using the program Vibram [95] to animate the vibrations.

5.3. Force Field Development

5.3.1. The training set

The parameterization of the force field was based entirely on the *ab initio* calculations of **Chapter 3**. The training set is made up of molecules of the form AH_nX_{4-n} (n=0-4) and Me_2AX_2, with A = C, Si, Ge and X = H, F, Cl, Br. Iodine was excluded from the force field at this stage due to the fact that a different basis set was used in the *ab initio* calculations for iodine containing molecules, and the results are therefore inconsistent with the rest of the experimental data. The data used for fitting the force field were the bond lengths, bond angles and vibrational frequencies of the above molecules.

5.3.2. Interactions and parameters

The energy of the force field can be described by the equation:

$$E_{FF} = \sum E_{str} + \sum E_{bend} + \sum E_{tors} + \sum E_{vdw} + \sum E_{sb} + \sum E_{bb} + \sum E_{btb}$$

The seven constituent terms describe the bond stretching, angle bending, torsion, van der Waals, stretch-bend, bend-bend and bend-torsion-bend interactions respectively. The equations defining the interactions are given in table 5.1, along with the code used by PEFF to identify the interaction and the variables found in each equation. The parameters defined in the cross-term interactions are shown in figure 5.1.

The bond stretching parameters (r_0 and k_s), angle bending parameters (θ_0 and k_b) and torsion parameters (V) were defined for each possible bonding pair, bond angle and torsion angle. The cross terms where not explicitly defined for each combination of atom types and generic terms were used instead. Only seven stretch-bend interaction parameters, two bend-bend interaction parameters and two bend-torsion-bend parameters were defined.

Table 5.I: Interactions used in the force field

Code	Formula	Variables
101	$E_{str} = \frac{1}{2} k_s (\Delta r)^2 , \quad \Delta r = r - r_0$	r_0 , k_s
201	$E_{bend} = \frac{1}{2} k_b (\Delta r)^2 , \quad \Delta\theta = \theta - \theta_0$	θ_0 , k_b
301	$E_{tors} = \frac{1}{2} V (1 + \cos 3\omega)$	V
506	$E_{vdw} = \varepsilon \left[\left(\frac{r_m}{r} \right)^{12} - 2 \left(\frac{r_m}{r} \right)^{6} \right]$	ε , r_m
801	$E_{sb} = k_{sb} \Delta r \Delta\theta , \quad \Delta r = r_{12} - r_0 , \quad \Delta\theta = \theta_{123} - \theta_0$	r_0 , θ_0 , k_{sb}
1301	$E_{bb} = k_{bb} \Delta\theta \Delta\theta' , \quad \Delta\theta = \theta_{123} - \theta_0 , \quad \Delta\theta' = \theta_{124} - \theta_0$	$\theta_0 , \theta_0' , k_{bb}$
1801	$E_{btb} = k_{btb} \Delta\theta (\cos \omega) \Delta\theta' , \quad \Delta\theta = \theta_{123} - \theta_0 , \quad \Delta\theta' = \theta_{234} - \theta_0'$	$\theta_0 , \theta_0' , k_{btb}$

Figure 5.1: The parameters used in the cross term interactions

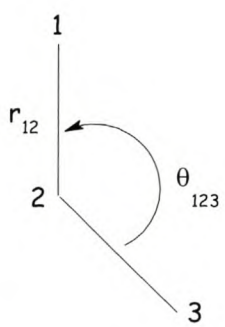

Stretch-bend (801)

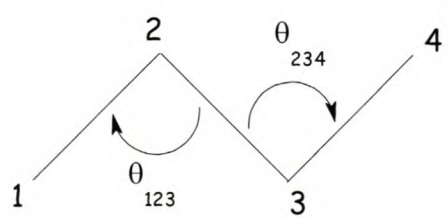

Bend-torsion-bend (1801)

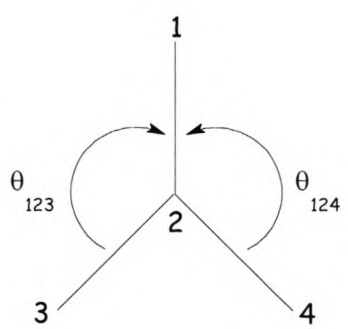

Bend-bend (1301)

5.3.3. Atom types

The atom types for which the force field is parameterized are listed in table 5.2, along with the element, atomic mass, ε and r_m value for each atom type. The van der Waals hardness (ε) and van der Waals radius (r_m) are used to calculate non-bonded or van der Waals interactions. The 3 in the naming of the atom types for C, Si and Ge indicates that the atom is, in the first approximation, sp^3 hybridized.

Table 5.2: Summary of the atom types used in the force field

Number	Type	Element	Weight	ε	r_m
1	H	H	1.0074	0.044	1.443
2	C3	C	12.011	0.105	1.9255
3	Si3	Si	28.0855	0.402	2.1475
4	Ge3	Ge	72.59	0.379	2.140
5	F	F	18.9984	0.050	1.682
6	Cl	Cl	35.4527	0.227	1.9735
7	Br	Br	79.904	0.251	2.250

5.3.4. Defining the force field

Before the force field can be refined, the atom types, interactions and parameters must be defined and the training set must be provided. The input file *MyMolecules* contains the Cartesian coordinates and connectivity of the atoms for each molecule of the training set, as well as all the all the experimental information (bond lengths, bond angles and frequencies) needed to optimize the force field, while the file *eff* contains the lists of the atom types, parameters and interactions that define the force field.

The molecules in the training set are added one by one and after each addition the parameters for that molecule are optimized. As each new molecule is added, the new interactions and parameters required for that molecule are defined in *eff*. If the molecule contains an atom that has not occurred yet in previous molecules, the new atom type is also defined. An initial value is given to the new parameters, the value of which is relatively unimportant, since it does not affect the outcome of the optimization. An inaccurate starting value for a parameter does however, increase the number of refinement cycles required to optimize the parameter, and thus also the calculation time. Mostly an educated guess is made, based on calculated parameters for similar molecules, spectroscopic parameters or, if neither are available, basic chemical knowledge.

5.3.5. Importing the training set

Each time a new molecule is added to the training set, the parameters for that molecule are optimized. The optimization is done in two cycles. In the first cycle, the program calculates a set of eigenvectors and corresponding eigenvalues for the molecule. These calculated values are compared to the observed frequencies and reassigned in *MyMolecules*. The parameters are then re-optimized, this time using the eigenvectors calculated in the first step to fit to the observed frequencies. This process is repeated until all the molecules in the training set have been introduced. Figure 5.2. gives a schematic representation of the force field optimization process.

When PEFF is run, the interactions, parameters and atom types that define the force field are copied from the external file *eff* to the file *PEFFINP*, which is then used as input for the program. The program reads the interactions, parameters and atom types that define the force field in from *PEFFINP* and the coordinates and observables from *MyMolecules* and then optimizes the parameters by fitting the calculated bond lengths, bond angles and frequencies to the observed values. The minimization method and conditions of the refinement are specified in the file *MyMolecules*.

When PEFF has completed the optimization, it generates three output files. The first, called *fort.28*, contains a list of the optimized parameters. The second is the *PEFFCRD* file, which contains the optimized geometries of all the molecules in the training set that have already been imported, as well as the eigenvectors and trajectories of each vibrational mode of the molecule, if this is specified. The third output file, *PEFFOUT*, contains information about the optimization process, including each step in the refinement, a table containing all the calculated and observed parameters and the statistics of the optimization, such as the standard deviations, percentage deviations and maximum deviations of the experimental observables.

Once the frequencies have been reassigned, the trajectories and eigenvalues of the new molecule are copied from *PEFFCRD* to the file *PEFFVEC*, which contains the trajectories and eigenvectors of all the molecules already added to the training set and is used as input for PEFF in the second cycle of the refinement. Note that the program associates the sets of eigenvectors in *PEFFVEC* as they occur and it is therefore imperative that the sets of eigenvectors are listed in the same order as the coordinates of the molecules in *MyMolecules*. In the second refinement cycle the program is instructed to read in the complete set of eigenvectors for the new molecule from the file *PEFFVEC*, to be used in the assignment of the vibrational frequencies. The procedure is much the same as in the first cycle except that no eigenvectors are calculated. The only difference in the output files is that *PEFFCRD* now contains only the optimized coordinates for the training set.

5.3.6. Frequency assignment

Each of the vibrational modes of a molecule is related to a vibrational frequency and its associated energy. In *MyMolecules,* the experimental frequencies are listed from the lowest to the highest value, corresponding to modes 1 to n, where n is the number of vibrational frequencies of that molecule. Next to these frequencies a number is given in parentheses, which corresponds to the force field modes, where these modes are also numbered

from lowest to highest value. Ideally, the order of the calculated frequencies should be the same as the order of the observed frequencies, but this is not always the case. When the force field is refined and the eigenvectors are calculated, the frequency assignment can sometimes change. After the first refinement step, the frequency assignments must therefore be checked and corrected if necessary.

The trajectories and eigenvalues of the vibrational modes of the molecule are copied from *PEFFCRD* to a dos file *peff.crd*. The frequencies and symmetries are assigned and compared to those of the *ab initio* vibrations. The necessary corrections are then made to the numbering of the observed vibrations in the file *MyMolecules* before the force field is optimized again.

5.3.7. Further refinement of the force field

While the training set is being imported, only those interactions and parameters absolutely necessary to define each new molecule are added. A preliminary force field is thus obtained, which can then be further modified and refined to obtain the final product. The basic interactions in the preliminary force field are the bend, stretch and torsion interactions, all that is needed to describe a molecule. The additional interactions added in the later refinement are the van der Waals, stretch-bend, bend-bend and bend-torsion-bend interactions. These were added one by one and the parameters re-optimized after each addition, first in sequence, then in groups of similar parameters and finally all together. Coulomb interactions were also added, but they caused an overall weakening of the force field and were eventually discarded. It is important to note that care must be taken when optimizing all the parameters together, since many of them are interdependent and there is a danger of the force field diverging. The parameters must already be fairly well optimized before this can be done. Once all the interactions and parameters have been added and the force field has been refined to within acceptable limits, the frequency assignments are checked for the last time and once again adjusted where necessary.

5.4. Results

5.4.1. Geometry

The bond distances can be calculated to within a root mean square deviation of 0.0143 Å (0.6%) and a maximum deviation of 0.0705 Å, for the diagonal force field. With the addition of cross terms this improves to a rms deviation of 0.0109 Å (0.4%) and a maximum deviation of 0.0702 Å. The difference between the calculated and observed values is less than 0.020 Å for all but the C-F bond lengths in CH_3F and in CH_2F_2, the Ge-Br bond lengths in GeH_3Br and GeH_2Br_2 and the Ge-Cl bond length in $GeCl_4$. The deviations between calculated and observed halosilane bond lengths all fall within the limit of 0.02 Å. For the dimethylated compounds (Me_2AX_2), the overall fit is exceptionally good and all the experimental deviations are within the limit of 0.020 Å. In general, the largest deviations are found in the A-X bonds, and it seems to be particularly the combination of C with F and Ge with Br that poses a problem.

The fit for the bond angles is also good and can be calculated to within a root mean square deviation of 1.003° (0.7%) and a maximum deviation of –4.091° for the diagonal force field. With the addition of cross terms the rms deviation more than halves to a value of 0.486° (0.4%) and the maximum deviation decreases to only 1.511°. The difference between the calculated and observed values is less than 1° for all but the F-C-F angle in CH_2F_2, the Br-Ge-Br angle in GeH_2Br_2 and the C-C-H angles in the dihalopropanes. The deviations in the halosilane bond angles all fall within the limit of 1°. As was the case for the bond lengths, the combination of C with F and Ge with Br leads to the largest errors.

The geometric parameters for the halomethanes, -silanes and -germanes are summarized in tables 5.3. to 5.5, along with the results of the *ab initio* calculations. In general the A-H distances are much closer to the observed values than the A-X distances. For the tetrahalomethanes, -silanes and -

germanes there is a systematic trend towards too large calculated A-X values. In the monohalomethanes, -silanes and –germanes the A-X bonds also show a systematic deviation, this time with the calculated values smaller than observed by an average of about 0.014 Å. Calculated bond lengths for the dihalomethanes, -silanes and -germanes fit very well, except for Ge-Br in GeH_2Br_2, which is a full 0.070 Å larger than the observed value, the largest experimental bond length error for the range AH_nX_{4-n}. For the trihalomethanes, -silanes and –germanes there is a systematic error towards too large calculated values, especially for the A-X bond distances where the average difference between calculated and observed values is about 0.010 Å.

Although the deviations in the angles for the monohalomethanes, -silanes and –germanes are not large, there is a systematic error in both the H-A-H and the H-A-X angles, the calculated values being too large in the case of the H-A-H angles and too small in the case of the H-A-X angles. For the dihalomethanes, -silanes and –germanes on the other hand, the calculated H-A-X angles are systematically too large and the H-A-H and X-A-X too small. The X-A-X angles for this group of molecules show the largest deviations and the F-C-F angle in CH_2F_2 has a deviation of –1.146°, the maximum experimental error for the range AH_nX_{4-n}. The trihalomethanes, -silanes and –germanes have an overall good fit for bond angles but there is once again a systematic error towards too large X-A-X angles and too small H-A-X angles.

The geometric parameters for the methylated compounds (Me_2AX_2 with A=C, Si, Ge and X=H, F, Cl, Br), together with the *ab initio* results, are also given in tables 5.3. to 5.5. The correspondence between calculated and observed values is excellent for the C-H bond distances in the methyl groups. The A-C and A-X bond lengths do not fit as well but the maximum deviation is still only –0.018 Å, between the calculated and observed values of the Ge-Br bond length in Me_2GeBr_2, and this is within the limit of 0.020 Å. There is a systematic deviation in the A-X bond lengths, with the calculated values being too small. For the A-Cl bond lengths the differences are –0.013 Å, -0.012 Å and –0.014 Å for A = C, Si and Ge respectively.

Table 5.3: Geometric Parameters of CH_nX_{4-n} and Me_2CX_2

Molecule	Parameter	Fore Field Value	*Ab initio* Value	Difference
CH_4	C-H	1.081	1.084	-0.003
CH_3F	C-H	1.079	1.082	-0.003
	C-F	1.338	1.365	-0.026
	H-C-H	110.5	109.8	0.7
	H-C-F	108.4	109.1	-0.7
CH_3Cl	C-H	1.079	1.078	0.001
	C-Cl	1.770	1.785	-0.014
	H-C-H	110.8	110.5	0.3
	H-C-Cl	108.1	108.5	-0.3
CH_3Br	C-H	1.077	1.076	0.001
	C-Br	1.934	1.948	-0.014
	H-C-H	111.4	111.2	0.2
	H-C-Br	107.4	107.7	-0.3
CH_2F_2	C-H	1.077	1.078	-0.001
	C-F	1.335	1.338	-0.004
	H-C-F	109.3	108.9	0.4
	H-C-H	111.9	112.5	-0.6
	F-C-F	107.5	108.6	-1.1
CH_2Cl_2	C-H	1.079	1.074	0.005
	C-Cl	1.770	1.768	0.002
	H-C-Cl	108.5	108.2	0.3
	H-C-H	111.0	111.1	-0.2
	Cl-C-Cl	112.0	112.9	-0.9
CH_2Br_2	C-H	1.076	1.072	0.004
	C-Br	1.932	1.930	0.002
	H-C-Br	108.2	107.9	0.3
	H-C-H	111.9	112.2	-0.3
	Br-C-Br	112.2	113.1	-0.9
CHF_3	C-H	1.075	1.074	0.001
	C-F	1.331	1.317	0.015
	H-C-F	110.7	110.4	0.2
	F-C-F	108.2	108.5	-0.3
$CHCl_3$	C-H	1.081	1.071	0.010
	C-Cl	1.774	1.763	0.011
	H-C-Cl	107.5	107.6	-0.1
	Cl-C-Cl	111.4	111.3	0.1

$CHBr_3$	C-H	1.079	1.069	0.009
	C-Br	1.936	1.926	0.010
	H-C-Br	107.2	107.5	-0.3
	Br-C-Br	111.7	111.4	0.3
CF_4	C-F	1.327	1.302	0.025
CCl_4	C-Cl	1.781	1.766	0.015
CBr4	C-Br	1.947	1.933	0.014
CMe_2H_2	C-C	1.521	1.528	-0.008
	C-X	1.087	1.087	0.000
	C-H4	1.083	1.086	-0.002
	C-H5	1.084	1.087	-0.003
	C-C-C	113.8	112.8	1.0
	C-C-X	109.0	109.4	-0.4
	X-C-X	106.7	106.3	0.4
	H4-C-C	110.6	111.3	-0.7
	H5-C-C	110.6	111.1	-0.5
CMe_2F_2	C-C	1.515	1.509	0.007
	C-X	1.345	1.354	-0.009
	C-H5	1.084	1.083	0.001
	C-H6	1.084	1.083	0.001
	C-C-C	115.8	116.1	-0.3
	C-C-X	108.6	108.6	0.0
	X-C-X	106.2	105.9	0.3
	C-C-H5	110.6	109.1	1.5
	C-C-H6	110.7	110.3	0.4
CMe_2Cl_2	C-C	1.523	1.521	0.002
	C-X	1.785	1.798	-0.013
	C-H5	1.083	1.081	0.002
	C-H6	1.083	1.084	0.000
	C-C-C	112.6	112.9	-0.4
	C-C-X	108.9	108.9	0.0
	X-C-X	108.6	108.4	0.2
	C-C-H5	110.7	110.9	-0.3
	C-C-H6	110.5	109.5	1.1
CMe_2Br_2	C-C	1.521	1.519	0.002
	C-X	1.953	1.964	-0.011
	C-H5	1.083	1.081	0.003
	C-H6	1.084	1.084	-0.001
	C-C-C	113.4	113.7	-0.3
	C-C-X	108.8	108.7	0.1
	X-C-X	108.1	108.1	0.0
	C-C-H5	110.6	111.2	-0.5
	C-C-H6	110.6	109.5	1.1

Table 5.4: Geometric Parameters of SiH_nX_{4-n} and Me_2SiX_2

Molecule	Parameter	Force Field Value	*Ab Initio* Value	Difference
SiH_4	Si-H	1.470	1.475	-0.006
	Si-H	1.465	1.470	-0.005
	Si-F	1.580	1.594	-0.014
	H-Si-H	110.9	110.2	0.8
SiH_3F	H-Si-F	108.0	108.8	-0.8
	Si-H	1.465	1.468	-0.002
	Si-Cl	2.053	2.067	-0.014
	H-Si-H	111.1	110.6	0.5
SiH_3Cl	H-Si-Cl	107.8	108.3	-0.5
	Si-H	1.465	1.467	-0.002
	Si-Br	2.208	2.222	-0.014
	H-Si-H	111.1	110.6	0.6
SiH_3Br	H-Si-Br	107.7	108.4	-0.6
	Si-H	1.460	1.462	-0.001
	Si-F	1.579	1.581	-0.002
SiH_2F_2	H-Si-F	109.2	108.9	0.3
	H-Si-H	112.9	113.4	-0.5
	F-Si-F	107.0	107.6	-0.5
	Si-H	1.462	1.460	0.002
	Si-Cl	2.050	2.050	-0.001
SiH_2Cl_2	H-Si-Cl	108.7	108.4	0.2
	H-Si-H	112.6	112.9	-0.3
	Cl-Si-Cl	109.5	110.2	-0.7
	Si-H	1.463	1.460	0.002
	Si-Br	2.205	2.206	-0.001
SiH_2Br_2	H-Si-Br	108.4	108.0	0.4
	H-Si-H	112.4	113.0	-0.6
	Br-Si-Br	111.0	111.9	-0.9
	Si-H	1.455	1.449	0.007
	Si-F	1.577	1.569	0.008
$SiHF_3$	H-Si-F	110.8	110.9	0.0
	F-Si-F	108.1	108.0	0.0
	Si-H	1.460	1.454	0.006
	Si-Cl	2.048	2.038	0.010
$SiHCl_3$	H-Si-Cl	109.2	109.4	-0.1
	Cl-Si-Cl	109.7	109.6	0.1

$SiHBr_3$	Si-H	1.462	1.454	0.008
	Si-Br	2.204	2.195	0.009
	H-Si-Br	108.3	108.7	-0.5
	Br-Si-Br	110.7	110.2	0.5
SiF_4	Si-F	1.576	1.557	0.019
$SiCl_4$	Si-Cl	2.047	2.029	0.018
$SiBr_4$	Si-Br	2.206	2.188	0.017
$SiMe_2H_2$	Si-C	1.883	1.890	-0.007
	Si-X	1.476	1.481	-0.005
	C-H6	1.084	1.086	-0.002
	C-H7	1.084	1.087	-0.002
	C-Si-C	111.8	111.5	0.3
	C-Si-X	109.4	109.5	0.0
	X-Si-X	107.2	107.5	-0.3
	Si-C-H6	111.2	111.2	0.0
	Si-C-H7	110.6	111.2	-0.6
$SiMe_2F_2$	Si-C	1.871	1.861	0.010
	Si-X	1.581	1.592	-0.010
	C-H5	1.084	1.086	-0.002
	C-H6	1.085	1.086	-0.002
	C-Si-C	115.1	115.0	0.1
	C-Si-X	108.9	108.9	0.0
	X-Si-X	105.9	105.8	0.1
	Si-C-H5	111.6	111.0	0.6
	Si-C-H6	110.6	111.2	-0.5
$SiMe_2Cl_2$	Si-C	1.875	1.880	-0.005
	Si-X	2.057	2.069	-0.012
	C-H5	1.084	1.085	-0.001
	C-H6	1.085	1.086	-0.002
	C-Si-C	114.3	114.4	-0.1
	C-Si-X	108.6	108.6	0.0
	X-Si-X	108.0	107.8	0.2
	Si-C-H5	111.4	111.2	0.2
	Si-C-H6	110.7	110.6	0.1
$SiMe_2Br_2$	Si-C	1.875	1.867	0.009
	Si-X	2.214	2.222	-0.009
	C-H5	1.084	1.084	0.000
	C-H6	1.085	1.086	-0.002
	C-Si-C	113.8	113.8	0.0
	C-Si-X	108.5	108.5	0.0
	X-Si-X	109.1	109.1	0.1
	Si-C-H5	111.4	111.2	0.3
	Si-C-H6	110.6	110.3	0.4

Table 5.5: Geometric Parameters of GeH_nX_{4-n} and Me_2GeX_2

Molecule	Parameter	Force Field Value	*Ab Initio* Value	Difference)
GeH_4	Ge-H	1.537	1.535	0.002
GeH_3F	Ge-H	1.528	1.531	-0.003
	Ge-F	1.716	1.727	-0.010
	H-Ge-H	112.5	111.8	0.7
	H-Ge-F	106.2	107.0	-0.8
GeH_3Cl	Ge-H	1.529	1.523	0.006
	Ge-Cl	2.151	2.168	-0.016
	H-Ge-H	112.2	111.8	0.4
	H-Ge-Cl	106.6	107.1	-0.5
GeH_3Br	Ge-H	1.530	1.530	0.000
	Ge-Br	2.284	2.309	-0.025
	H-Ge-H	112.0	111.5	0.5
	H-Ge-Br	106.8	107.4	-0.6
GeH_2F_2	Ge-H	1.519	1.523	-0.004
	Ge-F	1.708	1.709	-0.001
	H-Ge-F	109.0	108.7	0.3
	H-Ge-H	116.7	117.3	-0.6
	F-Ge-F	103.4	103.9	-0.5
GeH_2Cl_2	Ge-H	1.523	1.523	0.000
	Ge-Cl	2.145	2.146	-0.001
	H-Ge-Cl	108.4	108.2	0.2
	H-Ge-H	115.2	115.4	-0.2
	Cl-Ge-Cl	107.7	108.3	-0.6
GeH_2Br_2	Ge-H	1.524	1.526	-0.002
	Ge-Br	2.276	2.206	0.070
	H-Ge-Br	108.3	108.0	0.3
	H-Ge-H	114.7	114.8	-0.1
	Br-Ge-Br	108.9	110.0	-1.1
$GeHF_3$	Ge-H	1.510	1.510	0.000
	Ge-F	1.699	1.693	0.007
	H-Ge-F	112.7	112.9	-0.1
	F-Ge-F	106.0	105.9	0.2
$GeHCl_3$	Ge-H	1.518	1.517	0.000
	Ge-Cl	2.140	2.129	0.011
	H-Ge-Cl	110.3	110.4	-0.1
	Cl-Ge-Cl	108.6	108.5	0.1

$GeHBr_3$	Ge-H	1.521	1.523	-0.002
	Ge-Br	2.271	2.280	-0.009
	H-Ge-Br	109.6	110.1	-0.6
	Br-Ge-Br	109.4	108.8	0.6
GeF_4	Ge-F	1.690	1.677	0.013
$GeCl_4$	Ge-Cl	2.137	2.116	0.021
$GeBr_4$	Ge-Br	2.268	2.272	-0.003
$GeMe_2H_2$	Ge-C	1.946	1.951	-0.005
	Ge-X	1.552	1.549	0.002
	C-H4	1.083	1.084	-0.001
	C-H5	1.083	1.085	-0.003
	C-Ge-C	111.3	111.0	0.3
	C-Ge-X	109.7	109.6	0.1
	X-Ge-X	106.7	107.4	-0.7
	Ge-C-H4	109.8	111.1	-1.3
	Ge-C-H5	110.2	110.5	-0.3
$GeMe_2F_2$	Ge-C	1.921	1.921	0.000
	Ge-X	1.714	1.721	-0.007
	C-H5	1.083	1.084	-0.001
	C-H6	1.083	1.084	-0.001
	C-Ge-C	120.2	120.2	0.0
	C-Ge-X	108.2	108.2	0.0
	X-Ge-X	102.6	102.5	0.1
	Ge-C-H5	110.6	110.1	0.5
	Ge-C-H6	110.2	110.4	-0.2
$GeMe_2Cl_2$	Ge-C	1.930	1.926	0.004
	Ge-X	2.157	2.170	-0.014
	C-H5	1.083	1.083	0.000
	C-H6	1.083	1.084	-0.002
	C-Ge-C	117.9	118.1	-0.2
	C-Ge-X	107.9	108.0	0.0
	X-Ge-X	106.6	106.3	0.3
	Ge-C-H5	110.1	109.8	0.3
	Ge-C-H6	110.3	110.0	0.4
$GeMe_2Br_2$	Ge-C	1.935	1.927	0.008
	Ge-X	2.299	2.317	-0.018
	C-H5	1.083	1.082	0.001
	C-H6	1.083	1.084	-0.001
	C-Ge-C	118.1	118.3	-0.2
	C-Ge-X	107.6	107.6	-0.1
	X-Ge-X	108.0	107.6	0.5
	Ge-C-H5	109.5	108.8	0.7
	Ge-C-H6	110.5	110.0	0.6

The best fit between calculated and observed bond angles for Me_2AX_2 is seen for the C-A-X angles. The worst fit generally is for the A-C-H angles, especially in the dihalo-propanes, where the deviations are sometimes larger than 1°. The maximum error for the range Me_2AX_2 is for the C-C-H5 angle of 2,2-difluoropropane, which has a value of 1.511°. The X-A-X angles are all calculated slightly too large, except for the H-Si-H angle in dimethylsilane, which is smaller than the observed value. Calculated C-A-C angles are larger than the observed angles for Me_2AH_2 and smaller than the observed angles for Me_2AX_2, the only exception being difluoro(dimethyl)silane, in which the calculated the C-Si-C angle is larger than the observed angle. However, these errors are small and the fit for these angles is on the whole very good.

5.4.2. Vibrational frequencies

With the basic force field, containing only diagonal terms in the force constant matrix (stretch, bend, torsion and van der Waals interactions), it was possible to calculate the vibrational frequencies with an rms deviation of 41.10 cm^{-1} (4.0 %) and a maximum deviation of 189.66 cm^{-1}. The addition of the stretch-bend, bend-bend and bend-torsion-bend cross terms to the force constant matrix improved the fit to an rms value of 34.72 cm^{-1} (3.8%) and a maximum deviation of 154.11 cm^{-1}.

The vibrational analyses for the halomethanes, -silanes and -germanes are summarized in table I to III, and those for propane and the 2,2-dihalo-propanes, dimethylsilane, dimethylgermane, the dihalo(dimethyl)silanes and the dihalo(dimethyl)germanes in tables IV to VI of **Addendum B**. The tables contain the symmetries and assignment of each vibrational mode, the calculated force field frequencies, the observed *ab initio* frequencies, the absolute difference and percentage difference between the two and the numbering of the modes for both the calculated and observed frequencies, where the vibrations are numbered from lowest to highest frequency.

For the monohalomethanes, the only modes for which the order of the calculated and observed frequencies differ are A_1 symmetric C-F stretch, the B_2 asymmetric C-F stretch and the B_1 H-C-H rocking mode of difluoromethane. The correlation between the calculated and observed frequencies is good for both methane and the monohalomethanes. There are some fairly large absolute deviations, but these are found for the high frequency C-H stretching modes and the percentage deviation is therefore small. The fit for the dihalomethanes is not as good and there are four calculated frequencies that differ by more than 10% from the observed values, namely the A_1 symmetric X-C-X bending modes in CH_2F_2 and CH_2Br_2, the H-C-H twisting mode in CH_2F_2 and the H-C-H rocking mode in CH_2Cl_2. For the trihalomethanes, the low frequency A_1 symmetric H-C-X bend and symmetric C-X stretching modes are consistently calculated too low by the force field and the percentage deviations are high. The calculated E asymmetric X-C-X bending modes also deviate but not as much. Although the order of the vibrations in CF_4, CCl_4 and CBr_4 is correct, large percentage deviations between calculated and observed frequencies are seen for the F_2 bend deformation and the A_1 symmetric stretch in all three molecules and the calculated values are on the whole too low.

For the monohalosilanes, the assignment of a number of modes calculated by the force field differed from those of the observed modes. These are the T_2 asymmetric stretching and the A_1 symmetric stretching modes in silane, the E asymmetric and A_1 symmetric stretching modes in SiH_3F and the E asymmetric H-Si-H and A_1 symmetric H-Si-X bends in SiH_3Cl and SiH_3Br. In SiH_2F_2 the A_2 H-Si-H twisting and B_2 wagging modes and in SiH_2Cl_2 the B_2 asymmetric Si-Cl stretching and B_1 H-Si-H rocking vibrations are also inverted. Despite these differences in order, there are few large deviations between calculated and observed frequencies. As was the case for carbon, the fit for silane and the monohalosilanes is good. The only large deviation is found for the T_2 asymmetric stretches in silane, but they are high frequency vibrations and the percentage difference is therefore small. The 3 lowest frequency vibrations in SiH_2F_2 have quite high deviations, the largest being a

percentage deviation of 18.48% for the A_2 H-Si-H twist. The lowest frequency mode in SiH_2Cl_2 and SiH_2Br_2, the A_1 symmetric X-Si-X bend, also deviates from the observed value by about 10%. The rest of the calculated frequencies in the dihalosilanes correspond well to the observed values. For the trihalosilanes the low frequency E asymmetric X-Si-X bend and the high frequency A_1 symmetric Si-H stretch show the largest deviations. For SiF_4, $SiCl_4$ and $SiBr_4$, as for the carbon analogs, large percentage deviations, sometimes over 10%, are seen for the F_2 bend deformation and the A_1 symmetric stretch and also for the E bend deformation.

For the monohalogermanes, vibrations assigned by the force field differed from the observed vibrations in all four fluorinated germanes. In GeH_3F the E asymmetric H-Ge-H and A_1 symmetric H-Ge-F bends have been inverted, as have the A_1 symmetric and B_2 asymmetric Ge-F stretches in GeH_2F_2. The E asymmetric H-Ge-F bend, the A_1 symmetric Ge-F stretch and the E asymmetric Ge-F stretch in $GeHF_3$ and the E and T_2 bend deformations in GeF_4 are also different on the force field. Qualitatively, the differences between calculated and observed frequencies are similar to those in the halomethanes and the halosilanes. For germane and the monohalogermanes, the largest deviation is for the A_1 symmetric Ge-Br stretch in GeH_3Br and even for this frequency the percentage deviation is less than 10%. There are no large deviations for GeH_2F_2 or for GeH_2Cl_2. In GeH_2Br_2, the two lowest frequencies, the A_1 symmetric Br-Ge-Br bend and Ge-Br stretch, deviate by more than 10%, but these are the largest deviations for the dihalogermanes. The E asymmetric X-Ge-X and H-Ge-X bending modes have large deviations for all three trihalogermanes, but for the higher frequencies the fit is fine. As is the case for the tetrahalogenated carbon and silicon compounds, the fit for the low frequency E and F_2 bending deformations and the A_1 symmetric stretch in GeF4, $GeCl_4$ and $GeBr_4$ is poor, with a maximum 28.10% deviation for the E bend deformation in GeF_4.

For Me_2CX_2, the order of the frequencies calculated by the force field differs from the order of the observed frequencies for a number of modes. The

differences are mainly in the C-H stretching and H-C-H bending modes of the methyl groups however, which are found within a narrow frequency range. Aside from the methyl vibrations, the A_2 uneven torsion, A_2 X-A-X twisting mode and the B_1 even torsion in Me_2CCl_2, the A_2 uneven torsion, X-A-X rocking mode and symmetric C-A-C bend in Me_2CBr_2 and the X-A-X wagging mode in Me_2CH_2 are also assigned differently by the force field. Since most of these vibrations are closely spaced however, the overall fit of the frequencies is still good. The largest absolute deviation for the group is 78.10 cm^{-1}, for the B_1 asymmetric A-X stretch in Me_2CH_2, and there are only 6 vibrations for which the percentage deviation is greater than 10%.

For Me_2SiX_2, the errors are qualitatively much the same as for the analogous carbon compounds. Individual vibrations amongst the H-C-H bending and C-H stretching modes are assigned differently, but the positioning of the groups on the frequency scale are correct. Considerably more of the lower energy vibrations differ in order for Me_2SiX_2 than for Me_2CX_2, including the torsions in Me_2SiF_2 and Me_2SiCl_2, some of the asymmetric A-C-H bending modes in Me_2SiH_2 and Me_2SiF_2, the symmetric C-A-C bends in Me_2SiCl_2 and Me_2SiBr_2 and some of the C-A-X bending modes. The largest absolute deviation, a value of –113.65 cm^{-1} for the A1 symmetric A-C-H bend, is also much larger. The overall fit is still good however, with only three vibrations having deviations of more than 10%.

For Me_2GeX_2, the C-H stretching and H-C-H bending vibrations are once again mostly differently assigned by the force field. In Me_2GeH_2, the A-C-H bending vibrations as a group are in the same position relative to the other vibrations, but the order of the modes within the group differs. The order of the symmetric and asymmetric A-X stretching vibrations has also been inverted. In Me_2GeF_2, the only assignments that differ, aside from the methyl group vibrations, are the torsions, the order of which has been inverted. The calculated order of the five lowest energy modes in both Me_2GeCl_2 and Me_2GeBr_2 and the B_2 X-A-X wagging mode of Me_2GeCl_2 is also different from the observed order. The correlation between calculated and experimental

frequencies is worse for this group than for either the carbon or silicon analogs. Although the maximum deviations are only 109.20 cm^{-1} and 110.83 cm^{-1} for the two A-X vibrations of Me_2GeH_2, which is not too large, there are 11 vibrations for with the percentage deviation is over 10% and for 5 of these the difference is greater than 20%. The calculated frequency of the X-A-X twisting mode of Me_2GeBr_2 shows a 35.96% deviation from the observed value.

5.4.3. Interactions and parameters

A complete list of the optimized parameters is given in tables 5.6 to 5.11. As mentioned previously, the cross terms are not defined for each combination of atom types. Further differentiation of the cross terms did lead to a slight improvement of the force field, but the improvement was not large enough to warrant the increase in the amount of parameters required to describe these additional interactions and they were eventually discarded.

For the van der Waals interaction a generic term was used and the atomic parameters used to calculate the van der Waals parameters are given in table 5.2. At a point in the force field refinement a generic coulomb interaction was also added, but this worsened the fit of the force field and was eventually discarded.

5.4.4. Comparison with previous force fields

The main difference between this force field and previous force fields developed for the halogermanes, -silanes and –alkanes, is the addition of a generic van der Waals term to the interactions. Also, the previous force fields used experimental geometries or assumed an idealized tetrahedral geometry in the input and did not attempt to reproduce these geometries, but focused instead on the vibration frequencies and other properties related to the vibrational behavior. Nonetheless, where previously defined parameters are available, they are compared to those of this force field.

Table 5.6: Stretching Parameters

Bond	Description	r_0 (Å)	k_s (kcal/Å^2)
2-1	C3-H	1.0848	682.38
3-1	Si3-H	1.4519	395.80
4-1	Ge3-H	1.5092	333.10
2-5	C3-F	1.3506	927.53
3-5	Si3-F	1.5758	776.84
4-5	Ge3-F	1.6987	703.15
2-6	C3-Cl	1.7788	407.22
3-6	Si3-Cl	2.0416	375.05
4-6	Ge3-Cl	2.1339	313.77
2-7	C3-Br	1.948	322.78
3-7	Si3-Br	2.1937	304.41
4-7	Ge3-Br	2.2579	217.20
2-2	C3-C3	1.5195	591.32
3-2	Si3-C3	1.8538	363.80
4-2	Ge3-C3	1.9106	379.39

Table 5.7: Torsion parameters

Torsion	Description	V (kcal)
1-2-2-1	H-C3-C3-H	0.2672
1-2-2-2	H-C3-C3-C3	0.4406
1-2-3-1	H-C3-Si3-H	0.0731
1-2-3-2	H-C3-Si3-C3	0.2640
1-2-4-1	H-C3-Ge3-H	0.1668
1-2-4-2	H-C3-Ge3-C3	0.1321
1-2-2-5	H-C3-C3-F	0.2367
1-2-3-5	H-C3-Si3-F	0.0159
1-2-4-5	H-C3-Ge3-F	-0.0030
1-2-2-6	H-C3-C3-Cl	0.5033
1-2-3-6	H-C3-Si3-Cl	0.1000
1-2-4-6	H-C3-Ge3-Cl	0.1097
1-2-2-7	H-C3-C3-Br	0.5588
1-2-3-7	H-C3-Si3-Br	0.1945
1-2-4-7	H-C3-Ge3-Br	0.2584

Table 5.8: Bending Parameters

Angle	Description	θ_0 (°)	k_b (kcal/rad^2)
1-2-1	H-C3-H	107.7	77.33
1-3-1	H-Si3-H	118.4	59.24
1-4-1	H-Ge3-H	122.5	53.93
5-2-5	F-C3-F	105.5	233.09
5-3-5	F-Si3-F	109.2	128.78
5-4-5	F-Ge3-F	106.2	92.44
6-2-6	Cl-C3-Cl	110.1	141.99
6-3-6	Cl-Si3-Cl	112.2	120.63
6-4-6	Cl-Ge3-Cl	111.0	101.61
7-2-7	Br-C3-Br	109.2	114.30
7-3-7	Br-Si3-Br	114.1	112.20
7-4-7	Br-Ge3-Br	112.7	101.45
1-2-5	H-C3-F	106.3	128.83
1-3-5	H-Si3-F	112.6	87.86
1-4-5	H-Ge3-F	113.0	71.27
1-2-6	H-C3-Cl	105.8	98.70
1-3-6	H-Si3-Cl	113.3	73.81
1-4-6	H-Ge3-Cl	114.2	63.71
1-2-7	H-C3-Br	104.3	88.56
1-3-7	H-Si3-Br	113.3	71.80
1-4-7	H-Ge3-Br	114.9	62.36
2-2-2	C3-C3-C3	114.7	113.86
2-2-1	C3-C3-H	110.1	89.58
2-3-2	C3-Si3-C3	124.9	57.11
2-3-1	C3-Si3-H	122.2	55.09
3-2-1	Si3-C3-H	111.0	62.14
2-4-2	C3-Ge3-C3	128.1	54.96
2-4-1	C3-Ge3-H	131.7	41.13
4-2-1	Ge3-C3-H	109.5	64.63
2-2-5	C3-C3-F	107.6	147.95
2-3-5	C3-Si3-F	115.5	73.58
2-4-5	C3-Ge3-F	115.1	56.43
2-2-6	C3-C3-Cl	110.7	129.57
2-3-6	C3-Si3-Cl	117.6	62.55
2-4-6	C3-Ge3-Cl	120.9	41.46
2-2-7	C3-C3-Br	110.0	121.32
2-3-7	C3-Si3-Br	117.6	65.78
2-4-7	C3-Ge3-Br	124.4	34.06

Table 5.9: Stretch-bend parameters

Atoms	Description	k_{sb} (kcal/Å.rad)
X-2-X	X-C3-X	27.704
5-2-X	F-C3-X	103.603
X-3-X	X-Si3-X	15.055
5-3-X	F-Si3-X	14.487
X-4-X	X-Ge3-X	13.495
5-4-X	F-Ge3-X	34.878
X-X-X	X-X-X	6.699

Table 5.10: Bend-bend parameters

Atoms	Description	k_{bb} (kcal/rad^2)
X-X-X-X	X-X-X-X	1.3816
5-X-X-X	F-X-X-X	1.5573

Table 5.11: Bend-torsion-bend parameters

Atoms	Description	k_{btb} (kcal/rad^2)
1-2-X-2	H-C3-X-C3	-9.2137
1-2-X-X	H-C3-X-X	-7.4908

The comparison of the stretching and bending force constants of our force field with literature values is summarized in the tables of **Addendum F**. The general trend in the stretching force constants of this work is a decrease in the order A-F > A-H > A-Cl > A-Br for A=C, Si and Ge. The same trend is observed in the C-H and C-X stretching force constants of the previously reported force fields [41] for molecules of the form AH_nX_{4-n}, but for Si and Ge the A-Cl force constants are generally larger than the A-H stretching force constants. The numerical values differ quite largely in some cases, but this is to be expected, considering the difference in the parameterization and use of the force fields.

The general trend in the bending force constants of this work is a decrease in the order of X-A-X > X-A-H > H-A-H for a specific A and X. In the previous force fields this is also true for AH_3X and AHX_3 molecules, but for the AH_2X_2 molecules the H-A-H bending constants are consistently larger than the X-A-H bending constants. The numerical correspondence between the literature

values of the bending force constants and those of the present work is generally worse than was the case for the stretching constants.

In the case of the dimethylated compounds, the only molecule for which a force field has been previously defined is Me_2GeF_2 [32] and the force field is a vibrational one. Nonetheless, there is fairly good correspondence between the stretching force constants of this force field and that of the present work. Most of the bending force constants also correspond well, except for that of the C-Ge-C angle, which is almost double the literature value in our force field. As the previous force field assumed an idealized tetrahedral geometry for the Ge atom while our force field uses the large angles calculated with *ab initio* methods, it is only to be expected that these force constants would differ largely.

The values of the interaction parameters have not been directly compared to those of previous force fields, since the cross terms used in this work are generic and cannot therefore be expected to correspond to the explicit cross terms previously defined. However, the stretch-bend and bend-bend force constants of our force field are all positive, whereas they are negative in many of the force fields for AH_nX_{4-n} molecules. The previous force field for Me_2GeF_2 defines only stretch-stretch and bend-bend interactions and uses no stretch-bend or bend-torsion-bend terms. Once again many of the bend-bend interaction parameters are negative.

5.5. Discussion

Although there is room for improvement in the force field, the main aim was to create a force field that would be able to correctly predict the C-A-C angles in compounds of the form Me_2AX_2 for A= C, Si, Ge and X=H, F, Cl, Br and this has been successfully achieved. The close agreement between the force field and the *ab initio* calculations should make it possible to quantitatively predict the geometries and vibrational spectra of other halogenated organic compounds of germanium, silicon and carbon.

Furthermore, this was achieved using very basic functions for the interactions and a minimal number of cross-term interactions. The addition of further non-diagonal elements to the force constant matrix does lead to a better fit of the force field, but the improvement is too small to justify the number of additional parameters required for these cross terms.

An interesting point to note is that the addition of Coulomb interactions weakened the fit of the force field. The fact that *ab initio* calculations indicate that there is substantial ionic character in some of the molecules for which the force field was parameterized makes it strange that this should be the case. It is possible that the effect of the charge distribution on the valence angles was implicitly included in the other interactions, making it unnecessary to include an explicit charge interaction.

5.6. Conclusion

A force field has been developed for halogenated alkanes, silanes and germanes which is able to correctly predict the trend in C-A-C angles in molecules of the form Me_2AX_2, where A=C, Si or Ge and X=H, F, Cl or Br.

CHAPTER 6: Conclusion

6.1. Summary

In terms of the aims outlined in **Chapter 1**, the results of this work can be summarized as follows:

- An *ab initio* study has been conducted at HF level of theory and a set of consistent and reliable structural and vibrational data has been obtained for compounds of the general form AH_nX_{4-n}, $MeAH_2X$, $MeAHX_2$, Me_2AHX and Me_2AX_2, where A=C, Si, Ge and X=H, F, Cl, Br. Data were also obtained for compounds of the form Me_2AI_2 at HF level and for Me_2AX_2 at MP2 and DFT level.
- The results of the ab initio calculations confirmed the experimental findings, namely that the C-Ge-C angle in compounds of the form Me_2GeX_2 is substantially larger than the tetrahedral angle of 109.47°. The same effect is not seen in the analogous silicon and carbon compounds. Previous *ab initio* studies and a search of the Cambridge Structural Database indicate that the geometries of analogous Sn and Pb compounds show similar deviations from the tetrahedral.
- Factors that influence the C-A-C angle in compounds of the form Me_2AX_2 include the electronegativity of the substituent X and the degree of ionicity in the bonding. This is supported by statistical analysis of the Cambridge Structural Database and the total electron density distributions of some of the calculated structures. It is likely that the d-orbitals of germanium, in combination with the other factors, could also play a role in opening up the C-Ge-C angle.
- The observed effect seems to be a trend in the group IV elements rather than an anomaly in the germanium compounds. A second order polynomial function can be fitted to the calculated data for the C-A-C angles with a high degree of success and serves as a good starting approximation for describing the trend.

- Qualitatively, the deviations from idealized geometry in the germanium compounds can be justified in terms of three theories of structure and bonding, namely the Valence-Shell Electron-Repulsion theory, Bent's rule and the Ligand Close Packing model.
- A representative compound, dichlorobis(phenethyl)germane, has been synthesized and the crystal structure determined by means of X-ray diffraction techniques. The C-Ge-C angle was found to be 121.2°, which verifies the results of the *ab initio* and gas phase electron diffraction studies.
- A force field has been developed which is able to correctly predict the trend in the C-A-C and X-A-X angles in compounds of the form Me_2AX_2, with an error of less than 1° for these angles. Furthermore, this was achieved using only standard bond stretching, angle bending and torsional interactions, a generic van der Waals interaction and a few generic cross terms. Effects such as electronegativity and charge distribution, although found to influence the angles, were not explicitly included and seem to have been implicitly accounted for in the basic interactions.

6.2. Future research

There is much scope for further research on the dihalo(dimethyl)germanes and there are many gaps to be filled in the existing data, for these and other related compounds. A definite area for future research is the addition of the full range of iodine compounds and the analogous compounds of the other group IV elements tin and lead, to the existing *ab initio* study. This would require the use of a much larger basis set to include all the atoms and the consideration of relativistic effects in the heavier atoms, and a much higher level of theory than Hartree-Fock would be needed. This would however, demonstrate more clearly the nature of the trend in the C-A-C and X-A-X angles and provide a much larger set of data on which to base an analysis.

The deviations from idealized geometry have been explained in terms of existing theories and the hybridization of the central atom has formed a substantial part of the discussions on the bond angles. Although the molecular orbitals of some of the compounds were studied, they provided little insight into the problem of the large C-Ge-C angles in the dihalo-(dimethyl)germanes. A Natural Bond Orbital analysis would provide much valuable insight into the directional nature of the molecular orbitals and enable a better understanding of the effect.

As we have seen, there are few crystalline compounds of the form R_2GeX_2 in which the C-Ge-C angles are not sterically or electronically hindered in some way. The synthesis of dichlorobis(phenethyl)germane was successful and was performed under mild conditions with a relatively quick and easy method. The synthesis of more of these compound to increase the available experimental structural data, is another area of interest.

Lastly, the force field was parameterized for the atom types C, Si, Ge, H, F, Cl and Br. Another area of future research would be to expand the force field to include the atom types I, Sn and Pb. It would also be interesting to use the force field to calculate the structure of dichlorobis(phenethyl)germane and compare it to the experimentally determined structure. In order to do this the force field would have to be parameterized to accommodate for aromatic systems.

REFERENCES

1. V. W. Laurie, *J. Chem. Phys.*, **30**, 1210 (1959)

2. E. C. Thomas and V. W. Laurie, *J. Chem. Phys.*, **50(8)**, 3512 (1969)

3. Y. S. Li and J. R. Durig, *Inorg. Chem.*, **12(2)**, 306 (1973)

4. J. R. Durig and K. L. Hellams, *J. Mol. Struct.*, **29**, 349 (1975)

5. J. R. Durig, P. J. Cooper and Y. S. Li, *J. Mol. Spectroscopy*, **57**, 169 (1975)

6. R. W. Kilb and L. Pierce, *J. Chem. Phys.*, **27(1)**, 108 (1957)

7. L. Pierce, *J. Chem. Phys.*, **34(2)**, 498 (1961)

8. J. F. Ollom, A. A. Sinisgalli, H. N. Rexroad and R. C. Gunton, *J. Chem. Phys.*, **24**, 487 (1955)

9. P. Venkateswarlu, R. C. Mockler and W. Gordy, *J. Chem. Phys.*, **21(10)**, 1713 (1953)

10. S. N. Wolf, L. C. Krisher, *J. Chem. Phys.*, **56(3)**, 1041 (1972)

11. J. E. Drake, R. T. Hemmings, J. L. Hencher, F. M. Mustoe and Q. Shen, *J. Chem. Soc. Dalton Trans.*, 394 (1976)

12. J. E. Drake, J. L. Hencher and Q. Shen, *Can. J. Chem.*, **55**, 1104 (1977)

13. J. E. Drake, R. T. Hemmings, J. L. Hencher, F. M. Mustoe and Q. Shen, *J. Chem. Soc. Dalton Trans.*, 811 (1976)

14. B. Beagley, D. P. Brown and J. M. Freeman, *J. Mol. Structure*, **18**, 335 (1973)

15. J. L. Hencher and F. J. Mustoe, *Can. J. Chem.*, **53**, 3542 (1975)

16. B. Rempfer, H. Oberhammer and N. Auner, *J. Am. Chem. Soc.*, **108**, 3893 (1986)

17. G. Vacek, V. S. Mastryukov and H.F. Schaefer III, *J. Phys. Chem.*, **98**, 11337 (1994)

18. V. Jonas, C. Boehme and G. Frenking, *Inorg. Chem.*, **35**, 2097 (1996)

19. V. Jonas, G. Frenking and M. T. Reetz, *J. Comput. Chem.*, **13**, 919 (1992)

20. T. M. Klapotke and A. Schulz, *Quantum Chemical Methods in Main Group Chemistry*, John Wiley and Sons, Chichester, 1998

21. S. L. Mayo, B. D. Olafson, W. A. Goddard III, *J. Phys. Chem.*, **94**, 8897 (1990)

22. A. K. Rappe, C. J. Casewit, K. S. Colwell, W. A. Goddard III, W. M. Skiff, *J. Am. Chem. Soc.*, **114**, 10024 (1992)

23. D. M. Root, C. R. Landis, T. Cleveland, *J. Am. Chem. Soc.*, **115**, 4201 (1993)

24. J. E. Griffiths, *Spectrochimica Acta*, **20**, 1335 (1964)

25. J. R. Aronson and J. R. Durig, *Spectrochimica Acta*, **20**, 219 (1964)

26. R. J. Cross and F. Glockling, *J. Organomet. Chem.*, **3**, 146 (1965)

27. J. R. Durig, K. K. Lau, J. B. Turner and J. Bragin, *J. Mol. Spectroscopy*, **31**, 419 (1969)

28. D. F. van de Vondel and G. P. van der Kelen, *Bull. Soc. Chim. Belges*, **74**, 453 (1964)

29. D. F. van de Vondel, G. P. van der Kelen and G. van Hooydonk, *J. Organomet. Chem.*, **23**, 431 (1970)

30. J. R. Durig, C. F. Jumper and J. N. Willis Jr., *J. Mol. Spectroscopy*, **37**, 260 (1971)

31. J. W. Anderson, G. K. Barker, J. E. Drake and R. T. Hemmings, *Can. J. Chem.*, **49**, 2931 (1971)

32. J. W. Anderson, G. K. Barker, A. J. F. Clark, J. E. Drake and R. T. Hemmings, *Spectrochimica Acta*, **30A**, 1081 (1974)

33. G. K. Barker, J. E. Drake and R. T. Hemmings, *Can. J. Chem.*, **52**, 2622 (1974)

34. G. K. Barker, J. E. Drake and R. T. Hemmings and B. Rapp, *Spectrochimica Acta*, **28A**, 1113 (1972)

35. G. K. Barker, J. E. Drake, R. T. Hemmings and B. Rapp, *J. Chem. Soc. (A)*, 3291 (1971)

36. R. Aroca, E. A. Robinson and T. A. Ford, *J. Mol. Struct.*, **31**, 177 (1976)

37. R. Aroca, E. A. Robinson and T. A. Ford, *S. Afr. J. Chem.*, **30**, 95 (1977)

38. J. Bunnell and T. A. Ford, *J. Mol. Struct.*, **94**, 227 (1983)

39. J. Bunnell and T. A. Ford, *J. Mol. Spectroscopy*, **100**, 215 (1983)

40. N. Mercau, R. Aroca, E. A. Robinson, J. Aron, J. Bunnell and T. A. Ford, *J. Comput. Chem.*, **5(5)**, 427 (1984)

41. N. Mercau, R. Aroca, E. A. Robinson, J. Aron, J. Bunnell and T. A. Ford, *J. Mol. Struct.*, **110**, 361 (1984)

42. J. S. Weaving and T. A. Ford, *J. Mol. Struct.*, **161**, 245 (1987)

43. F. A. Cotton, G. Wilkinson and P. L. Gaus, *Basic Inorganic Chemistry*, 2nd ed., John Wiley and Sons, 1987

44. F. A. Cotton and G. Wilkinson, *Advanced Inorganic Chemistry*, 5th ed., John Wiley and Sons, 1988

45. L. Pauling, *The Nature of the Chemical Bond*, 3rd ed., Cornell University Press, Ithaca, New York, 1962

46. N. V. Sidgwick and H. M. Powell, *Proc. Roy. Soc.*, **A176**, 153 (1940)

47. C. E. Mellish and J. W. Linnet, *Trans. Faraday Soc.*, **50**, 657 (1954)

48. G. W. A. Fowles, *J. Chem. Educ.*, **34**, 187 (1957)

49. R. J. Gillespie and R. S. Nyholm, *Quart. Rev. (London)*, **11**, 339 (1957)

50. R. J. Gillespie, *J. Chem. Educ.*, **40**, 295 (1963)

51. H. A. Bent, *Chem. Rev.*, **61**, 275 (1961)

52. R. J. Gillespie and E. A. Robinson, *Advances in Molecular Structure Research*, **4**, 14 (1998)

53. R. F. W. Bader, *Atoms in Molecules: A Quantum Theory*, Clarendon Press, Oxford, 1990

54. P. Comba and T. W. Hambley, *Molecular Modelling*, Weinheim, VCH, 1995

55. J. L. M. Dillen, unpublished notes

56. F. Jensen, *Introduction to Computational Chemistry*, John Wiley and Sons, 1999

57. J. B. Foresman and . Frisch, *Exploring Chemistry with electronic structure methods*, 2nd ed., Gaussian Inc., Pittsburgh PA, 1995

58. A. Hinchliffe, *Computational Quantum Chemistry*, John Wiley and Sons, 1988

59. J. M. Goodman, *Chemical applications of molecular modelling*, Cambridge, Royal Society of Chemistry, 1998

60. A. Hinchliffe, *Modelling Molecular Structures*, John Wiley and Sons, 2000

61. G. Frenking, personal communication

62. Z. Barandiarán and L. Seijo, *J. Chem. Phys.*, **101(5)**, 4049 (1994)

63. J. Bunnell, B. C. Crafford and T. A. Ford, *J. Mol. Struct.*, **61**, 383 (1980)

64. J. Bunnell and T. A. Ford, *Spectrochimica Acta*, **42A**, 543 (1986)

65. J. Bunnell and T. A. Ford, *Spectrochimica Acta*, **42A**, 551 (1986)

66. *Cerius2, Software Environment for Chemical Computing*, Molecular Simulations Inc., San Diego, 1998

67. Morgan and Drew, *J. Chem. Soc.*, **125**, 1261 (1924)

68. Tabern, Orndorff and Dennis, *J. Am. Chem. Soc.*, **49**, 2512 (1927)

69. C. A. Kraus and Foster, *J. Am. Chem. Soc.*, **49**, 457 (1927)

70. C. A. Kraus and C. L. Brown, *J. Am. Chem. Soc.*, **52**, 3690 (1930)

71. T. S. Piper and M. K. Wilson, *J. Inorg. Nucl. Chem.*, **4**, 22 (1957)

72. H. H. Anderson, *J. Am. Chem. Soc.*, **82**, 3016 (1960)

73. J. E. Griffiths, *Inorganic Chemistry*, **2**, 375 (1963)

74. K. Moedritzer, *J. Organometallic Chem.*, **6**, 282 (1966)

75. E. G. Rochow, *J. Am. Chem. Soc.*, **69**, 1729 (1947)

76. O. H. Johnson, *Inorganic Synthesis*, **18**, 64 (1978)

77. D. M. Harris, W. H. Nebergall and O. H. Johnson, *Inorganic Synthesis*, **18**, 70 (1978)

78. D. M. Harris, W. H. Nebergall and O. H. Johnson, *Inorganic Syntheses*, **18**, 72 (1978)

79. D. M. Harris and O. H. Johnson, *Inorganic Syntheses*, **18**, 74 (1978)

80. O. H. Johnson, W. H. Nebergall and D. M. Harris, *Inorganic Syntheses*, **18**, 76 (1978)

81. L. Fajarí, J. Carilla, L. Juliá, J. Riera, A. Párraga, M. Coll and X. Solans, *J. Organomet. Chem.*, **474**, 89 (1994)

82. F. H. Allen, S. Bellard, M. D. Brice, B. A. Cartwright, A. Doubleday, H. Higgs, T. Hummelink, B. G. Hummelink-Peters, O. Kennard, W. D. S. Motherwell, J. R. Rodgers, D. G. Watson, *Acta Cryst.*, **B35**, 2331 (1979)

83. *Gaussian98, Revision A.7.*, M. J. Frisch, G. W. Trucks, H. B. Schlegel, G. E. Scuseria, M. A. Robb, J. R. Cheeseman, V. G. Zakrzewski, J. A. Montgomery, J. A. Montgomery, Jr., R. E. Stratmann, J. C. Burant, S. Dapprich, J. M. Millam, A. D. Daniels, K. N. Kudin, M. C. Strain, O. Farkas, J. Tomasi, V. Barone, M. Cossi, R. Cammi, B. Mennucci, C. Pomelli, C. Adamo, S. Clifford, J. Ochterski, G. A. Petersson, P. Y. Ayala, Q. Cui, K. Morokuma, D. K. Malick, A. D. Rabuck, K. Raghavachari, J. B. Foresman, J. Cioslowski, J. V. Ortiz, A. G. Baboul, B. B. Stefanov, G. Liu, A. Liashenko, P. Piskorz, I. Komaromi, R. Gomperts, R. L. Martin, D. J. Fox, T. Keith, M. A. Al-Laham, C. Y. Peng, A. Nanayakkara, C. Gonzalez, M. Challacombe, P. M. W. Gill, B. Johnson, W. Chen, M. W. Wong, J. L. Andres, C. Gonzalez, M. Head-Gordon, E. S. Replogle, and J. A. Pople, Gaussian Inc., Pittsburgh PA, 1998

84. *Gopenmol, Version 1.31.*, Leif Laaksonen, 1997

85. E. Frisch and M. J. Frisch, *Gaussian 98 User's reference*, 2nd ed., Gaussian Inc., Pittsburgh PA, 1999

86. *WebLab ViewerPro 3.7.*, Molecular Simulations Inc., San Diego, 2000

87. Herrmann and Brauer, *Synthetic Methods of Organometallic and Inorganic Chemistry, Volume 1*, Thieme Medical Publishers, New York, 1996

88. B. S. Furniss, A. J. Hannaford, P. W. G. Smith and A. R. Tatchell, *Vogel's Textbook of Practical Organic Chemistry*, 5th ed., Longman Scientific and Technical, Essex, 1989

89. B. V. Nonius, *COLLECT. Data collection Software*, Delft, The Netherlands, 1998

90. G. M. Sheldrick, *SHELX-97. Program for Crystal structure analysis*, Univ. of Göttingen, Germany, 1997

91. L. J. Farrugia, *J. Appl. Cryst.*, **32**, 837 (1999)

92. L. J. Farrugia, *J. Appl. Cryst.*, **30**, 565 (1997)

93. J. L. M. Dillen, *J. Comp. Chem.*, **13(3)**, 257 (1992)

94. J. L. M. Dillen, *PEFF User's Guide*, 1995, unpublished

95. J. L. M. Dillen, *Vibram*, Univ. of Stellenbosch, South Africa, unpublished

Addendum A: Valence Molecular Orbitals of Me_2CF_2, Me_2GeF_2 and Me_2GeH_2

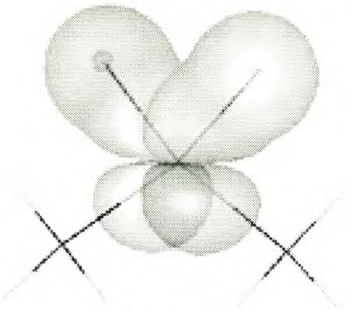

GeF14

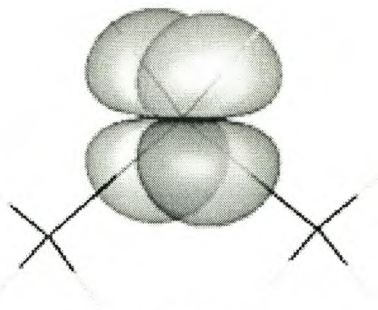

GeH12

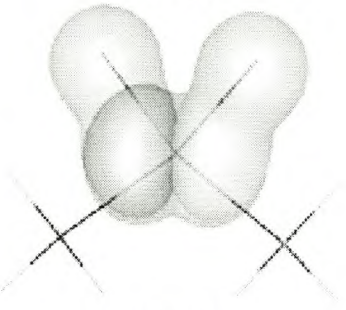

GeF15

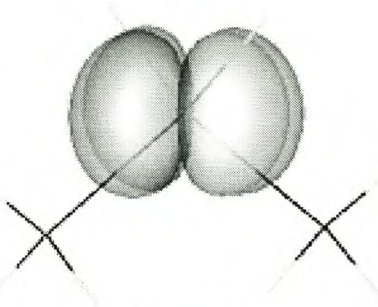

GeH13

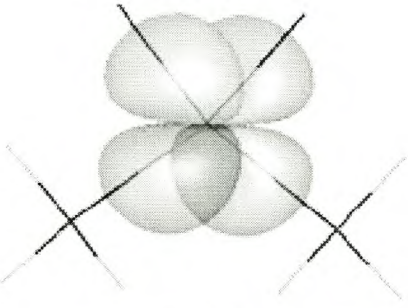

GeF16

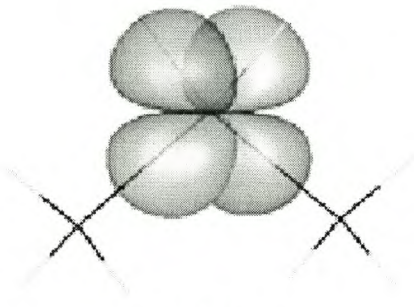

GeH14

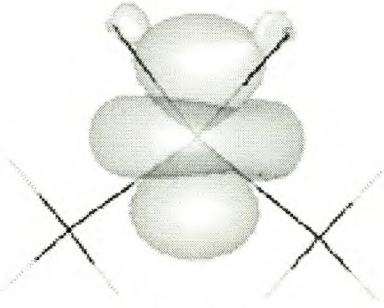

GeF17

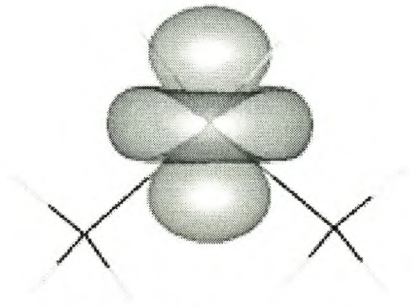

GeH15

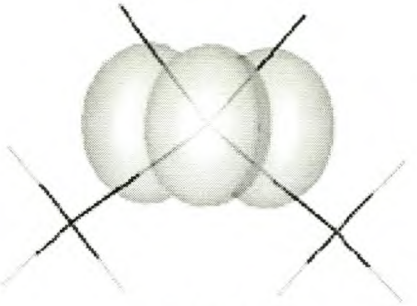

GeF18

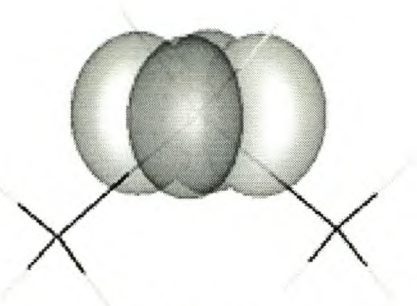

GeH16

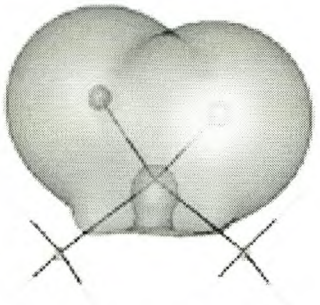

CF6

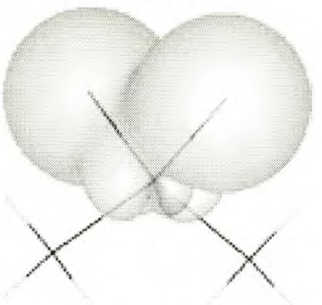

GeF19

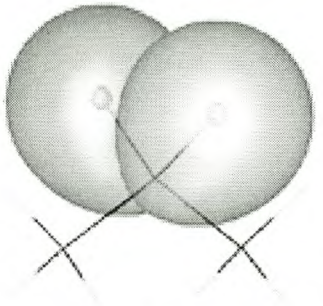

CF7

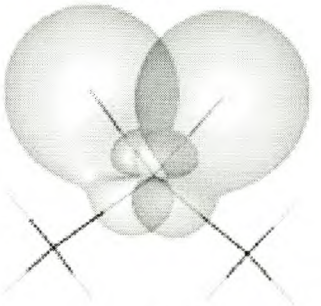

GeF20

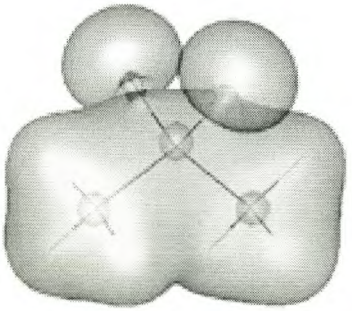

CF8

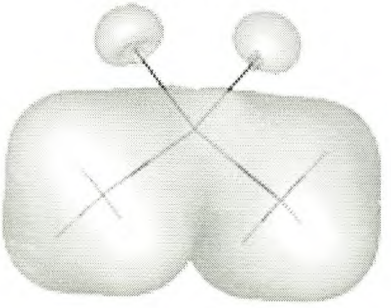

GeF21

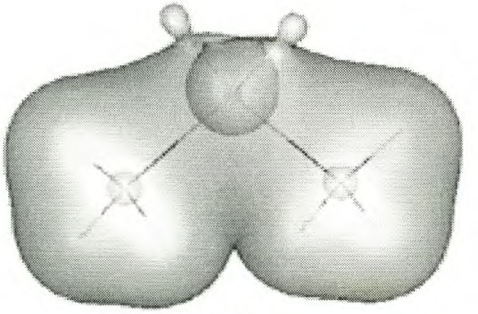

GeH17

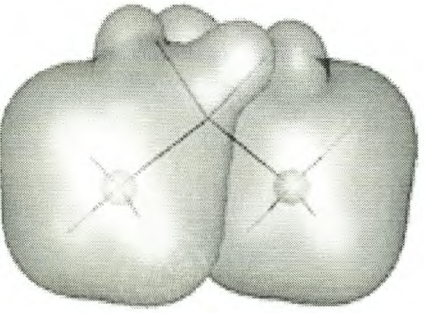

CF9

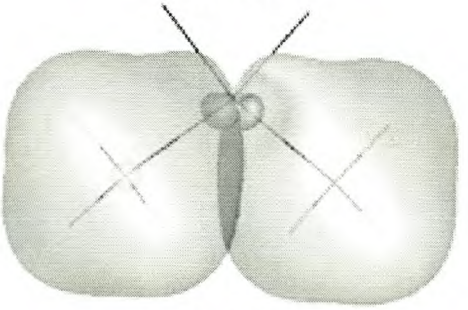

GeF22

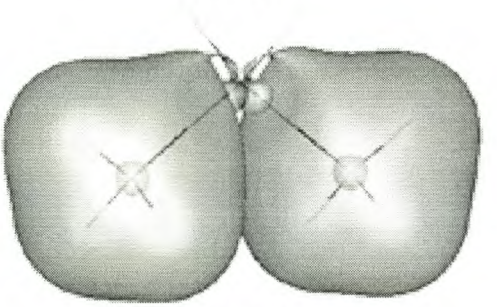

GeH18

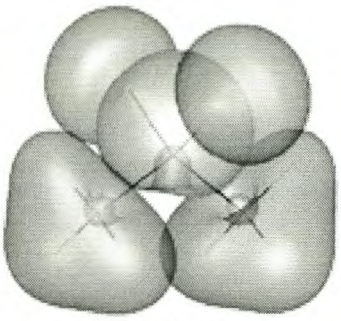

CF10

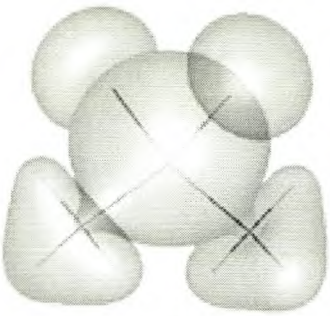

GeF23

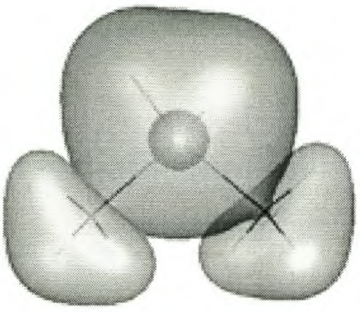

GeH19

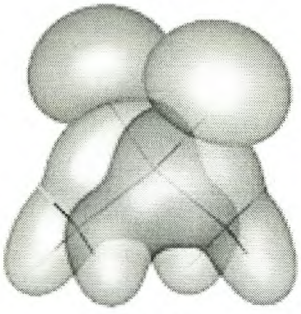

CF11

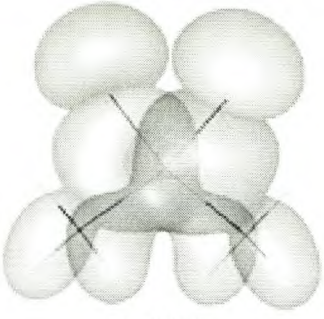

GeF24

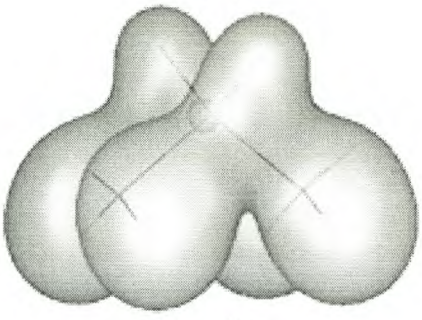

GeH20

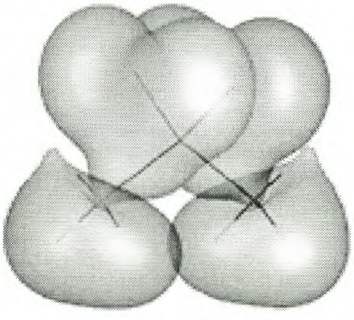

CF13

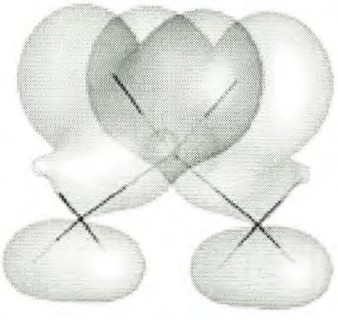

GeF25

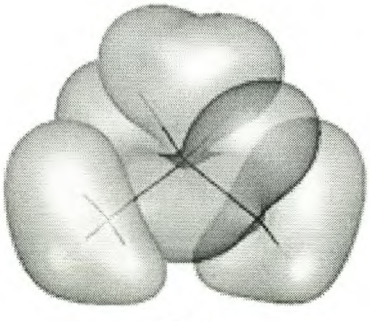

CF12

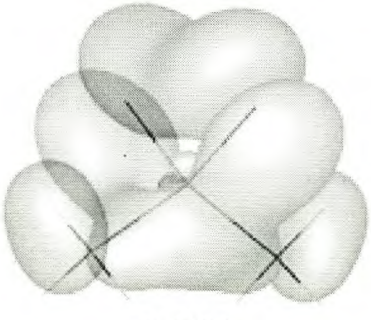

GeF26

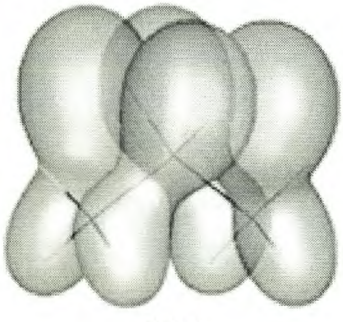

CF14

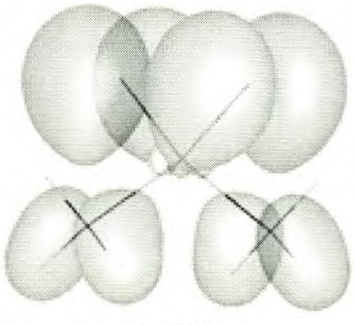

GeF27

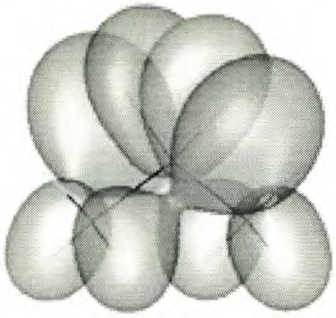

CF16

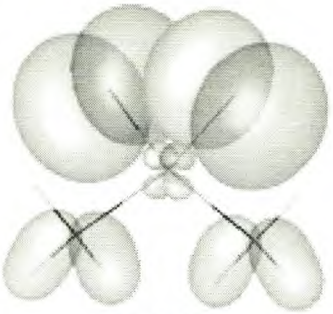

GeF28

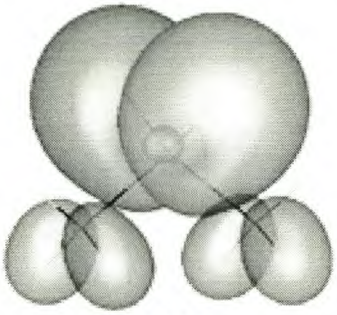

GeH24

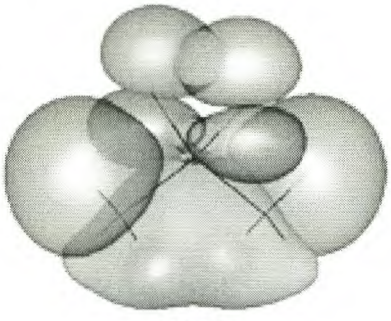

CF15

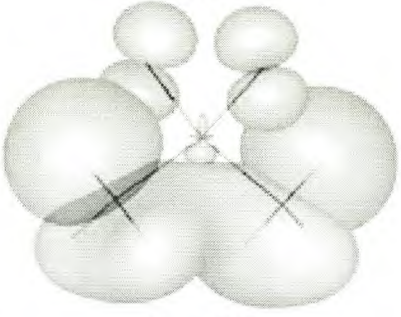

GeF29

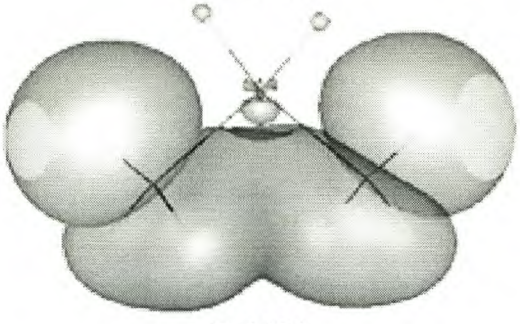

GeH21

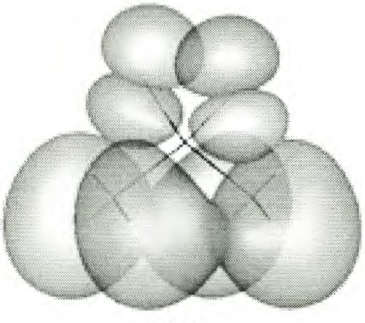

CF17

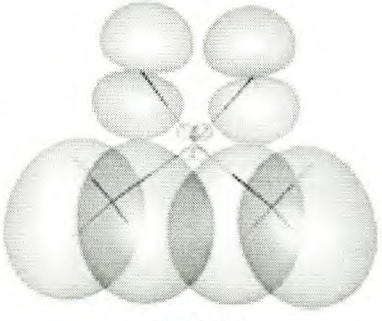

GeF30

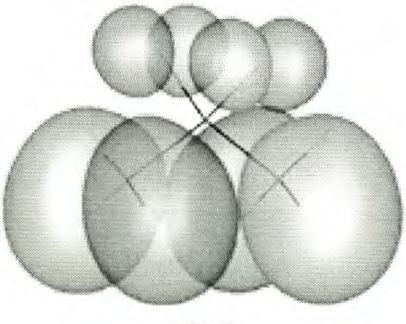

CF18

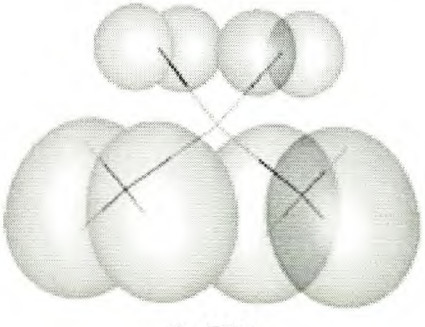

GeF31

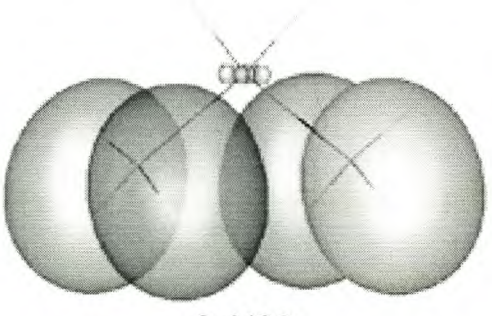

GeH23

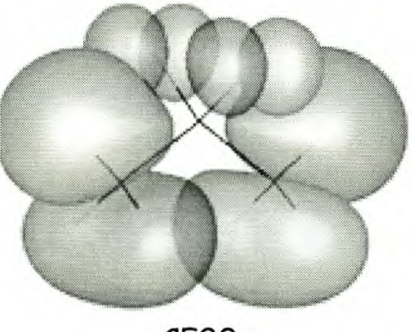

CF20

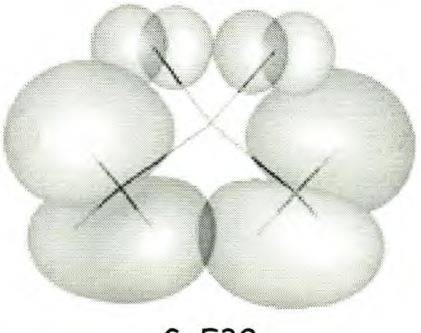

GeF32

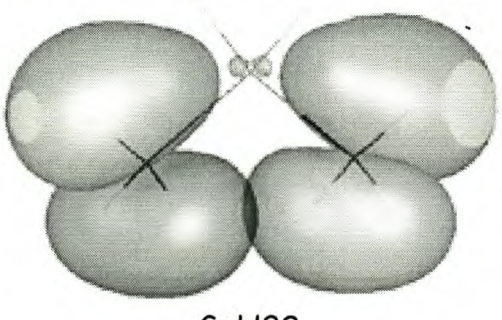

GeH22

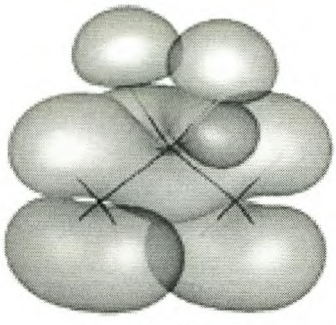

CF19

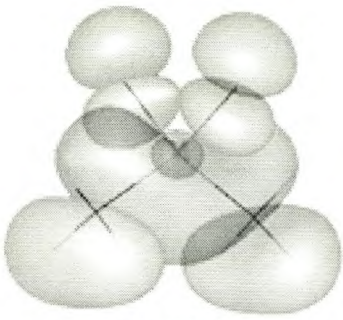

GeF33

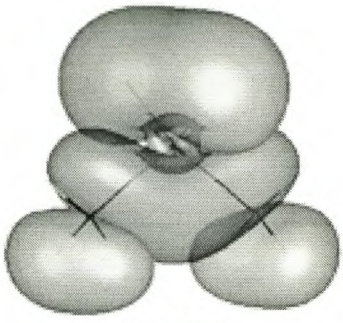

GeH25

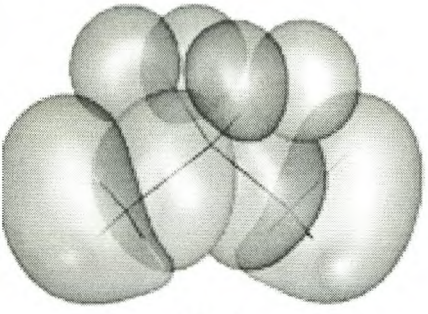

CF21

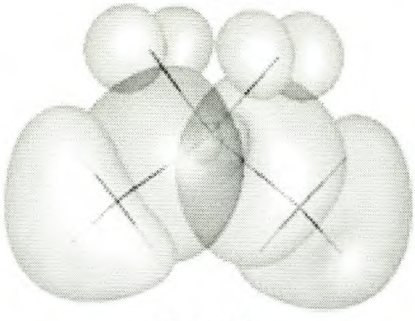

GeF34

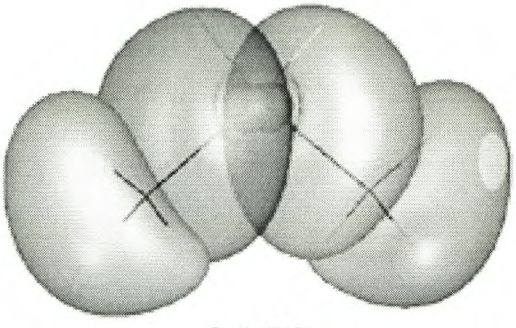

GeH26

Addendum B: Vibrational Analysis

Table I: Vibrations of the halomethanes (CH_nX_{4-n})

Molecule	Symmetry	Assignment	Observed Frequency	Calculated Frequency	Difference (Calc-Obs)	%Diff.	Mode ab initio	Mode FF
CH_4	F2	bend def	1328.5	1330.6	2.1	0.16	1,2,3	2
	E	bend def	1520.3	1505.0	-15.3	1.01	4,5	5
	A1	symm str	2854.8	2825.5	-29.3	1.03	6	6
	F2	asymm str	2948.1	2957.9	9.8	0.33	7,8,9	8
CH_3F	A1	symm CF str	1059.3	1095.0	35.7	3.37	1	1
	E	asymm HCF bend	1171.4	1166.3	-5.0	0.43	2,3	3
	A1	symm HCF bend	1474.8	1444.8	-29.9	2.03	4	4
	E	asymm HCH bend	1476.2	1485.5	9.4	0.64	5,6	6
	A1	symm CH str	2887.0	2858.5	-28.4	0.99	7	7
	E	asymm CH str	2958.7	2960.5	1.9	0.06	8,9	8
CH_3Cl	A1	symm CCl str	698.8	674.1	-24.7	3.53	1	1
	E	asymm HCCl bend	1016.4	990.7	-25.8	2.53	2,3	2
	A1	symm HCCl bend	1373.4	1371.3	-2.0	0.15	4	4
	E	asymm HCH bend	1454.5	1468.6	14.1	0.97	5,6	5
	A1	symm CH str	2917.4	2856.2	-61.2	2.10	7	7
	E	asymm CH str	3010.0	2961.9	-48.1	1.60	8,9	8
CH_3Br	A1	symm CBr str	570.0	547.7	-22.3	3.92	1	1
	E	asymm HCBr bend	946.5	930.5	-16.1	1.70	2,3	2
	A1	symm HCBr bend	1323.9	1292.9	-31.0	2.34	4	4
	E	asymm HCH bend	1451.0	1472.5	21.5	1.48	5,6	5
	A1	symm CH str	2926.2	2853.7	-72.6	2.48	7	7
	E	asymm CH str	3028.0	2963.3	-64.7	2.14	8,9	8
CH_2F_2	A1	symm FCF bend	509.6	565.1	55.5	10.90	1	1
	A1	symm CF str	1105.5	1054.5	-51.0	4.61	2	3
	B2	asymm CF str	1122.8	1194.7	71.9	6.40	3	4
	B1	HCH rocking	1164.3	1052.5	-111.9	9.61	4	2
	A2	HCH twist	1258.6	1396.1	137.5	10.93	5	5
	B2	HCH wagging	1463.7	1408.3	-55.4	3.79	6	6
	A1	HCH symm bend	1529.3	1502.3	-27.1	1.77	7	7
	A1	symm CH str	2942.1	2893.6	-48.5	1.65	8	8
	B1	asymm CH str	3006.4	2963.9	-42.5	1.42	9	9
CH_2Cl_2	A1	symm ClCCl bend	278.4	259.6	-18.8	6.75	1	1
	A1	symm CCl str	691.5	639.6	-51.9	7.50	2	2
	B2	asymm CCl str	752.4	759.9	7.5	1.00	3	3
	B1	HCH rocking	888.7	798.2	-90.5	10.18	4	4
	A2	HCH twist	1174.3	1229.7	55.4	4.72	5	5
	B2	HCH wagging	1295.1	1314.7	19.6	1.51	6	6
	A1	symm HCH bend	1445.5	1446.0	0.5	0.04	7	7
	A1	symm CH str	2979.6	2892.8	-86.9	2.92	8	8
	B1	asymm CH str	3053.3	2964.5	-88.8	2.91	9	9

CH_2Br_2	A1	symm BrCBr bend	170.2	151.0	-19.2	11.28	1	1
	A1	symm CBr str	556.0	509.3	-46.7	8.39	2	2
	B2	asymm CBr str	630.3	634.3	4.0	0.64	3	3
	B1	HCH rocking	788.8	730.9	-57.8	7.33	4	4
	A2	HCH twist	1107.4	1165.2	57.8	5.21	5	5
	B2	HCH wagging	1213.2	1216.5	3.4	0.28	6	6
	A1	symm HCH bend	1423.1	1429.6	6.5	0.46	7	7
	A1	symm CH str	2992.9	2890.8	-102.1	3.41	8	8
	B1	asymm CH str	3077.9	2966.7	-111.2	3.61	9	9
CHF_3	E	asymm FCF bend	491.9	540.6	48.7	9.90	1,2	1
	A1	symm HCF bend	680.6	630.8	-49.8	7.31	3	3
	A1	symm CF str	1126.7	979.7	-147.1	13.05	4	4
	E	asymm CF str	1185.7	1240.7	55.0	4.64	5,6	5
	E	asymm HCF bend	1413.5	1419.8	6.3	0.44	7,8	7
	A1	symm CH str	3036.8	2931.7	-105.2	3.46	9	9
$CHCl_3$	E	asymm ClCCl bend	257.8	241.5	-16.2	6.29	1,2	1
	A1	symm HCCl bend	360.3	295.0	-65.3	18.13	3	3
	A1	symm CCl str	652.5	562.5	-90.0	13.79	4	4
	E	asymm CCl str	780.8	812.2	31.4	4.02	5,6	6
	E	asymm HCCl bend	1248.8	1268.4	19.6	1.57	7,8	8
	A1	symm CH str	3043.2	2930.4	-112.8	3.71	9	9
$CHBr_3$	E	asymm BrCBr bend	154.1	136.3	-17.8	11.54	1,2	1
	A1	symm HCBr bend	215.8	177.8	-37.9	17.58	3	3
	A1	symm CBr str	512.5	440.8	-71.6	13.98	4	4
	E	asymm CBr str	657.6	676.2	18.6	2.84	5,6	6
	E	asymm HCBr bend	1156.8	1185.6	28.8	2.49	7,8	7
	A1	symm CH str	3059.3	2930.6	-128.7	4.21	9	9
CF_4	E	bend def	472.7	497.6	24.9	5.27	1,2	1
	F2	bend def	683.1	592.4	-90.7	13.28	3,4,5	5
	A1	symm str	896.2	758.8	-137.4	15.34	6	6
	F2	asymm str	1315.1	1292.9	-22.2	1.69	7,8,9	9
CCl_4	E	bend def	217.6	208.9	-8.7	4.00	1,2	2
	F2	bend def	311.0	259.9	-51.1	16.43	3,4,5	3
	A1	symm str	449.2	368.0	-81.2	18.07	6	6
	F2	asymm str	805.7	867.7	62.0	7.69	7,8,9	7
CBr_4	E	bend def	129.4	114.3	-15.1	11.69	1,2	1
	F2	bend def	182.1	148.1	-34.0	18.67	3,4,5	4
	A1	symm str	262.4	218.3	-44.1	16.82	6	6
	F2	asymm str	682.5	713.3	30.8	4.51	7,8,9	7

Table II: Vibrations of the halosilanes (SiH_nX_{4-n})

Molecule	Symmetry	Assignment	Observed Value	Calculated Value	Difference (Calc-Obs)	%Diff	Mode ab initio	Mode FF
SiH_4	F2	bend def	907.1	899.9	-7.2	0.79	1,2,3	3
	E	bend def	938.0	928.8	-9.2	0.99	4,5	5
	F2	asymm str	2130.0	2198.5	68.5	3.22	6,7,8	9
	A1	symm str	2136.9	2151.9	15.0	0.70	9	6
SiH_3F	E	asymm HSiF bend	710.1	717.6	7.5	1.05	1,2	1
	A1	symm SiF str	842.0	860.0	18.0	2.14	3	3
	E	asymm HSiH bend	938.4	936.8	-1.6	0.17	4,5	4
	A1	symm HSiF bend	992.3	994.4	2.1	0.21	6	6
	E	asymm SiH str	2161.7	2198.7	37.1	1.71	7,8	8
	A1	symm SiH str	2168.5	2162.7	-5.7	0.26	9	7
SiH_3Cl	A1	symm SiCl str	509.5	516.5	7.0	1.37	1	1
	E	asymm HSiCl bend	641.5	638.2	-3.3	0.52	2,3	2
	E	asymm HSiH bend	931.1	932.2	1.1	0.12	4,5	5
	A1	symm HSiCl bend	937.1	919.1	-18.0	1.92	6	4
	A1	symm SiH str	2168.5	2162.1	-6.5	0.30	7	7
	E	asymm SiH str	2172.3	2199.2	27.0	1.24	8,9	8
SiH_3Br	A1	symm SiBr str	405.1	400.3	-4.8	1.19	1	1
	E	asymm HSiBr bend	628.7	623.6	-5.1	0.82	2,3	2
	E	asymm HSiH bend	929.9	931.9	2.0	0.22	4,5	6
	A1	symm HSiBr bend	932.2	910.0	-22.2	2.38	6	4
	A1	symm SiH str	2167.4	2162.0	-5.4	0.25	7	7
	E	asymm SiH str	2173.0	2199.4	26.4	1.22	8,9	9
SiH_2F_2	A1	symm FSiF bend	305.5	333.6	28.1	9.18	1	1
	B1	HSiH rocking	697.2	631.1	-66.1	9.48	2	2
	A2	HSiH twist	722.3	855.8	133.5	18.48	3	5
	A1	symm SiF str	832.3	839.3	7.0	0.84	4	4
	B2	HSiH wagging	877.5	832.1	-45.4	5.17	5	3
	A1	symm HSiH bend	967.5	973.2	5.7	0.59	6	6
	B2	asymm SiF str	975.7	998.8	23.1	2.37	7	7
	B1	asymm SiH str	2213.6	2199.3	-14.4	0.65	8	9
	A1	symm SiH str	2214.3	2174.2	-40.1	1.81	9	8
SiH_2Cl_2	A1	symm ClSiCl bend	179.4	196.2	16.8	9.37	1	1
	A1	symm SiCl str	493.7	483.6	-10.1	2.04	2	2
	B2	asymm SiCl str	551.2	559.7	8.5	1.54	3	4
	B1	HSiH rocking	578.6	529.3	-49.3	8.53	4	3
	A2	HSiH twist	698.0	754.9	56.9	8.15	5	5
	B2	HSiH wagging	866.6	850.2	-16.5	1.90	6	6
	A1	symm HSiH bend	934.2	937.2	3.1	0.33	7	7
	A1	symm SiH str	2203.9	2173.9	-30.0	1.36	8	8
	B1	asymm SiH str	2213.8	2199.9	-13.9	0.63	9	9

SiH_2Br_2	A1	symm BrSiBr bend	113.7	127.0	13.3	11.68	1	1
	A1	symm SiBr str	378.5	368.6	-9.9	2.62	2	2
	B2	asymm SiBr str	451.3	449.5	-1.8	0.39	3	3
	B1	HSiH rocking	527.7	504.6	-23.1	4.38	4	4
	A2	HSiH twist	719.8	745.0	25.2	3.51	5	5
	B2	HSiH wagging	853.3	840.0	-13.3	1.56	6	6
	A1	symm HSiH bend	924.4	929.6	5.2	0.56	7	7
	A1	symm SiH str	2200.7	2173.9	-26.8	1.22	8	8
	B1	asymm SiH str	2214.2	2200.1	-14.1	0.64	9	9
$SiHF_3$	E	asymm FSiF bend	286.0	323.6	37.7	13.17	1,2	2
	A1	symm HSiF bend	399.6	366.9	-32.7	8.19	3	3
	A1	symm SiF str	814.9	785.5	-29.4	3.61	4	4
	E	asymm HSiF bend	831.6	855.7	24.1	2.90	5,6	5
	E	asymm SiF str	966.8	985.3	18.4	1.91	7,8	8
	A1	symm SiH str	2285.2	2186.9	-98.3	4.30	9	9
$SiHCl_3$	E	asymm ClSiCl bend	168.3	186.4	18.0	10.71	1,2	1
	A1	symm HSiCl bend	241.4	222.7	-18.7	7.77	3	3
	A1	symm SiCl str	465.4	433.2	-32.2	6.91	4	4
	E	asymm SiCl str	566.4	575.8	9.4	1.66	5,6	6
	E	asymm HSiCl bend	793.5	808.2	14.7	1.85	7,8	7
	A1	symm SiH str	2243.0	2187.0	-56.0	2.50	9	9
$SiHBr_3$	E	asymm BrSiBr bend	103.0	116.1	13.1	12.76	1,2	2
	A1	symm HSiBr bend	155.0	152.3	-2.6	1.70	3	3
	A1	symm SiBr str	343.1	319.0	-24.1	7.01	4	4
	E	asymm SiBr str	462.6	468.4	5.8	1.26	5,6	6
	E	asymm HSiBr bend	772.2	792.4	20.1	2.61	7,8	8
	A1	symm SiH str	2235.7	2187.1	-48.6	2.17	9	9
SiF_4	E	bend def	274.1	307.3	33.2	12.11	1,2	1
	F2	bend def	406.4	346.9	-59.5	14.65	3,4,5	5
	A1	symm str	848.5	694.4	-154.1	18.16	6	6
	F2	asymm str	988.9	973.3	-15.6	1.58	7,8,9	7
$SiCl_4$	E	bend def	142.2	166.0	23.8	16.76	1,2	1
	F2	bend def	212.4	205.2	-7.2	3.37	3,4,5	4
	A1	symm str	398.2	353.2	-45.0	11.30	6	6
	F2	asymm str	585.9	597.7	11.8	2.01	7,8,9	7
$SiBr_4$	E	bend def	85.6	98.3	12.7	14.86	1,2	2
	F2	bend def	124.0	130.0	6.0	4.85	3,4,5	3
	A1	symm str	238.0	212.0	-26.0	10.94	6	6
	F2	asymm str	475.9	490.2	14.3	3.01	7,8,9	7

Table III: Vibrations of the halogermanes (GeH_nX_{4-n})

Molecule	Symmetry	Assignment	Observed Value	Calculated Value	Difference (Calc-Obs)	%Diff	Mode ab initio	Mode FF
GeH_4	F2	bend def	805.1	825.4	20.3	2.52	1,2,3	2
	E	bend def	895.1	832.7	-62.4	6.97	4,5	4
	A1	symm str	1952.6	1974.1	21.5	1.10	6	6
	F2	asymm str	1955.1	1992.6	37.5	1.92	7,8,9	9
GeH_3F	E	asymm HGeF bend	616.8	605.4	-11.4	1.84	1,2	1
	A1	symm GeF str	691.6	717.8	26.2	3.79	3	3
	E	asymm HGeH bend	844.4	851.8	7.4	0.88	4,5	6
	A1	symm HGeF bend	847.5	848.6	1.1	0.12	6	4
	E	asymm GeH str	1980.7	1992.4	11.7	0.59	7,8	9
	A1	symm GeH str	1980.9	1977.4	-3.5	0.18	9	7
GeH_3Cl	A1	symm GeCl str	377.4	390.5	13.2	3.49	1	1
	E	asymm HGeCl bend	574.2	559.8	-14.4	2.51	2,3	3
	A1	symm HGeCl bend	821.5	817.5	-3.9	0.48	4	4
	E	asymm HGeH bend	849.4	847.6	-1.8	0.21	5,6	6
	A1	symm GeH str	1976.3	1977.5	1.2	0.06	7	7
	E	asymm GeH str	1986.2	1992.4	6.2	0.31	8,9	8
GeH_3Br	A1	symm GeBr str	282.5	255.5	-27.0	9.57	1	1
	E	asymm HGeBr bend	561.6	549.7	-11.9	2.12	2,3	2
	A1	symm HGeBr bend	817.6	815.7	-1.8	0.22	4	4
	E	asymm HGeH bend	848.6	846.1	-2.4	0.29	5,6	6
	A1	symm GeH str	1969.6	1977.6	8.0	0.40	7	7
	E	asymm GeH str	1981.0	1992.4	11.4	0.58	8,9	9
GeH_2F_2	A1	symm FGeF bend	230.2	235.5	5.3	2.31	1	1
	B1	HGeH rocking	575.4	532.1	-43.3	7.52	2	2
	A2	HGeH twist	662.2	698.7	36.5	5.51	3	3
	A1	symm GeF str	710.4	711.8	1.5	0.21	4	5
	B2	asymm GeF str	720.4	710.9	-9.5	1.32	5	4
	B2	HGeH wagging	791.6	793.0	1.4	0.17	6	6
	A1	symm HGeH bend	829.1	880.4	51.4	6.20	7	7
	A1	symm GeH str	2025.9	1981.4	-44.5	2.20	8	8
	B1	asymm GeH str	2026.6	1992.2	-34.4	1.70	9	9
GeH_2Cl_2	A1	symm ClGeCl bend	142.6	154.7	12.1	8.49	1	1
	A1	symm GeCl str	384.7	373.0	-11.7	3.04	2	2
	B2	asymm GeCl str	394.6	409.1	14.5	3.67	3	3
	B1	HGeH rocking	495.1	463.0	-32.1	6.48	4	4
	A2	HGeH twist	632.2	660.3	28.1	4.45	5	5
	B2	HGeH wagging	754.3	738.7	-15.5	2.06	6	6
	A1	symm HGeH bend	826.3	850.8	24.5	2.97	7	7
	A1	symm GeH str	2001.5	1981.7	-19.8	0.99	8	8
	B1	asymm GeH str	2012.7	1992.2	-20.5	1.02	9	9

GeH_2Br_2	A1	symm BrGeBr bend	96.2	106.2	10.1	10.47	1	1
	A1	symm GeBr str	274.8	239.7	-35.0	12.75	2	2
	B2	asymm GeBr str	302.3	275.9	-26.4	8.72	3	3
	B1	HGeH rocking	452.4	446.6	-5.8	1.27	4	4
	A2	HGeH twist	640.7	652.1	11.5	1.79	5	5
	B2	HGeH wagging	745.9	736.7	-9.2	1.23	6	6
	A1	symm HGeH bend	818.6	845.1	26.5	3.23	7	7
	A1	symm GeH str	1985.7	1981.8	-3.9	0.20	8	8
	B1	asymm GeH str	2000.0	1992.1	-7.9	0.39	9	9
$GeHF_3$	E	asymm FGeF bend	216.4	234.4	18.0	8.34	1,2	2
	A1	symm HGeF bend	272.3	250.9	-21.4	7.85	3	3
	E	asymm HGeF bend	695.7	780.7	85.1	12.23	4,5	7
	A1	symm GeF str	723.2	693.6	-29.5	4.08	6	4
	E	asymm GeF str	752.8	720.1	-32.7	4.34	7,8	5
	A1	symm GeH str	2091.0	1986.3	-104.7	5.01	9	9
$GeHCl_3$	E	asymm ClGeCl bend	138.4	153.6	15.2	11.02	1,2	1
	A1	symm HGeCl bend	169.9	163.9	-6.0	3.55	3	3
	A1	symm GeCl str	382.2	350.9	-31.2	8.17	4	4
	E	asymm GeCl str	408.5	412.2	3.6	0.89	5,6	6
	E	asymm HGeCl bend	685.7	707.3	21.7	3.16	7,8	7
	A1	symm GeH str	2029.1	1986.5	-42.6	2.10	9	9
$GeHBr_3$	E	asymm BrGeBr bend	91.7	101.7	10.0	10.86	1,2	1
	A1	symm HGeBr bend	112.7	120.5	7.8	6.89	3	3
	A1	symm GeBr str	258.2	216.8	-41.4	16.05	4	4
	E	asymm GeBr str	309.0	282.1	-26.9	8.71	5,6	6
	E	asymm HGeBr bend	665.9	698.6	32.6	4.90	7,8	8
	A1	symm GeH str	2004.5	1986.5	-17.9	0.90	9	9
GeF_4	E	bend def	190.2	243.6	53.4	28.10	1,2	4
	F2	bend def	251.2	238.6	-12.6	5.03	3,4,5	1
	A1	symm str	712.5	660.6	-51.9	7.28	6	6
	F2	asymm str	783.3	755.5	-27.8	3.54	7,8,9	9
$GeCl_4$	E	bend def	121.2	146.2	25.0	20.64	1,2	2
	F2	bend def	161.9	163.9	2.0	1.22	3,4,5	4
	A1	symm str	366.0	323.1	-42.9	11.73	6	6
	F2	asymm str	420.2	415.7	-4.5	1.08	7,8,9	7
$GeBr_4$	E	bend def	78.3	91.2	12.9	16.47	1,2	1
	F2	bend def	101.8	112.2	10.4	10.24	3,4,5	5
	A1	symm str	221.6	179.0	-42.6	19.21	6	6
	F2	asymm str	314.6	288.9	-25.7	8.16	7,8,9	9

Table IV: Vibrations of the 2,2-dihalopropanes (Me_2CX_2)

Molecule	Symmetry	Assignment	Calculated Value	Observed Value	Difference (Calc-Obs)	%Diff.	Mode ab initio	Mode FF
CMe_2H_2	A2	uneven torsion	225.7	208.8	16.9	8.10	1	1
	B1	even torsion	254.4	261.9	-7.5	2.86	2	2
	A1	CAC bend	348.1	350.6	-2.4	0.69	3	3
	B1	XAX rocking	719.8	721.6	-1.8	0.24	4	4
	A1	symm AC str	822.2	830.7	-8.5	1.02	5	5
	A2	asymm ACH bend	914.3	879.5	34.8	3.96	6	6
	B2	asymm ACH bend	927.5	905.4	22.1	2.44	7	7
	B2	asymm AC str	1028.5	1007.1	21.4	2.12	8	8
	A1	symm ACH bend	1108.2	1148.2	-40.0	3.48	9	9
	B1	asymm ACH bend	1126.8	1188.4	-61.6	5.19	10	10
	A2	XAX twisting	1227.3	1281.8	-54.5	4.25	11	11
	B2	XAX wagging	1429.9	1342.3	87.7	6.53	12	14
	B2	symm HCH bend	1392.6	1394.2	-1.6	0.11	13	12
	A1	symm HCH bend	1440.9	1403.0	37.9	2.70	14	15
	A2	asymm HCH bend	1449.3	1459.5	-10.2	0.70	15	16
	A1	asymm HCH bend	1425.2	1460.6	-35.4	2.43	16	13
	B2	asymm HCH bend	1453.6	1466.4	-12.9	0.88	17	18
	B1	asymm HCH bend	1451.5	1475.4	-23.9	1.62	18	17
	A1	symm XAX bend	1458.3	1480.8	-22.5	1.52	19	19
	B2	symm CH str	2865.6	2851.1	14.5	0.51	20	21
	A1	symm AX str	2901.6	2851.9	49.7	1.74	21	22
	A1	symm CH str	2865.3	2857.9	7.4	0.26	22	20
	B1	asymm AX & CH str	2950.7	2872.7	78.1	2.72	23	23
	A2	asymm CH str	2958.3	2901.7	56.6	1.95	24	25
	B2	asymm CH str	2957.5	2909.6	48.0	1.65	25	24
	A1	asymm CH str	2959.7	2912.9	46.8	1.61	26	26
	B1	asymm AX & CH str	2965.6	2914.8	50.8	1.74	27	27
CMe_2F_2	A1	uneven torsion	217.6	206.8	10.8	5.23	1	1
	B1	even torsion	220.2	241.3	-21.1	8.73	2	2
	A1	CAC bend	322.8	316.1	6.7	2.12	3	3
	A2	XAX twisting	364.8	337.8	27.0	7.99	4	4
	B1	XAX rocking	402.7	409.5	-6.9	1.68	5	5
	B2	XAX wagging	461.6	493.6	-32.0	6.48	6	6
	A1	symm XAX bend	525.3	504.7	20.5	4.06	7	7
	A1	symm AC str	713.8	750.6	-36.8	4.90	8	8
	B2	asymm ACH bend	936.3	912.9	23.5	2.57	9	9
	B1	asymm AX str	951.7	930.1	21.6	2.32	10	10
	A1	symm AX str	960.2	988.7	-28.5	2.88	11	11
	A2	asymm ACH bend	981.9	994.6	-12.8	1.28	12	12
	B1	asymm ACH bend	1299.1	1229.1	70.0	5.69	13	15
	B2	asymm AC str	1237.4	1250.1	-12.7	1.02	14	13
	A1	symm ACH bend	1286.8	1257.0	29.8	2.37	15	14
	B2	symm HCH bend	1431.9	1407.7	24.2	1.72	16	17
	A1	symm HCH bend	1429.5	1413.4	16.2	1.14	17	16
	A2	asymm HCH bend	1448.4	1447.1	1.3	0.09	18	18
	B2	asymm HCH bend	1450.4	1451.1	-0.7	0.05	19	19
	A1	asymm HCH bend	1454.4	1462.4	-7.9	0.54	20	20
	B1	asymm HCH bend	1457.9	1467.2	-9.4	0.64	21	21
	B2	symm CH str	2865.8	2882.9	-17.1	0.59	22	23
	A1	symm CH str	2865.7	2887.9	-22.2	0.77	23	22
	A2	asymm CH str	2958.5	2948.9	9.7	0.33	24	25
	B2	asymm CH str	2957.6	2955.7	1.9	0.06	25	24
	B1	asymm CH str	2959.5	2956.2	3.4	0.11	26	27
	A1	asymm CH str	2958.7	2957.5	1.2	0.04	27	26

CMe_2Cl_2	A1	symm XAX bend	239.3	250.1	-10.9	4.34	1	1
	A2	uneven torsion	276.6	261.9	14.7	5.61	2	4
	A2	XAX twisting	262.4	274.1	-11.7	4.28	3	2
	B1	even torsion	273.6	294.1	-20.5	6.96	4	3
	B1	XAX rocking	308.9	347.7	-38.8	11.16	5	5
	A1	symm CAC bend	312.5	351.2	-38.7	11.02	6	6
	B2	XAX wagging	342.7	375.3	-32.5	8.67	7	7
	A1	symm AX str	509.9	541.3	-31.4	5.80	8	8
	B1	asymm AX str	740.0	662.9	77.2	11.64	9	9
	A1	symm AC str	880.2	896.0	-15.8	1.77	10	10
	B2	asymm ACH bend	936.5	929.5	7.1	0.76	11	11
	A2	asymm ACH bend	981.8	1011.8	-30.0	2.97	12	12
	B1	asymm ACH bend	1164.1	1123.3	40.8	3.63	13	13
	A1	symm ACH bend	1181.6	1163.1	18.5	1.59	14	14
	B2	asymm AC str	1183.8	1175.6	8.2	0.70	15	15
	B2	symm HCH bend	1429.3	1394.6	34.7	2.49	16	17
	A1	symm HCH bend	1459.2	1410.8	48.4	3.43	17	20
	B2	asymm HCH bend	1459.2	1448.3	11.0	0.76	18	19
	A2	asymm HCH bend	1457.7	1449.6	8.1	0.56	19	18
	A1	asymm HCH bend	1427.0	1460.0	-32.9	2.25	20	16
	B1	asymm HCH bend	1460.4	1468.1	-7.7	0.52	21	21
	B2	symm CH str	2865.5	2881.1	-15.6	0.54	22	23
	A1	symm CH str	2865.4	2886.7	-21.3	0.74	23	22
	A2	asymm CH str	2958.6	2944.6	13.9	0.47	24	25
	B1	asymm CH str	2958.8	2951.5	7.3	0.25	25	26
	B2	asymm CH str	2957.7	2951.5	6.2	0.21	26	24
	A1	asymm CH str	2959.6	2969.6	-10.0	0.34	27	27
CMe_2Br_2	A1	symm XAX bend	145.9	165.8	-19.9	11.98	1	1
	A2	XAX twisting	232.5	242.7	-10.2	4.22	2	2
	A2	uneven torsion	284.6	272.6	12.0	4.39	3	5
	B1	XAX rocking	247.8	280.8	-33.0	11.75	4	3
	A1	symm CAC bend	268.9	295.1	-26.2	8.88	5	4
	B1	even torsion	285.1	300.9	-15.7	5.23	6	6
	B2	XAX wagging	300.3	330.0	-29.7	9.01	7	7
	A1	symm AX str	438.8	462.6	-23.8	5.15	8	8
	B1	asymm AX str	649.3	584.3	65.0	11.13	9	9
	A1	symm AC str	862.9	880.4	-17.5	1.99	10	10
	B2	asymm ACH bend	938.5	932.9	5.7	0.61	11	11
	A2	asymm ACH bend	981.7	1008.4	-26.7	2.65	12	12
	B1	asymm ACH bend	1130.3	1108.2	22.0	1.99	13	13
	A1	symm ACH bend	1161.8	1154.8	7.1	0.61	14	14
	B2	asymm AC str	1174.8	1167.0	7.8	0.67	15	15
	B2	symm HCH bend	1460.8	1395.2	65.6	4.70	16	20
	A1	symm HCH bend	1427.5	1410.6	16.9	1.20	17	16
	B2	asymm HCH bend	1429.8	1449.6	-19.8	1.36	18	17
	A2	asymm HCH bend	1459.3	1449.9	9.4	0.65	19	18
	A1	asymm HCH bend	1460.6	1461.4	-0.8	0.06	20	19
	B1	asymm HCH bend	1461.7	1468.1	-6.4	0.44	21	21
	B2	symm CH str	2865.6	2876.1	-10.5	0.37	22	23
	A1	symm CH str	2865.5	2881.6	-16.1	0.56	23	22
	A2	asymm CH str	2958.5	2936.7	21.8	0.74	24	25
	B1	asymm CH str	2958.6	2942.7	16.0	0.54	25	26
	B2	asymm CH str	2957.6	2969.3	-11.6	0.39	26	24
	A1	asymm CH str	2959.5	2970.5	-11.0	0.37	27	27

Table V: Vibrations of the dihalo-dimethylsilanes (Me_2SiX_2)

Molecule	Symmetry	Assignment	Calculated Value	Observed Value	Difference (Calc-Obs)	%Diff.	Mode ab initio	Mode FF
$SiMe_2H_2$	A2	uneven torsion	146.2	137.6	8.7	6.31	1	1
	B1	even torsion	155.6	153.0	2.5	1.64	2	2
	A1	CAC bend	188.5	195.9	-7.4	3.79	3	3
	B1	XAX rocking	450.0	446.5	3.5	0.79	4	4
	A2	XAX twisting	594.4	566.7	27.7	4.88	5	5
	A1	symm AC str	604.5	606.6	-2.1	0.35	6	6
	B2	XAX wagging	702.8	630.6	72.2	11.45	7	8
	B2	asymm AC str	683.4	673.7	9.7	1.44	8	7
	A1	symm ACH bend	831.8	842.8	-11.0	1.31	9	10
	A2	asymm ACH bend	829.0	866.2	-37.3	4.30	10	9
	B1	asymm ACH bend	844.6	868.5	-23.9	2.75	11	11
	B2	asymm ACH bend	871.8	910.1	-38.3	4.21	12	12
	A1	symm XAX bend	910.3	941.3	-31.0	3.29	13	13
	B2	symm HCH bend	1296.3	1295.9	0.4	0.03	14	15
	A1	symm HCH bend	1296.0	1300.7	-4.6	0.36	15	14
	A2	asymm HCH bend	1427.0	1429.8	-2.8	0.19	16	18
	B2	asymm HCH bend	1427.3	1432.5	-5.1	0.36	17	19
	A1	asymm HCH bend	1426.0	1437.5	-11.5	0.80	18	16
	B1	asymm HCH bend	1426.9	1440.1	-13.2	0.91	19	17
	B1	asymm AX str	2196.8	2088.9	108.0	5.17	20	21
	A1	symm AX str	2177.0	2099.9	77.1	3.67	21	20
	B2	symm CH str	2865.1	2849.7	15.3	0.54	22	23
	A1	symm CH str	2865.0	2850.1	14.9	0.52	23	22
	A2	asymm CH str	2957.9	2909.3	48.6	1.67	24	25
	B1	asymm CH str	2958.2	2911.2	47.0	1.61	25	26
	B2	asymm CH str	2957.7	2913.7	43.9	1.51	26	24
	A1	asymm CH str	2958.4	2914.0	44.4	1.52	27	27
$SiMe_2F_2$	A2	uneven torsion	123.7	118.8	5.0	4.17	1	2
	B1	even torsion	122.7	130.3	-7.6	5.82	2	1
	A1	CAC bend	181.5	179.0	2.5	1.40	3	3
	A2	XAX twisting	208.2	195.6	12.5	6.41	4	4
	B1	XAX rocking	236.9	237.3	-0.4	0.15	5	5
	B2	XAX wagging	274.9	303.6	-28.8	9.48	6	6
	A1	symm XAX bend	321.6	310.5	11.2	3.60	7	7
	A1	symm AC str	565.6	596.3	-30.7	5.14	8	8
	B2	asymm AC str	693.6	677.1	16.5	2.43	9	9
	A2	asymm ACH bend	794.8	745.8	49.0	6.57	10	12
	B1	asymm ACH bend	787.4	781.6	5.9	0.75	11	10
	A1	symm ACH bend	792.1	787.2	4.8	0.61	12	11
	B2	asymm ACH bend	809.9	792.7	17.2	2.17	13	13
	A1	symm AX str	918.7	889.1	29.7	3.34	14	14
	B1	asymm AX str	979.5	927.8	51.8	5.58	15	15
	B2	symm HCH bend	1300.7	1311.9	-11.2	0.85	16	17
	A1	symm HCH bend	1300.6	1314.7	-14.1	1.08	17	16
	A2	asymm HCH bend	1423.9	1426.8	-2.9	0.20	18	19
	B2	asymm HCH bend	1424.0	1427.8	-3.9	0.27	19	20
	A1	asymm HCH bend	1422.8	1433.3	-10.5	0.73	20	18
	B1	asymm HCH bend	1424.0	1436.7	-12.7	0.88	21	21
	B2	symm CH str	2865.5	2854.8	10.7	0.38	22	23
	A1	symm CH str	2865.5	2856.7	8.8	0.31	23	22
	A2	asymm CH str	2957.8	2915.6	42.2	1.45	24	25
	B1	asymm CH str	2958.0	2918.1	39.9	1.37	25	26
	B2	asymm CH str	2957.4	2922.8	34.6	1.18	26	24
	A1	asymm CH str	2958.2	2923.1	35.1	1.20	27	27

$SiMe_2Cl_2$	A2	uneven torsion	157.6	149.3	8.3	5.54	1	4
	A1	symm XAX bend	156.7	152.3	4.3	2.85	2	3
	B1	even torsion	151.6	158.2	-6.6	4.17	3	2
	A2	XAX twisting	145.3	161.5	-16.1	9.99	4	1
	B1	XAX rocking	193.7	210.6	-16.9	8.04	5	5
	A1	symm CAC bend	206.6	212.2	-5.6	2.63	6	7
	B2	XAX wagging	193.7	226.6	-32.8	14.48	7	6
	A1	symm AX str	431.2	439.0	-7.7	1.76	8	8
	B1	asymm AX str	556.4	517.3	39.1	7.56	9	9
	A1	symm AC str	638.9	645.5	-6.7	1.03	10	10
	B2	asymm AC str	690.5	682.1	8.4	1.23	11	11
	A2	asymm ACH bend	794.7	761.6	33.1	4.34	12	12
	B2	asymm ACH bend	805.2	782.4	22.8	2.91	13	13
	B1	asymm ACH bend	838.5	835.7	2.8	0.34	14	14
	A1	symm ACH bend	843.0	956.6	-113.6	11.88	15	15
	B2	symm HCH bend	1298.9	1306.0	-7.1	0.54	16	17
	A1	symm HCH bend	1298.8	1311.0	-12.1	0.92	17	16
	A2	asymm HCH bend	1427.2	1421.6	5.6	0.39	18	19
	B2	asymm HCH bend	1427.4	1421.7	5.7	0.40	19	21
	A1	asymm HCH bend	1426.2	1427.2	-1.1	0.07	20	18
	B1	asymm HCH bend	1427.2	1432.2	-5.0	0.35	21	20
	B2	symm CH str	2865.3	2857.3	8.0	0.28	22	23
	A1	symm CH str	2865.3	2858.9	6.5	0.23	23	22
	A2	asymm CH str	2957.8	2920.8	37.0	1.27	24	25
	B1	asymm CH str	2958.1	2923.0	35.1	1.20	25	26
	B2	asymm CH str	2957.5	2934.7	22.8	0.78	26	24
	A1	asymm CH str	2958.3	2935.0	23.3	0.79	27	27
$SiMe_2Br_2$	A1	symm XAX bend	116.8	109.1	7.6	7.00	1	1
	A2	XAX twisting	137.5	150.3	-12.8	8.48	2	2
	A1	symm CAC bend	172.8	181.1	-8.3	4.56	3	4
	A2	uneven torsion	184.2	182.4	1.8	0.98	4	6
	B1	XAX rocking	166.7	182.5	-15.8	8.66	5	3
	B2	XAX wagging	177.5	190.7	-13.2	6.91	6	5
	B1	even torsion	187.8	192.0	-4.1	2.14	7	7
	A1	symm AX str	336.3	340.3	-4.0	1.18	8	8
	B1	asymm AX str	457.0	430.4	26.6	6.18	9	9
	A1	symm AC str	624.3	638.2	-13.9	2.18	10	10
	B2	asymm AC str	690.4	680.6	9.8	1.43	11	11
	A2	asymm ACH bend	796.0	759.2	36.8	4.85	12	12
	B2	asymm ACH bend	805.7	775.1	30.6	3.95	13	13
	B1	asymm ACH bend	835.7	828.4	7.4	0.89	14	14
	A1	symm ACH bend	841.2	853.5	-12.2	1.43	15	15
	B2	symm HCH bend	1298.8	1299.0	-0.2	0.02	16	17
	A1	symm HCH bend	1298.7	1304.2	-5.5	0.43	17	16
	A2	asymm HCH bend	1430.6	1422.9	7.7	0.54	18	20
	B2	asymm HCH bend	1430.7	1423.2	7.6	0.53	19	21
	A1	asymm HCH bend	1429.5	1429.4	0.2	0.01	20	18
	B1	asymm HCH bend	1430.6	1433.1	-2.5	0.18	21	19
	B2	symm CH str	2865.3	2857.1	8.2	0.29	22	23
	A1	symm CH str	2865.3	2858.6	6.7	0.23	23	22
	A2	asymm CH str	2957.9	2920.6	37.3	1.28	24	25
	B1	asymm CH str	2958.1	2922.8	35.4	1.21	25	26
	B2	asymm CH str	2957.5	2939.1	18.4	0.62	26	24
	A1	asymm CH str	2958.3	2939.4	18.9	0.64	27	27

Table VI: Vibrations of the dihalo-dimethylgermanes (Me_2GeX_2)

Molecule	Symmetry	Assignment	Calculated Value	Observed Value	Difference (Calc-Obs)	%Diff.	Mode ab initio	Mode FF
$GeMe_2H_2$	A2	uneven torsion	154.0	125.0	29.1	23.27	1	1
	B1	even torsion	156.3	142.7	13.5	9.49	2	2
	A1	CAC bend	161.2	170.0	-8.8	5.20	3	3
	B1	XAX rocking	398.9	398.1	0.9	0.22	4	4
	A2	XAX twisting	480.0	560.9	-80.9	14.43	5	5
	A1	symm AC str	576.9	564.2	12.7	2.25	6	6
	B2	asymm AC str	604.9	585.2	19.7	3.36	7	7
	B2	XAX wagging	639.9	633.2	6.7	1.06	8	8
	B2	asymm ACH bend	832.2	832.5	-0.3	0.03	9	11
	B1	asymm ACH bend	833.8	839.4	-5.6	0.66	10	12
	A1	symm ACH bend	808.2	839.7	-31.5	3.75	11	9
	A2	asymm ACH bend	819.4	854.6	-35.1	4.11	12	10
	A1	symm XAX bend	838.4	861.5	-23.1	2.68	13	13
	B2	symm HCH bend	1281.8	1286.6	-4.8	0.37	14	15
	A1	symm HCH bend	1281.7	1291.6	-9.9	0.76	15	14
	A2	asymm HCH bend	1438.0	1441.0	-3.0	0.21	16	18
	B2	asymm HCH bend	1438.5	1445.0	-6.4	0.45	17	19
	A1	asymm HCH bend	1437.0	1446.4	-9.3	0.65	18	16
	B1	asymm HCH bend	1437.7	1451.6	-14.0	0.96	19	17
	B1	asymm AX str	1990.3	1881.1	109.2	5.81	20	21
	A1	symm AX str	1983.5	1882.7	100.8	5.36	21	20
	B2	symm CH str	2862.4	2862.1	0.3	0.01	22	23
	A1	symm CH str	2862.4	2862.5	-0.1	0.00	23	22
	A2	asymm CH str	2959.2	2927.3	31.9	1.09	24	25
	B1	asymm CH str	2959.5	2928.7	30.9	1.05	25	26
	B2	asymm CH str	2959.2	2933.8	25.4	0.87	26	24
	A1	asymm CH str	2959.9	2934.1	25.7	0.88	27	27
$GeMe_2F_2$	A2	uneven torsion	80.4	74.8	5.6	7.53	1	2
	B1	even torsion	79.3	90.3	-11.0	12.17	2	1
	A1	symm CAC bend	164.5	150.4	14.0	9.33	3	3
	A2	XAX twisting	171.4	173.5	-2.1	1.19	4	4
	B1	XAX rocking	173.4	183.8	-10.4	5.66	5	5
	B2	XAX wagging	202.3	233.1	-30.8	13.22	6	6
	A1	symm XAX bend	231.2	233.9	-2.7	1.16	7	7
	A1	symm AC str	560.8	576.4	-15.6	2.70	8	8
	B2	asymm AC str	618.4	624.9	-6.5	1.04	9	9
	A1	symm AX str	722.3	699.6	22.7	3.24	10	10
	B1	asymm AX str	742.2	703.0	39.2	5.58	11	11
	B2	asymm ACH bend	802.8	764.8	38.1	4.98	12	12
	A2	asymm ACH bend	804.4	768.2	36.2	4.71	13	13
	B1	asymm ACH bend	821.7	817.8	4.0	0.48	14	14
	A1	symm ACH bend	831.0	840.8	-9.8	1.16	15	15
	B2	symm HCH bend	1292.3	1295.5	-3.2	0.25	16	17
	A1	symm HCH bend	1292.2	1300.6	-8.4	0.64	17	16
	A2	asymm HCH bend	1429.4	1429.9	-0.5	0.04	18	20
	B2	asymm HCH bend	1429.6	1435.1	-5.4	0.38	19	21
	A1	asymm HCH bend	1428.2	1436.2	-8.0	0.55	20	18
	B1	asymm HCH bend	1429.3	1438.9	-9.6	0.66	21	19
	B2	symm CH str	2863.4	2869.9	-6.4	0.22	22	23
	A1	symm CH str	2863.4	2871.6	-8.1	0.28	23	22
	A2	asymm CH str	2958.8	2939.1	19.7	0.67	24	25
	B1	asymm CH str	2959.0	2940.3	18.7	0.64	25	26
	B2	asymm CH str	2958.6	2950.0	8.6	0.29	26	24
	A1	asymm CH str	2959.3	2950.4	8.9	0.30	27	27

$GeMe_2Cl_2$	A2	uneven torsion	134.1	124.7	9.4	7.56	1	4
	A1	symm XAX bend	135.8	133.0	2.8	2.09	2	5
	B1	even torsion	132.2	137.4	-5.2	3.81	3	2
	A2	XAX twisting	112.5	145.8	-33.3	22.85	4	1
	A1	symm CAC bend	172.4	165.8	6.6	3.96	5	7
	B1	XAX rocking	147.8	167.7	-19.9	11.86	6	6
	B2	XAX wagging	133.4	170.1	-36.6	21.55	7	3
	A1	symm AX str	366.2	359.7	6.5	1.82	8	8
	B1	asymm AX str	405.8	367.8	38.0	10.32	9	9
	A1	symm AC str	576.6	577.2	-0.5	0.09	10	10
	B2	asymm AC str	616.9	617.3	-0.3	0.05	11	11
	B2	asymm ACH bend	802.4	770.6	31.8	4.13	12	12
	A2	asymm ACH bend	804.7	790.6	14.1	1.79	13	13
	B1	asymm ACH bend	818.9	826.2	-7.3	0.88	14	14
	A1	symm ACH bend	829.1	852.3	-23.2	2.72	15	15
	B2	symm HCH bend	1288.4	1292.7	-4.3	0.33	16	17
	A1	symm HCH bend	1288.4	1296.5	-8.1	0.62	17	16
	A2	asymm HCH bend	1434.1	1432.8	1.3	0.09	18	20
	B2	asymm HCH bend	1434.6	1435.4	-0.8	0.06	19	21
	A1	asymm HCH bend	1433.2	1435.5	-2.4	0.16	20	18
	B1	asymm HCH bend	1434.0	1441.8	-7.8	0.54	21	19
	B2	symm CH str	2863.0	2871.7	-8.6	0.30	22	23
	A1	symm CH str	2863.0	2873.0	-9.9	0.35	23	22
	A2	asymm CH str	2958.9	2944.5	14.5	0.49	24	25
	B1	asymm CH str	2959.1	2945.6	13.5	0.46	25	26
	B2	asymm CH str	2958.8	2959.1	-0.3	0.01	26	24
	A1	asymm CH str	2959.5	2959.5	0.0	0.00	27	27
$GeMe_2Br_2$	A1	symm XAX bend	97.4	96.0	1.4	1.46	1	2
	B2	XAX wagging	108.0	140.5	-32.5	23.12	2	3
	A2	XAX twisting	90.3	141.0	-50.7	35.96	3	1
	A1	symm CAC bend	155.1	151.7	3.4	2.27	4	5
	B1	XAX rocking	127.1	157.2	-30.1	19.12	5	4
	A2	uneven torsion	181.6	182.0	-0.4	0.23	6	6
	B1	even torsion	181.8	191.5	-9.7	5.04	7	7
	A1	symm AX str	237.6	258.2	-20.5	7.95	8	8
	B1	asymm AX str	273.6	284.6	-11.0	3.87	9	9
	A1	symm AC str	573.9	573.7	0.2	0.04	10	10
	B2	asymm AC str	617.1	616.2	0.9	0.15	11	11
	B2	asymm ACH bend	803.8	767.7	36.1	4.70	12	12
	A2	asymm ACH bend	806.2	794.4	11.8	1.49	13	13
	B1	asymm ACH bend	819.8	822.8	-3.0	0.36	14	14
	A1	symm ACH bend	830.4	851.3	-20.9	2.46	15	15
	B2	symm HCH bend	1286.4	1286.5	-0.1	0.01	16	16
	A1	symm HCH bend	1286.4	1288.6	-2.2	0.17	17	17
	A2	asymm HCH bend	1439.6	1440.9	-1.4	0.10	18	20
	A1	asymm HCH bend	1438.9	1441.9	-3.1	0.21	19	18
	B2	asymm HCH bend	1440.3	1442.1	-1.8	0.12	20	21
	B1	asymm HCH bend	1439.5	1447.8	-8.3	0.57	21	19
	B2	symm CH str	2862.9	2872.4	-9.6	0.33	22	23
	A1	symm CH str	2862.9	2873.5	-10.6	0.37	23	22
	A2	asymm CH str	2959.0	2947.6	11.4	0.39	24	25
	B1	asymm CH str	2959.2	2948.6	10.6	0.36	25	26
	B2	asymm CH str	2958.9	2962.2	-3.3	0.11	26	24
	A1	asymm CH str	2959.6	2962.6	-3.0	0.10	27	27

Addendum C: Point group characterization of molecules

Molecules of the form AH_2X_2:

Number of molecules = n

= 5

Degrees of freedom = 3n

= 15

Number of vibrations = 3n-6

= 9

Symmetry elements: E, C_2, σ_v, σ_v'

Point group: C_{2v}

Cartesian Coordinate representation:

C_{2v}	E	C_2	σ_v	σ_v'
Γ_{xyz}	15	-1	3	3

$\Gamma_{xyz} = 5A_1 + 2A_2 + 4B_1 + 4B_2$

$\Gamma_{trans} = A_1 + B_1 + B_2$

$\Gamma_{rot} = A_2 + B_1 + B_2$

Therefore $\Gamma_{vib} = 4A_1 + A_2 + 2B_1 + 2B_2$

AH stretching vibration representation:

C_{2v}	E	C_2	σ_v	σ_v'
Γ_{AH}	2	0	2	0

$\Gamma_{AH} = A_1 + B_1$

C_{2v}	E	C_2	σ_v	σ_v'
Γ_{AX}	2	0	0	2

$\Gamma_{AX} = A_1 + B_2$

Therefore $\Gamma_\theta = 2A_1 + A_2 + B_1 + B_2$

Molecules of the form AH_3X:

Number of molecules = n

= 5

Degrees of freedom = 3n

= 15

Number of vibrations = 3n-6

= 9

Symmetry elements: E, $2C_3$, $3\sigma_v$

Point group: C_{3v}

Cartesian Coordinate representation:

C_{3v}	E	$2C_3$	$3\sigma_v$
Γ_{xyz}	15	0	3

$\Gamma_{xyz} = 4A_1 + A_2 + 5E$

$\Gamma_{trans} = A_1 + E$

$\Gamma_{rot} = A_2 + E$

Therefore $\Gamma_{vib} = 3A_1 + 3E$

AH stretching vibration representation:

C_{3v}	E	$2C_3$	$3\sigma_v$
Γ_{AH}	3	0	1

$\Gamma_{AH} = A_1 + E$

C_{2v}	E	C_2	σ_v
Γ_{AX}	1	1	1

$\Gamma_{AX} = A_1$

Bending vibration representation:

C_{2v}	E	C_2	σ_v
Γ_{HAH}	3	0	1
Γ_{HAX}	3	0	1

$\Gamma_{HAH} = A_1 + E$

$\Gamma_{HAX} = A_1 + E$

Molecules of the form AHX_3:

Number of molecules = n

= 5

Degrees of freedom = 3n

= 15

Number of vibrations = 3n-6

= 9

Symmetry elements: E, $2C_3$, $3\sigma_v$

Point group: C_{3v}

Cartesian Coordinate representation:

C_{3v}	E	$2C_3$	$3\sigma_v$
Γ_{xyz}	15	0	3

$\Gamma_{xyz} = 4A_1 + A_2 + 5E$

$\Gamma_{trans} = A_1 + E$

$\Gamma_{rot} = A_2 + E$

Therefore $\Gamma_{vib} = 3A_1 + 3E$

AH stretching vibration representation:

C_{3v}	E	$2C_3$	$3\sigma_v$
Γ_{AH}	1	1	1

$\Gamma_{AH} = A_1$

C_{2v}	E	C_2	σ_v
Γ_{AX}	3	0	1

$\Gamma_{AX} = A_1 + E$

Bending vibration representation:

C_{2v}	E	C_2	σ_v
Γ_{HAH}	3	0	1
Γ_{HAX}	3	0	1

$\Gamma_{HAH} = A_1 + E$

$\Gamma_{HAX} = A_1 + E$

Molecules of the form $(CH_3)_2AX_2$:

Number of molecules = n

= 11

Degrees of freedom = 3n

= 33

Number of vibrations = 3n-6

= 27

Symmetry elements: E, C_2, σ_v, σ_v'

Point group: C_{2v}

Cartesian Coordinate representation:

C_{2v}	E	C_2	σ_v	σ_v'
Γ_{xyz}	33	-1	3	5

$\Gamma_{xyz} = 10A_1 + 6A_2 + 8B_1 + 9B_2$

$\Gamma_{trans} = A_1 + B_1 + B_2$

$\Gamma_{rot} = A_2 + B_1 + B_2$

Therefore $\Gamma_{vib} = 9A_1 + 5A_2 + 6B_1 + 7B_2$

Stretching vibration representation:

C_{2v}	E	C_2	σ_v	σ_v'
Γ_{AX}	2	0	2	0
Γ_{AC}	2	0	0	2
Γ_{CH}	6	0	0	2

$\Gamma_{AX} = A_1 + B_1$

$\Gamma_{AC} = A_1 + B_2$

$\Gamma_{CH} = 2A_1 + A_2 + B_1 + 2B_2$

Therefore $\Gamma_{str} = 4A_1 + A_2 + 2B_1 + 3B_2$

Bending vibration representation:

C_{2v}	E	C_2	σ_v	σ_v'
Γ_{XAX}	1	1	1	1
Γ_{CAC}	1	1	1	1
Γ_{CAX}	4	0	0	0
Γ_{HCH}	6	0	0	2
Γ_{HCA}	6	0	0	2

$\Gamma_{XAX} = A_1$

$\Gamma_{CAC} = A_1$

$\Gamma_{CAX} = A_1 + A_2 + B_1 + B_2$

But the A_1 CAX vibration is redundant, therefore it becomes

$\Gamma_{CAX} = A_2 + B_1 + B_2$

$\Gamma_{HCH} = 2A_1 + A_2 + B_1 + 2B_2$

$\Gamma_{HCA} = 2A_1 + A_2 + B_1 + 2B_2$

One A_1 and one B_2 vibration are redundant, therefore it becomes

$\Gamma_{HCA} = A_1 + A_2 + B_1 + B_2$

Torsion vibration representation:

C_{2v}	E	C_2	σ_v	σ_v'
Γ_{uneven}	1	1	-1	-1
Γ_{even}	1	-1	-1	1

$\Gamma_{uneven} = A_2$

$\Gamma_{even} = B_1$

Therefore $\Gamma_{tors} = A_2 + B_1$

Addendum D: Comparison of MP2, DFT and RHF heavy atom geometric parameters of Me_2AX_2 molecules

Molecule	Parameter	RHF value	MP2 value	Difference (RHF-MP2)	% Diff	DFT value	Difference (RHF-DFT)	% Diff
Me_2CH_2	A-C	1.528	1.526	0.002	0.146	1.532	-0.004	0.252
	A-X	1.087	1.096	-0.009	0.809	1.099	-0.011	1.040
	C-A-C	112.8	112.4	0.4	0.336	112.9	-0.1	0.129
	C-A-X	109.4	109.5	-0.1	0.089	109.4	0.0	0.016
	X-A-X	106.3	106.3	0.0	0.012	106.1	0.2	0.226
Me_2SiH_2	A-C	1.890	1.885	0.005	0.266	1.891	-0.001	0.056
	A-X	1.481	1.491	-0.009	0.641	1.493	-0.012	0.782
	C-A-C	111.5	111.0	0.4	0.393	111.9	-0.5	0.407
	C-A-X	109.5	109.6	-0.1	0.090	109.4	0.0	0.033
	X-A-X	107.5	107.5	-0.1	0.056	107.1	0.3	0.318
Me_2GeH_2	A-C	1.951	1.950	0.001	0.066	1.954	-0.003	0.168
	A-X	1.549	1.561	-0.012	0.758	1.555	-0.005	0.339
	C-A-C	111.0	110.9	0.1	0.050	111.1	-0.1	0.070
	C-A-X	109.6	109.7	-0.1	0.058	109.6	0.0	0.011
	X-A-X	107.4	107.2	0.2	0.188	107.2	0.1	0.121
Me_2CF_2	A-C	1.509	1.506	0.002	0.165	1.516	-0.007	0.460
	A-X	1.354	1.384	-0.030	2.200	1.381	-0.027	1.957
	C-A-C	116.1	116.7	-0.6	0.530	116.4	-0.3	0.296
	C-A-X	108.6	108.4	0.2	0.178	108.4	0.2	0.141
	X-A-X	105.9	106.0	-0.1	0.118	106.2	-0.3	0.256
Me_2SiF_2	A-C	1.861	1.855	0.005	0.291	1.862	-0.002	0.082
	A-X	1.592	1.617	-0.026	1.606	1.613	-0.022	1.360
	C-A-C	115.0	114.6	0.4	0.357	114.9	0.1	0.105
	C-A-X	108.9	108.9	0.0	0.033	108.9	0.0	0.011
	X-A-X	105.8	106.1	-0.3	0.309	106.0	-0.2	0.187
Me_2GeF_2	A-C	1.921	1.919	0.002	0.105	1.927	-0.007	0.349
	A-X	1.721	1.762	-0.042	2.420	1.751	-0.030	1.727
	C-A-C	120.2	121.1	-0.8	0.691	121.0	-0.7	0.618
	C-A-X	108.2	107.9	0.3	0.244	107.9	0.3	0.276
	X-A-X	102.5	102.6	-0.1	0.126	102.9	-0.4	0.417

Me_2CCl_2	A-C	1.521	1.517	0.004	0.256	1.522	-0.001	0.085
	A-X	1.798	1.795	0.003	0.172	1.828	-0.030	1.673
	C-A-C	112.9	113.1	-0.2	0.140	113.8	-0.9	0.781
	C-A-X	108.9	108.7	0.1	0.114	108.7	0.2	0.190
	X-A-X	108.4	108.7	-0.4	0.324	108.3	0.1	0.086
Me_2SiCl_2	A-C	1.867	1.862	0.005	0.272	1.870	-0.002	0.127
	A-X	2.069	2.064	0.005	0.255	2.087	-0.018	0.867
	C-A-C	114.4	114.2	0.2	0.162	114.7	-0.3	0.255
	C-A-X	108.6	108.6	0.0	0.034	108.5	0.1	0.112
	X-A-X	107.8	108.2	-0.4	0.343	108.0	-0.2	0.181
Me_2GeCl_2	A-C	1.926	1.925	0.002	0.083	1.934	-0.007	0.385
	A-X	2.170	2.168	0.002	0.081	2.194	-0.024	1.092
	C-A-C	118.1	118.2	-0.1	0.110	118.7	-0.6	0.517
	C-A-X	108.0	107.9	0.1	0.066	107.7	0.2	0.210
	X-A-X	106.3	106.5	-0.2	0.159	106.6	-0.3	0.269
Me_2CBr_2	A-C	1.519	1.516	0.003	0.220	1.519	0.000	0.000
	A-X	1.964	1.974	-0.010	0.506	1.993	-0.029	1.459
	C-A-C	113.7	114.1	-0.5	0.423	114.7	-1.0	0.884
	C-A-X	108.7	108.7	0.1	0.079	108.6	0.2	0.161
	X-A-X	108.1	107.9	0.2	0.156	107.7	0.4	0.348
Me_2SiBr_2	A-C	1.867	1.861	0.006	0.295	1.870	-0.003	0.183
	A-X	2.222	2.226	-0.004	0.167	2.234	-0.012	0.551
	C-A-C	113.8	114.2	-0.3	0.297	113.9	0.0	0.014
	C-A-X	108.5	108.4	0.1	0.093	108.4	0.1	0.068
	X-A-X	109.1	109.1	-0.1	0.055	109.4	-0.3	0.273
Me_2GeBr_2	A-C	1.927	1.925	0.002	0.114	1.935	-0.008	0.408
	A-X	2.317	2.326	-0.009	0.382	2.337	-0.020	0.850
	C-A-C	118.3	119.4	-1.1	0.913	118.6	-0.3	0.244
	C-A-X	107.6	107.3	0.3	0.269	107.5	0.2	0.151
	X-A-X	107.6	107.6	0.0	0.009	108.0	-0.4	0.369

Addendum E: Enlargements of ESMS and NMR spectra of dichlorobis(phenethyl)germane

Figure I: Enlargement of ESMS from 100-250 (m/z)

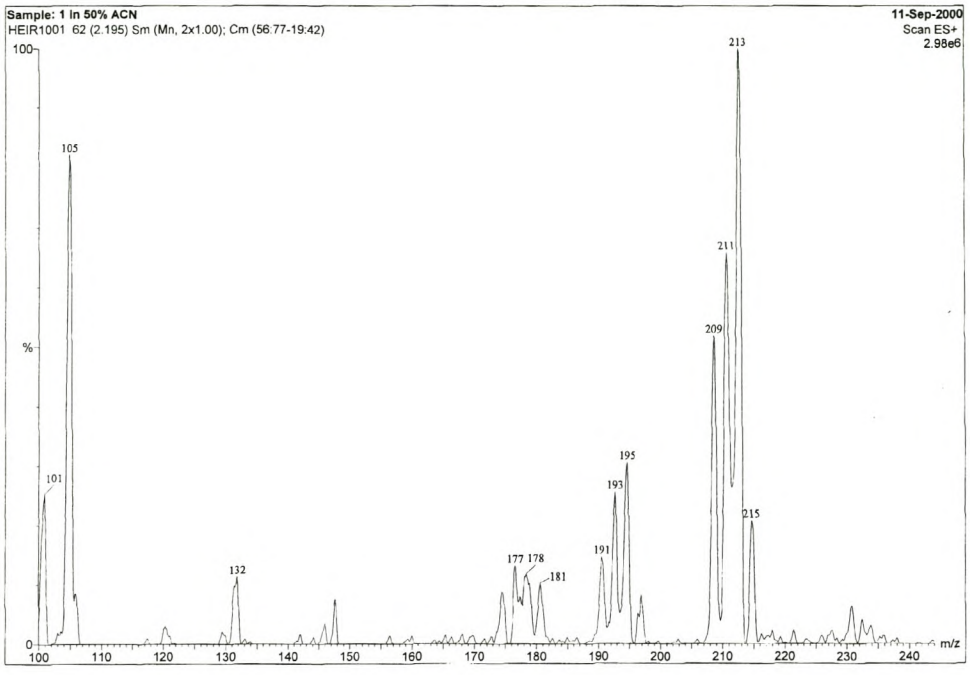

Figure II: Enlargement of ESMS from 250-450 (m/z)

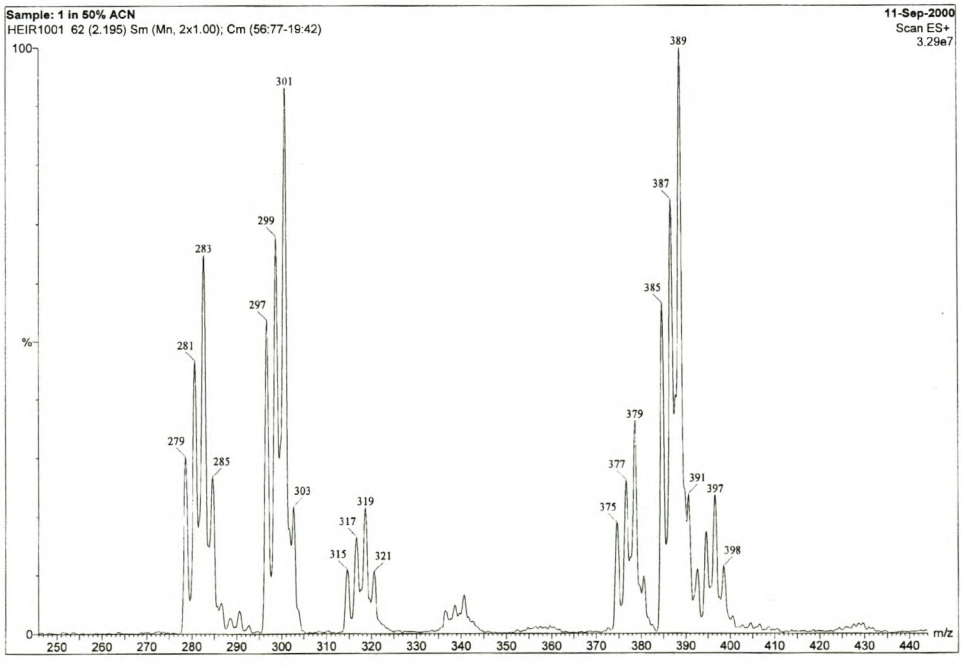

Figure III: Enlargement of ESMS from 450-630 (m/z)

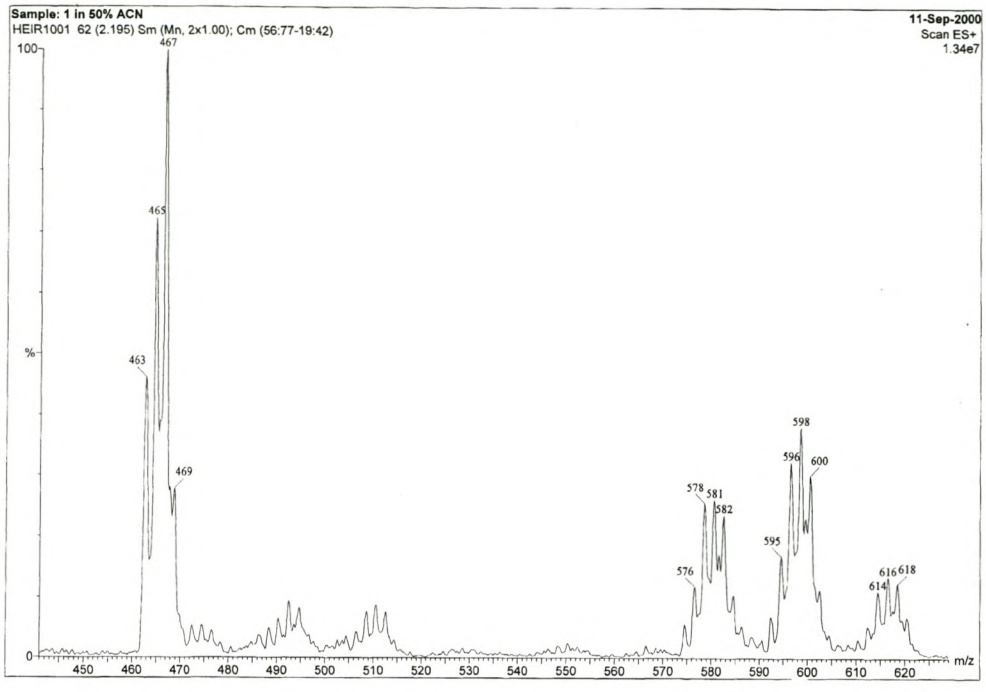

Figure IV: Enlargement of ESMS from 630-1000 (m/z)

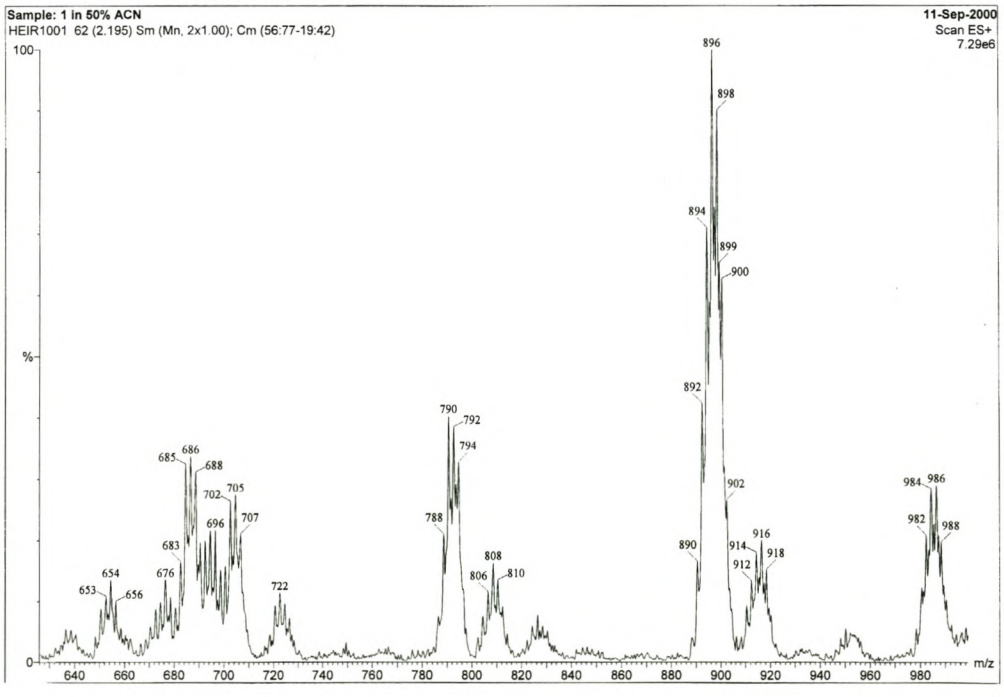

Figure V: Enlargement of ^{1}H NMR from 1.20-1.90 ppm

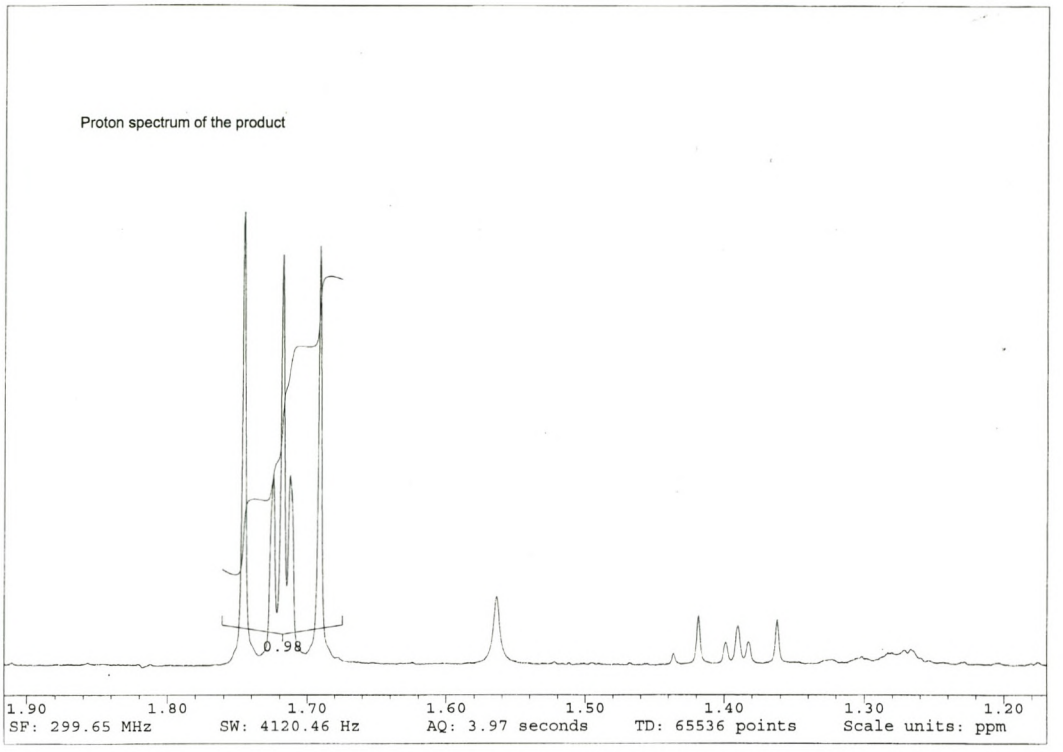

Figure VI: Enlargement of 1H NMR from 2.30-3.10 ppm

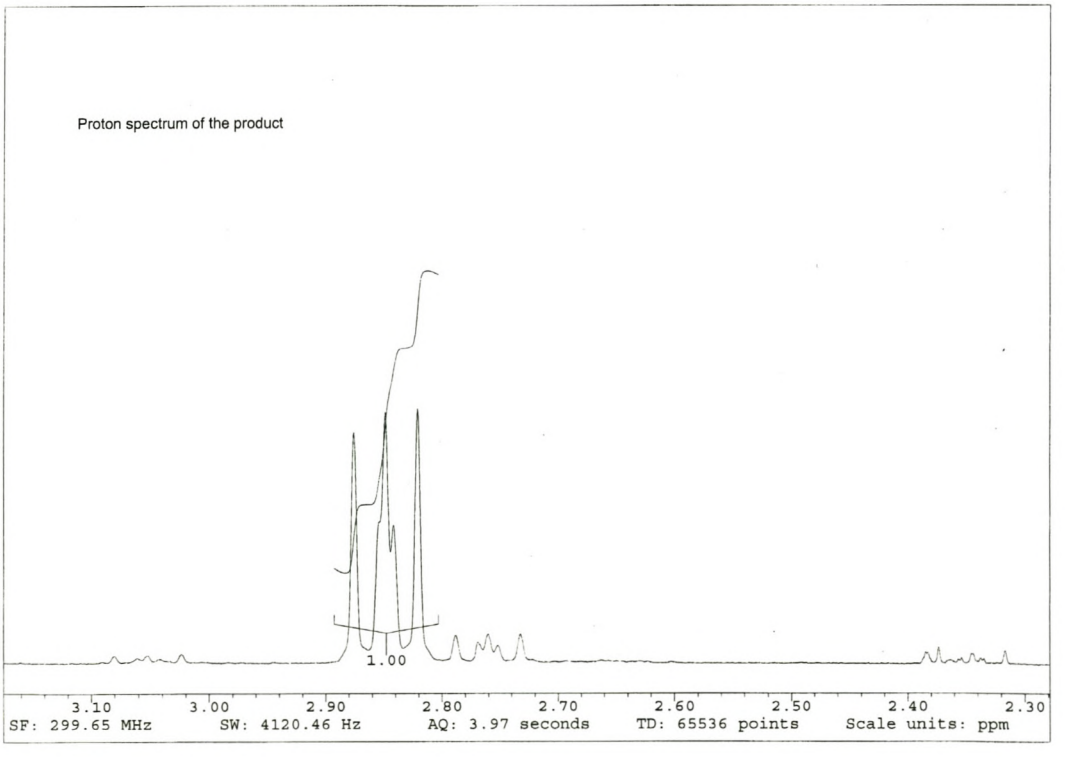

Figure VII: Enlargement of ^{1}H NMR from 7.10-7.40 ppm

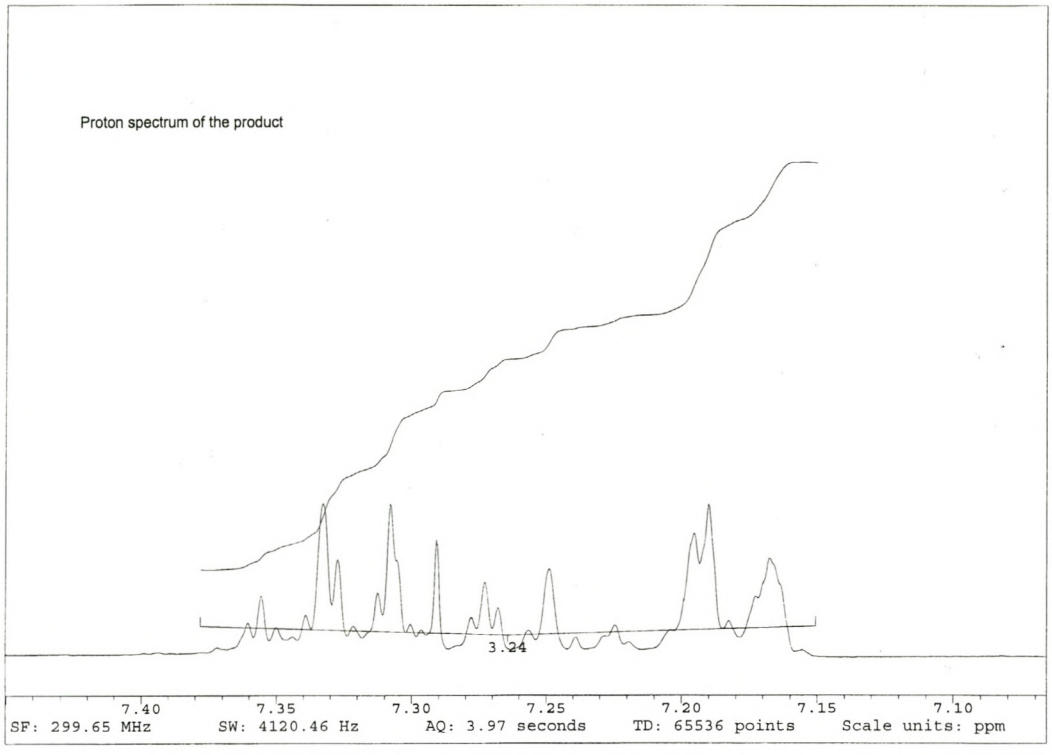

Figure VIII: Enlargement of $^{13}C\{^{1}H\}$ NMR from 124-133 ppm

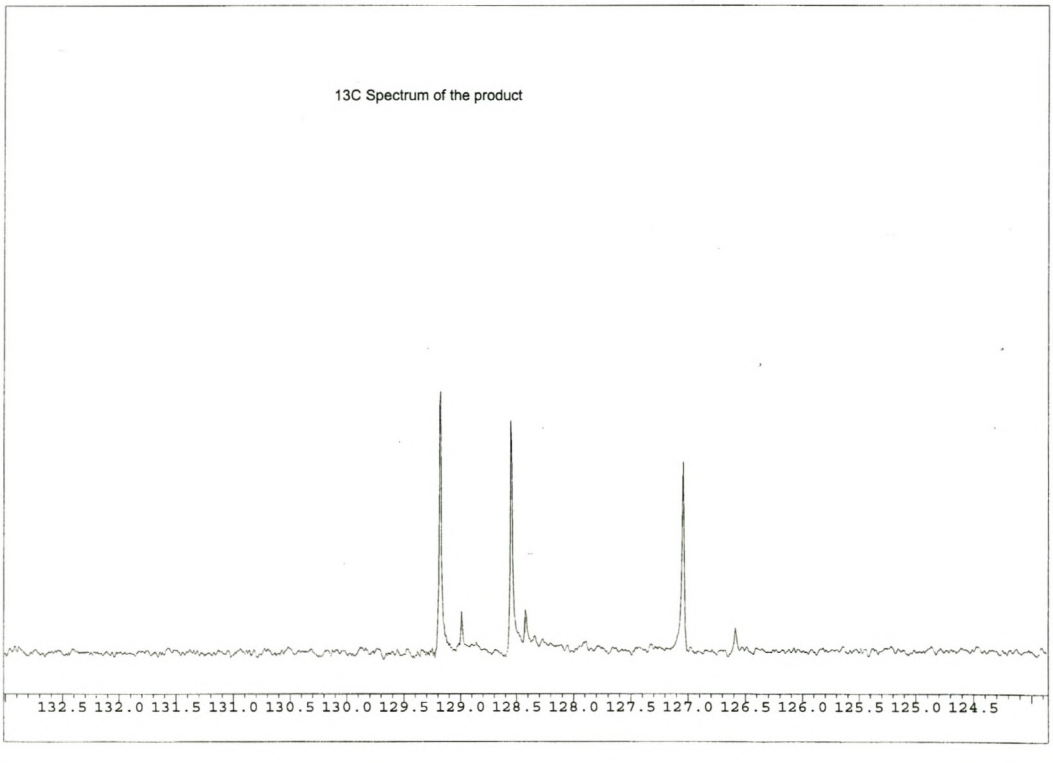

Figure IX: Enlargement of $^{13}C\{^{1}H\}$ NMR from 66-88 ppm

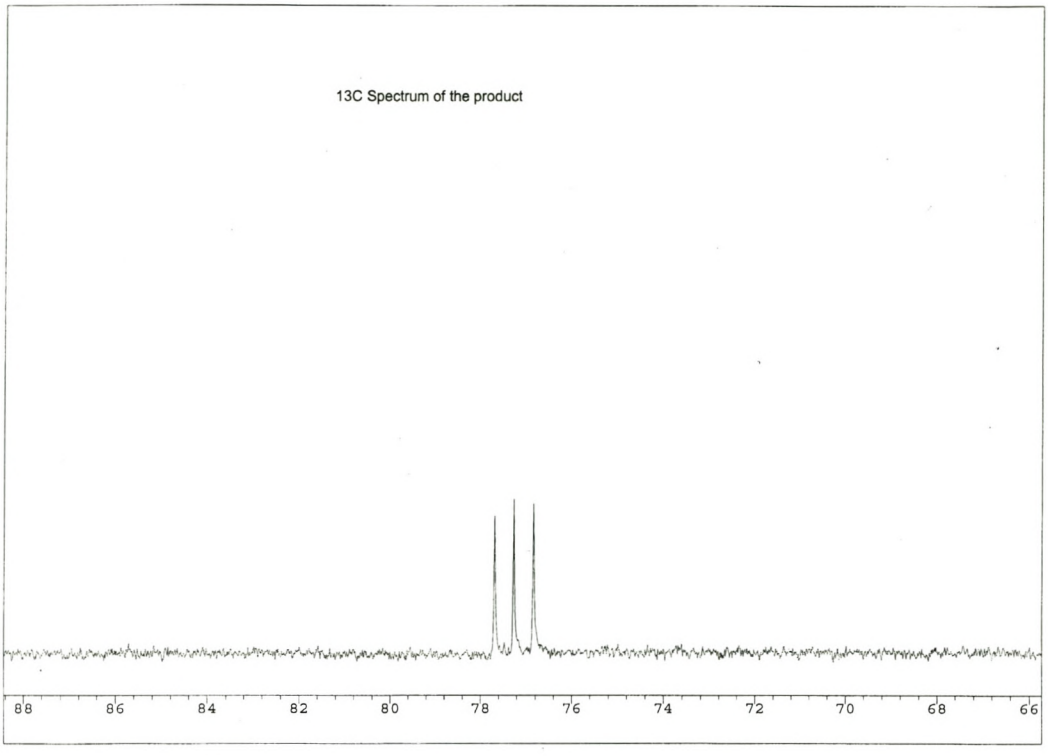

Figure X: Enlargement of $^{13}C\{^{1}H\}$ NMR from 18-38 ppm

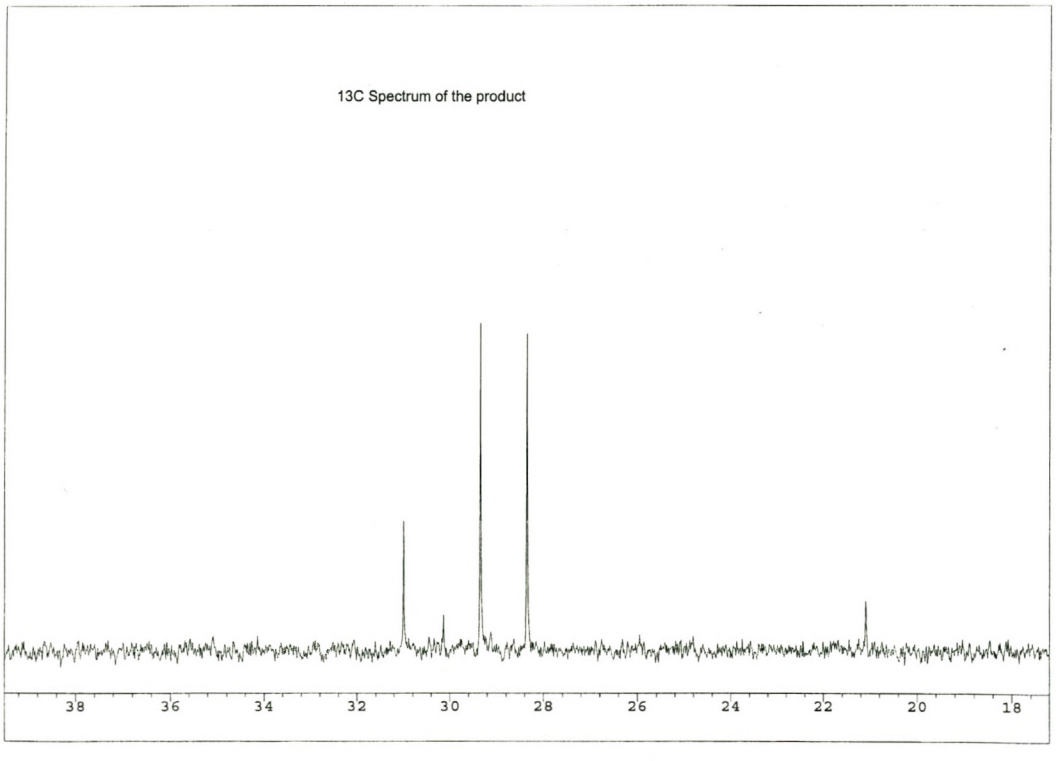

Addendum F: Comparison of Force Field Parameters to Literature Values

Table I: Stretching parameters for AH_nX_{4-n}

Molecule	Bond	Previous value ($N.m^{-1}$)	Previous value ($kcal.Å^{-2}$)	Present value ($kcal.Å^{-2}$)	Difference	% Diff.
CH_3F	C-H	487.8	702.1	682.4	19.7	2.9
	C-F	553.5	796.6	927.5	130.9	14.1
CH_3Cl	C-H	495.9	713.7	682.4	31.4	4.6
	C-Cl	351.5	505.9	407.2	98.7	24.2
CH_3Br	C-H	496.8	715.0	682.4	32.6	4.8
	C-Br	295.3	425.0	322.8	102.2	31.7
SiH_3F	Si-H	254.0	365.6	395.8	30.2	7.6
	Si-F	536.1	771.6	776.8	5.3	0.7
SiH_3Cl	Si-H	261.5	376.4	395.8	19.4	4.9
	Si-Cl	303.4	436.7	375.1	61.6	16.4
SiH_3Br	Si-H	270.3	389.0	395.8	6.8	1.7
	Si-Br	252.8	363.8	304.4	59.4	19.5
GeH_3F	Ge-H	260.1	374.4	333.1	41.3	12.4
	Ge-F	451.4	649.7	703.2	53.5	7.6
GeH_3Cl	Ge-H	264.6	380.8	333.1	47.7	14.3
	Ge-Cl	297.2	427.7	313.8	114.0	36.3
GeH_3Br	Ge-H	264.2	380.3	333.1	47.2	14.2
	Ge-Br	234.4	337.4	217.2	120.2	55.3
CH_2F_2	C-H	490.1	705.4	682.4	23.0	3.4
	C-F	604.6	870.2	927.5	57.4	6.2
CH_2Cl_2	C-H	490.7	706.2	682.4	23.9	3.5
	C-Cl	286.1	411.8	407.2	4.6	1.1
CH_2Br_2	C-H	492.2	708.4	682.4	26.0	3.8
	C-Br	229.7	330.6	322.8	7.8	2.4
SiH_2F_2	Si-H	285.6	411.1	395.8	15.3	3.9
	Si-F	571.7	822.8	776.8	46.0	5.9
SiH_2Cl_2	Si-H	283.4	407.9	395.8	12.1	3.1
	Si-Cl	310.7	447.2	375.1	72.1	19.2

GeH_2Cl_2	Ge-H	237.0	341.1	333.1	8.0	2.4
	Ge-Cl	246.0	354.1	313.8	40.3	12.8
GeH_2Br_2	Ge-H	262.4	377.7	333.1	44.6	13.4
	Ge-Br	232.2	334.2	217.2	117.0	53.9
CHF_3	C-H	511.9	736.8	682.4	54.4	8.0
	C-F	696.3	1002.2	927.5	74.6	8.0
$CHCl_3$	C-H	504.1	725.5	682.4	43.2	6.3
	C-Cl	310.7	447.2	407.2	40.0	9.8
$CHBr_3$	C-H	503.3	724.4	682.4	42.0	6.2
	C-Br	312.3	449.5	322.8	126.7	39.3
$SiHF_3$	Si-H	304.4	438.1	395.8	42.3	10.7
	Si-F	607.9	874.9	776.8	98.1	12.6
$SiHCl_3$	Si-H	289.6	416.8	395.8	21.0	5.3
	Si-Cl	323.9	466.2	375.1	91.1	24.3
$SiHBr_3$	Si-H	285.2	410.5	395.8	14.7	3.7
	Si-Br	289.2	416.2	304.4	111.8	36.7
$GeHCl_3$	Ge-H	273.9	394.2	333.1	61.1	18.3
	Ge-Cl	290.3	417.8	313.8	104.0	33.2

Table II: Bending parameters for AH_nX_{4-n}

Molecule	Angle	Previous value ($N.m^{-1}$)	Previous value (kcal)	Present value (kcal)	Difference	% Diff.
CH_3F	H-C-H	72.9	104.9	77.3	27.6	35.7
	H-C-F	90.0	129.5	128.8	0.7	0.5
CH_3Cl	H-C-H	68.1	98.0	77.3	20.7	26.7
	H-C-Cl	77.2	111.1	98.7	12.4	12.6
CH_3Br	H-C-H	67.8	97.6	77.3	20.3	26.2
	H-C-Br	73.2	105.4	88.6	16.8	19.0
SiH_3F	H-Si-H	39.1	56.3	59.2	3.0	5.0
	H-Si-F	46.7	67.2	87.9	20.6	23.5
SiH_3Cl	H-Si-H	35.3	50.8	59.2	8.4	14.2
	H-Si-Cl	38.8	55.8	73.8	18.0	24.3
SiH_3Br	H-Si-H	33.4	48.1	59.2	11.2	18.9
	H-Si-Br	35.3	50.8	71.8	21.0	29.2

GeH_3F	H-Ge-H	25.6	36.8	53.9	17.1	31.7
	H-Ge-F	36.6	52.7	71.3	18.6	26.1
GeH_3Cl	H-Ge-H	24.9	35.8	53.9	18.1	33.5
	H-Ge-Cl	31	44.6	63.7	19.1	30.0
GeH_3Br	H-Ge-H	27.8	40.0	53.9	13.9	25.8
	H-Ge-Br	35.9	51.7	62.4	10.7	17.1
CH_2F_2	H-C-H	63.3	91.1	77.3	13.8	17.8
	H-C-F	57.8	83.2	128.8	45.6	35.4
	F-C-F	131.8	189.7	233.1	43.4	18.6
CH_2Cl_2	H-C-H	63.4	91.2	77.3	13.9	18.0
	H-C-Cl	45.4	65.3	98.7	33.4	33.8
	Cl-C-Cl	195.9	282.0	142.0	140.0	98.6
CH_2Br_2	H-C-H	53.6	77.1	77.3	0.2	0.2
	H-C-Br	43.9	63.2	88.6	25.4	28.7
	Br-C-Br	161.8	232.9	114.3	118.6	103.7
SiH_2F_2	H-Si-H	27.0	38.9	59.2	20.4	34.4
	H-Si-F	24.7	35.5	87.9	52.3	59.5
	F-Si-F	44.9	64.6	128.8	64.2	49.8
SiH_2Cl_2	H-Si-H	26.2	37.7	59.2	21.5	36.3
	H-Si-Cl	20.9	30.1	98.7	68.6	69.5
	Cl-Si-Cl	38.3	55.1	120.6	65.5	54.3
GeH_2Cl_2	H-Ge-H	45.2	65.1	53.9	11.1	20.6
	H-Ge-Cl	17.8	25.6	63.7	38.1	59.8
	Cl-Ge-Cl	132.6	190.8	101.6	89.2	87.8
GeH_2Br_2	H-Ge-H	21.6	31.1	53.9	22.8	42.4
	H-Ge-Br	17.5	25.2	62.4	37.2	59.6
	Br-Ge-Br	35.0	50.4	101.5	51.1	50.3
CHF_3	H-C-F	119	171.3	128.8	42.4	32.9
	F-C-F	156.1	224.7	233.1	8.4	3.6
$CHCl_3$	H-C-Cl	135.8	195.5	98.7	96.8	98.0
	Cl-C-Cl	158	227.4	142.0	85.4	60.2
$CHBr_3$	H-C-Br	91.3	131.4	88.6	42.8	48.4
	Br-C-Br	114.8	165.2	114.3	50.9	44.6

Table III: Stretching parameters for Me_2AX_2

Molecule	Bond	Present Value (kcal/Å)	Present Value (mdyn/Å)	Previous Value (mdyn/Å)	Difference	% Diff.
Me_2GeF_2	C-H	682.38	4.74	4.88	0.14	2.9
	Ge-C	379.39	2.64	3.25	0.61	23.3
	Ge-F	703.15	4.89	4.17	0.72	14.7

Table IV: Bending parameters for Me_2AX_2

Molecule	Angle	Present Value (kcal.Å)	Present Value (mdyn.Å)	Previous Value (mdyn.Å)	Difference	% Diff.
Me_2GeF_2	C-Ge-C	54.96	0.38	0.68	0.30	78.0
	C-Ge-F	56.43	0.39	0.44	0.05	12.2
	F-Ge-F	92.44	0.64	0.77	0.13	19.8
	Ge-C-H6	64.63	0.45	0.42	0.03	6.5
	Ge-C-H4	64.63	0.45	0.45	0.00	0.2
	H-C-H	77.33	0.54	0.49	0.05	8.8